Diboson precision measurements

With the Higgs at LHC and FCC-hh

University of Birmingham

Particle Physics Seminar

16 November 2022

Birmingham, England

Alejo N. Rossia

Department of Physics and Astronomy

University of Manchester

With F. Bishara, S. De Curtis, L. Delle Rose, P. Englert, C. Grojean, M. Montull, G. Panico.

arXiv 2004.06122 (JHEP 07 (2020) 075)

arXiv 2011.13941 (JHEP 04 (2021) 154)

arXiv 2208.11134

We need something Beyond the Standard Model

Dark matter

Dark energy

Baryon asymmetry

EWSB mechanism

Neutrino masses

Quantum gravity

And many more

We haven't even measured all the SM yet!

How to look for BSM

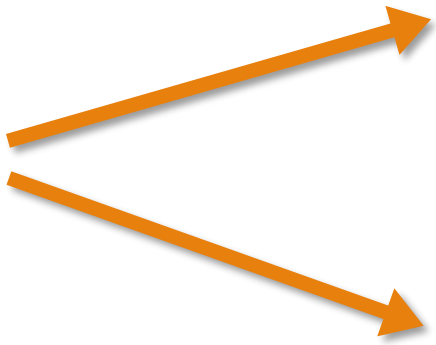

Resonance (particle) searches

Precision measurements

A trick of the tail

Precision with hadron colliders? Yes!

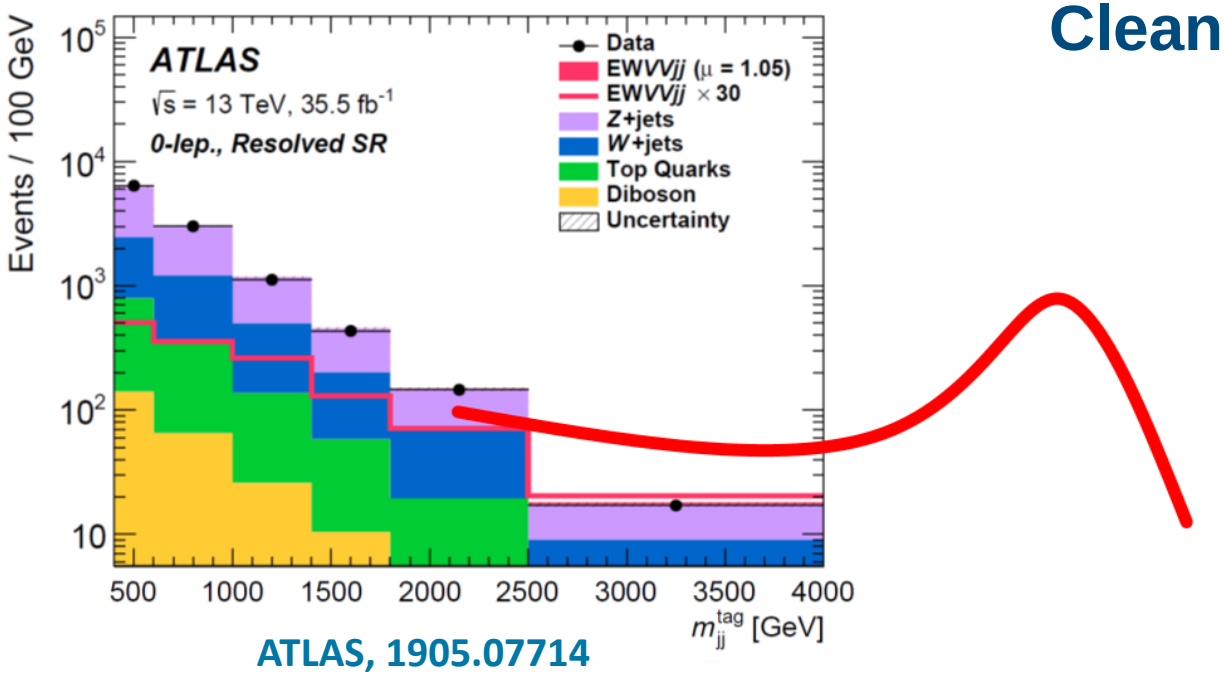

ATLAS, 1905.07714

Clean channels + NP effects that grow with E

Tail hunting!

Heavy New Physics

Effective Field Theories

Diboson processes offer a window into EW and Higgs dynamics.

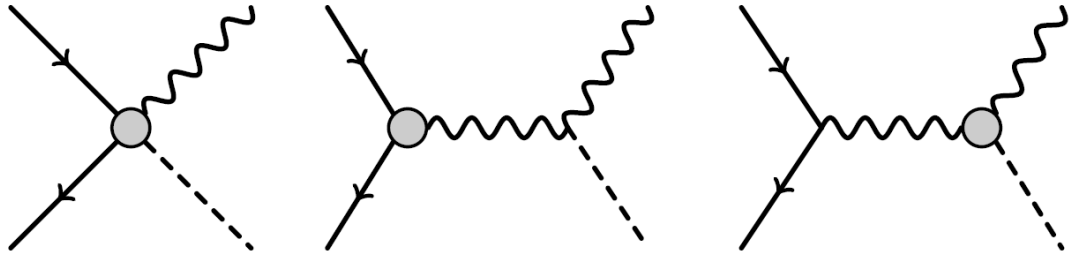

Diboson in the present

$(W/Z)h$ @ LHC

- ATLAS, *Eur. Phys. J. C 81 (2021) 2, 178*, ArXiv: 2007.02873
- ATLAS, *Phys. Lett. B 816 (2021) 136204*, ArXiv: 2008.02508
- CMS, *JHEP07 (2021) 027*, ArXiv: 2103.06956
- And more!

What will change in the future?

(HL-)LHC $\xrightarrow{e^{-i\hat{H}t}}$ FCC-hh

- FCC: Future Circular Collider
- FCC-ee + FCC-hh: like LEP+LHC

	HL-LHC	FCC-hh
C.o.M. energy	14 TeV	100 TeV
Int. Luminosity	3 ab^{-1}	30 ab^{-1}

FCC-hh: The LHC of the future

2021-2025 → **Feasibility study**

2030-2045 → **Construction**

2045-2060 → **FCC-ee operation**

2070-2095 → **FCC-hh operation**

$e^{-i\hat{H}t}$

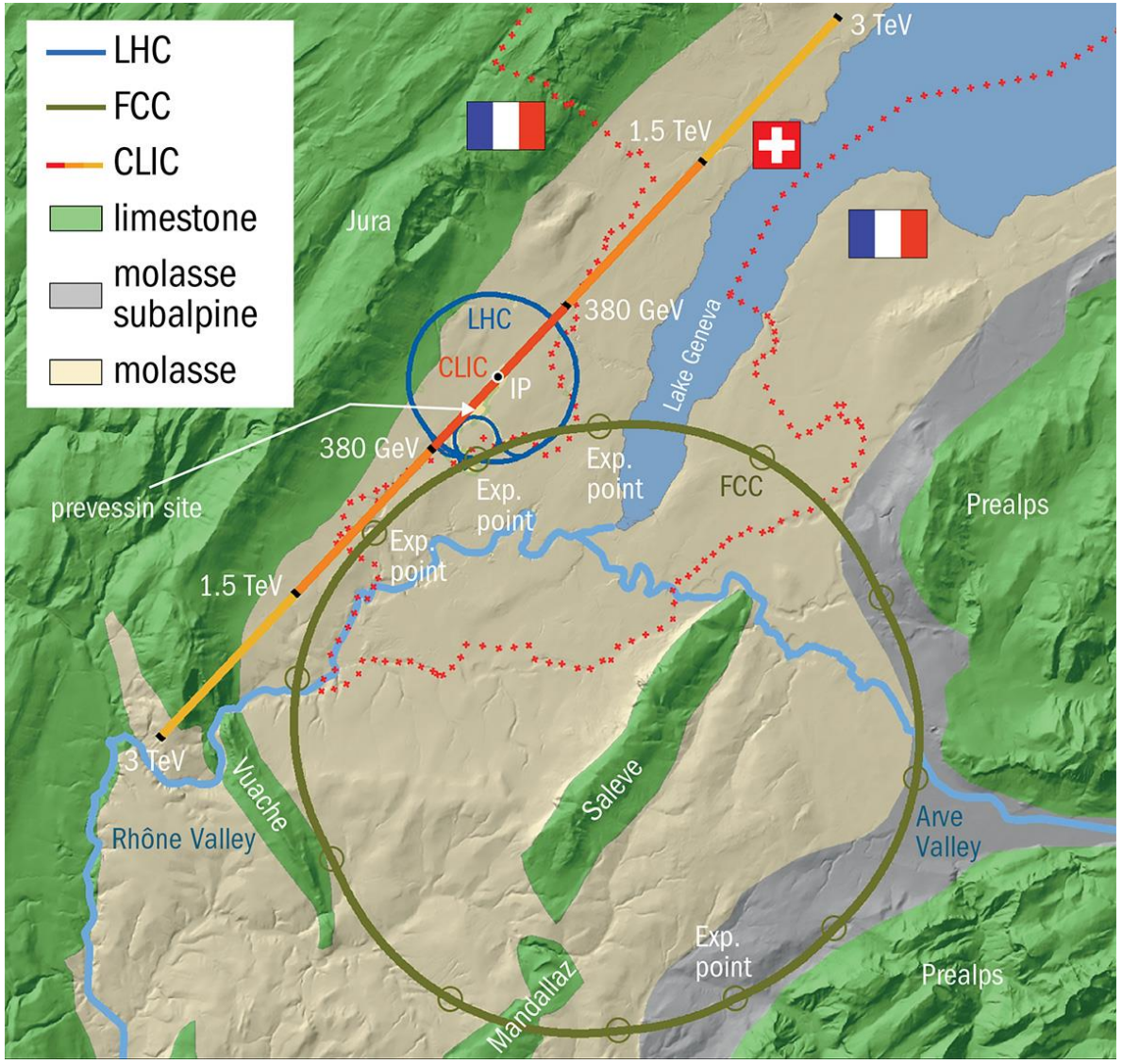

Timeline from talk by M. Benedikt (CERN) at FCC Workshop 2022

New collider, new opportunities

For $p_T^h > 550$ GeV:

$$pp \to W^{\pm} h$$

	Higgs decay	Higgs BR	n_{HL-LHC}	n_{HE-LHC}	n_{FCC-hh}
Today	$\bar{b}b$	$6 \cdot 10^{-1}$	10^3	10^4	10^5
	$\tau\tau$	$6 \cdot 10^{-2}$	10^2	10^3	10^4
Future	$\gamma\gamma$	$2 \cdot 10^{-3}$			10^3
	$4l$	$2 \cdot 10^{-3}$	10^0	10^2	10^3
	$\mu\mu$	$4 \cdot 10^{-4}$	10^0	10^1	10^2

$$\frac{s}{\sqrt{s+b}} \ll 1$$

$$\frac{s}{\sqrt{s+b}} \approx 1$$

Why Effective Field Theories?

- The main idea behind EFTs is in all fields of Physics.
- NP at a higher scale affect the interactions seen at a lower scale.

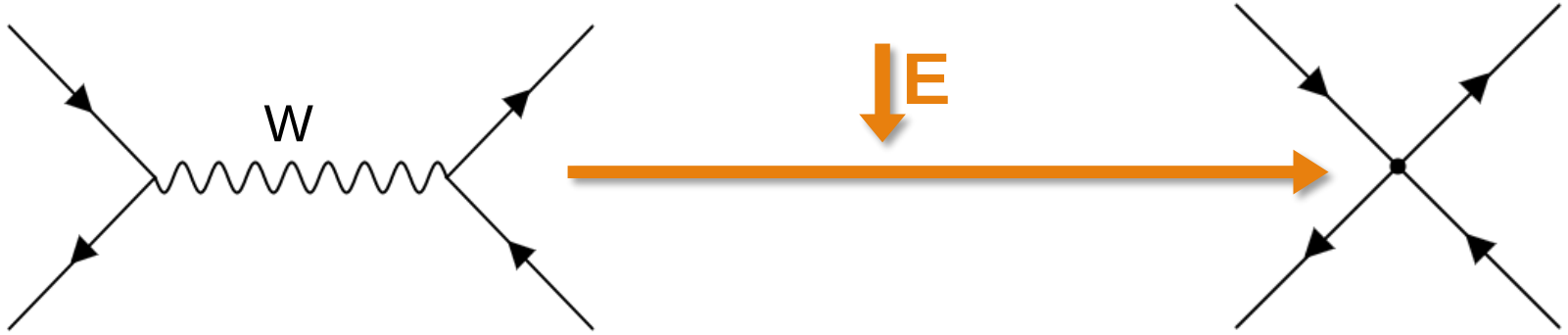

$$g\ \bar{q_L}\gamma^\mu W_\mu q_L \qquad \frac{g^2}{m_W^2}\ \bar{q_L}\gamma^\mu q_L \bar{l_L}\gamma_\mu l_L$$

- Operators with dimension>4 encode the NP effects in the EFT.
- Offer a more model-independent way of searching for NP.

Standard Model EFT (SMEFT) and Interference

- Field content and gauge symmetries of the SM and linearly realized EW sym.
- Add gauge invariant operators with dimension bigger than 4.

$$\mathcal{L} = \mathcal{L}_{SM} + \sum_i \frac{c_i^{(6)}}{\Lambda^2}\mathcal{O}_i^{(6)} + \sum_i \frac{c_i^{(8)}}{\Lambda^4}\mathcal{O}_i^{(8)} + \dots$$

- Leading deviations from the SM appear at dimension 6.

$$\sigma = |\mathcal{M}_{SM}|^2 + 2\mathrm{Re}\left(\mathcal{M}_{SM}\mathcal{M}_{BSM}^*\right) + |\mathcal{M}_{BSM}|^2$$

$$\propto c_i^{(6)}/\Lambda^2 \qquad \propto \left(c_i^{(6)}/\Lambda^2\right)^2$$

Interference

Leptonic diphoton Wh.

arXiv 2004.06122 (JHEP 07 (2020) 075)

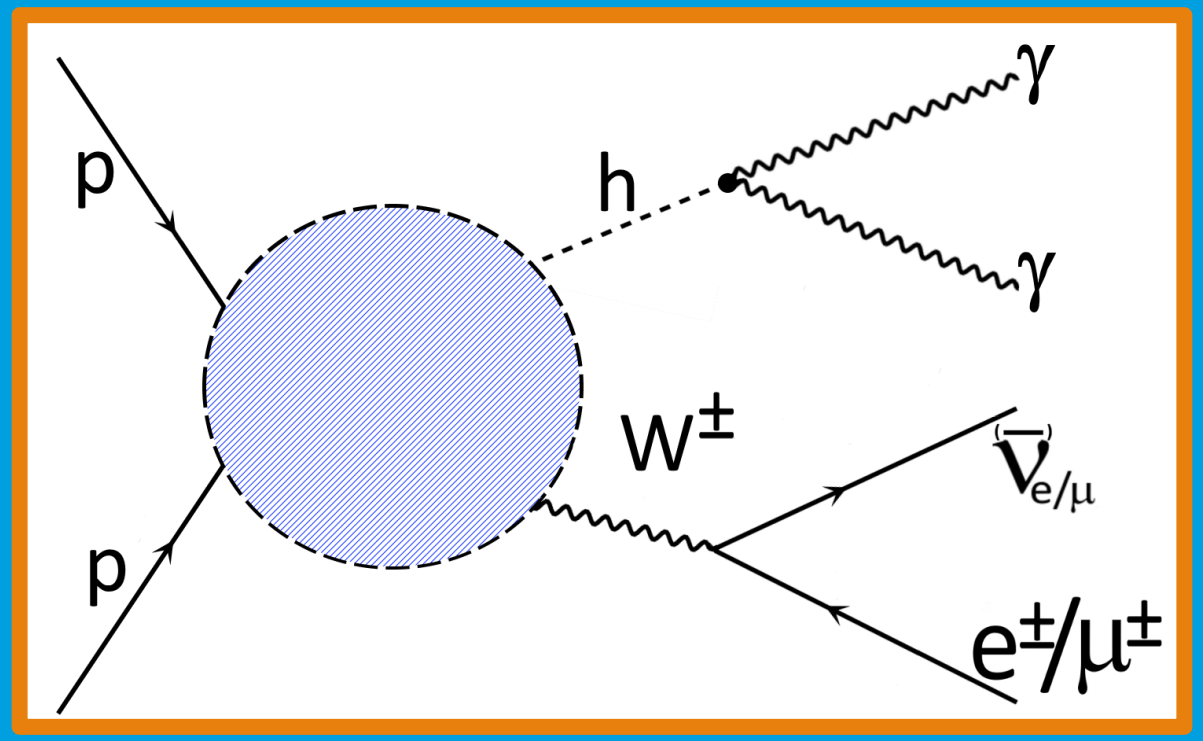

$$pp \to W^{\pm} h \to l^{\pm} \nu \, \gamma\gamma$$

Wh. What New Physics can we probe?

- Assumptions: SMEFT + Dim. 6 op. in Warsaw basis

High energy behavior

$$\frac{c_{\varphi q}^{(3)}}{\Lambda^2}\left(\overline{Q}_L\sigma^a\gamma^\mu Q_L\right)\left(iH^\dagger\sigma^a\overleftrightarrow{D}_\mu H\right) \longrightarrow \frac{\mathcal{A}_{BSM}}{\mathcal{A}_{SM}} \sim \hat{s} = E_{CM}^2$$

$$\frac{c_{\varphi \mathrm{W}}}{\Lambda^2} H^\dagger H\, W^{a,\mu\nu} W^a_{\mu\nu}$$

$$\frac{c_{\varphi \widetilde{\mathrm{W}}}}{\Lambda^2} H^\dagger H\, W^{a,\mu\nu} \widetilde{W}^a_{\mu\nu}$$

$$\longrightarrow \frac{\mathcal{A}_{BSM}}{\mathcal{A}_{SM}} \sim \sqrt{\hat{s}} = E_{CM}$$

$$\widetilde{W}^{a,\mu\nu} \equiv \frac{1}{2}\epsilon^{\mu\nu\rho\sigma} W^a_{\rho\sigma}$$

Wh. Interference patterns

High energy behaviour

V polarization	SM	$\mathcal{O}_{\varphi f}$	$\mathcal{O}_{\varphi \mathrm{W}}$	$\mathcal{O}_{\varphi \widetilde{\mathrm{W}}}$
$\lambda = 0$	1	$\frac{\hat{s}}{\Lambda^2}$	$\frac{M_W^2}{\Lambda^2}$	0
$\lambda = \pm$	$\frac{M_W}{\sqrt{\hat{s}}}$	$\frac{\sqrt{\hat{s}}\, M_W}{\Lambda^2}$	$\frac{\sqrt{\hat{s}}\, M_W}{\Lambda^2}$	$\frac{\sqrt{\hat{s}}\, M_W}{\Lambda^2}$

$V = W, Z$ $\qquad$ $\mathcal{O}_{\varphi f} = \mathcal{O}_{\varphi q}^{(3)}, \mathcal{O}_{\varphi q}^{(1)}, \mathcal{O}_{\varphi u}, \mathcal{O}_{\varphi d}$

Differential in p_T

↓

Interference between same polarisation

Wh.

Interference patterns

Measuring angles resurrects interference

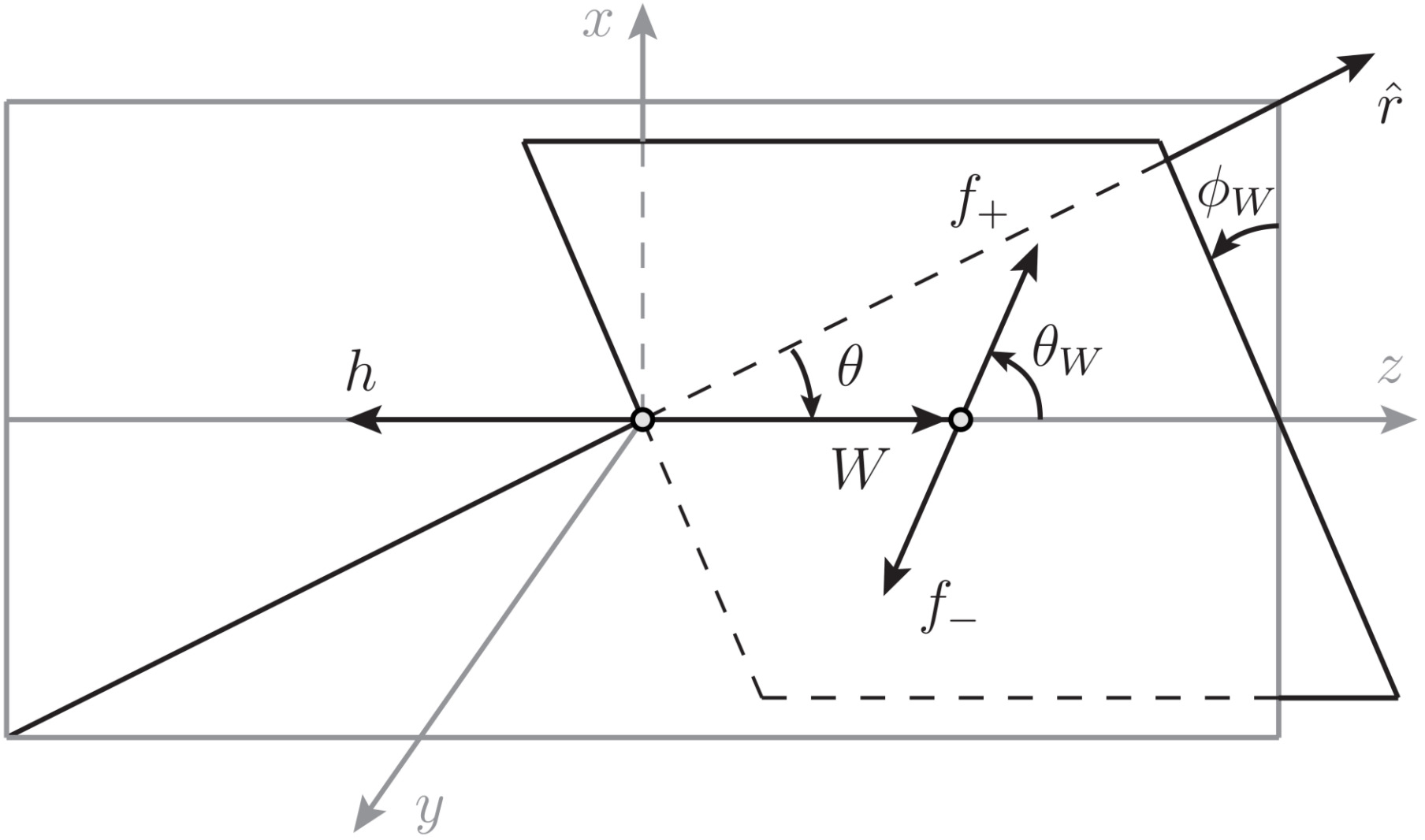

Wh. Interference patterns

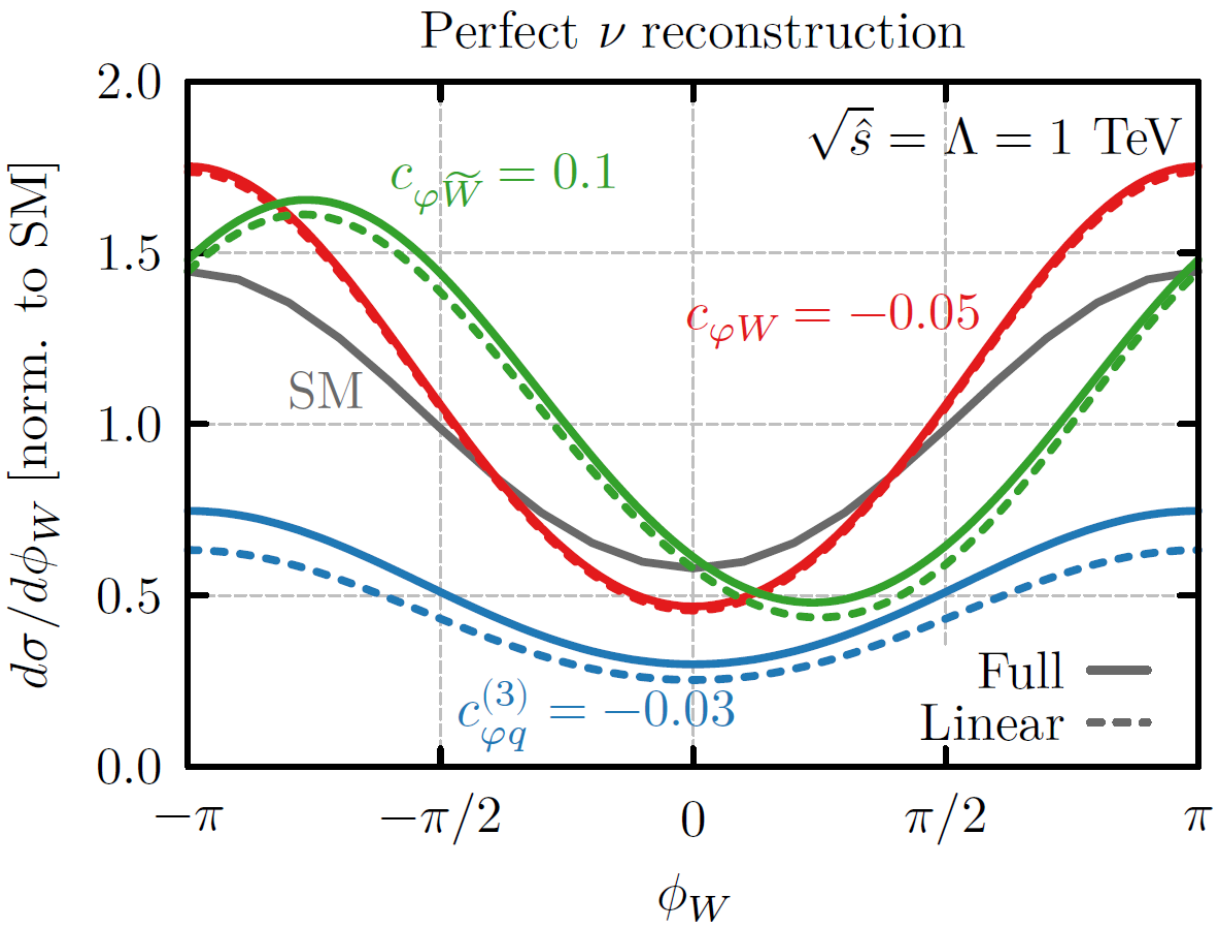

Differential in p_T^h and ϕ_W

$$\sigma^{int}_{\mathcal{O}^{(3)}_{\varphi q}} \sim \frac{\hat{s}}{\Lambda^2}$$

$$\sigma^{int}_{\mathcal{O}_{\varphi \mathrm{W}}} \sim \frac{\sqrt{\hat{s}} M_W}{\Lambda^2} \cos(\phi_W)$$

$$\sigma^{int}_{\mathcal{O}_{\varphi \widetilde{\mathrm{W}}}} \sim \frac{\sqrt{\hat{s}} M_W}{\Lambda^2} \sin(\phi_W)$$

$$p_T^h \in \{200, 400, 600, 800, 1000, \infty\}\,\mathrm{GeV} \qquad \phi_W \in [-\pi, 0],\ [0, \pi]$$

Wh. Interference patterns

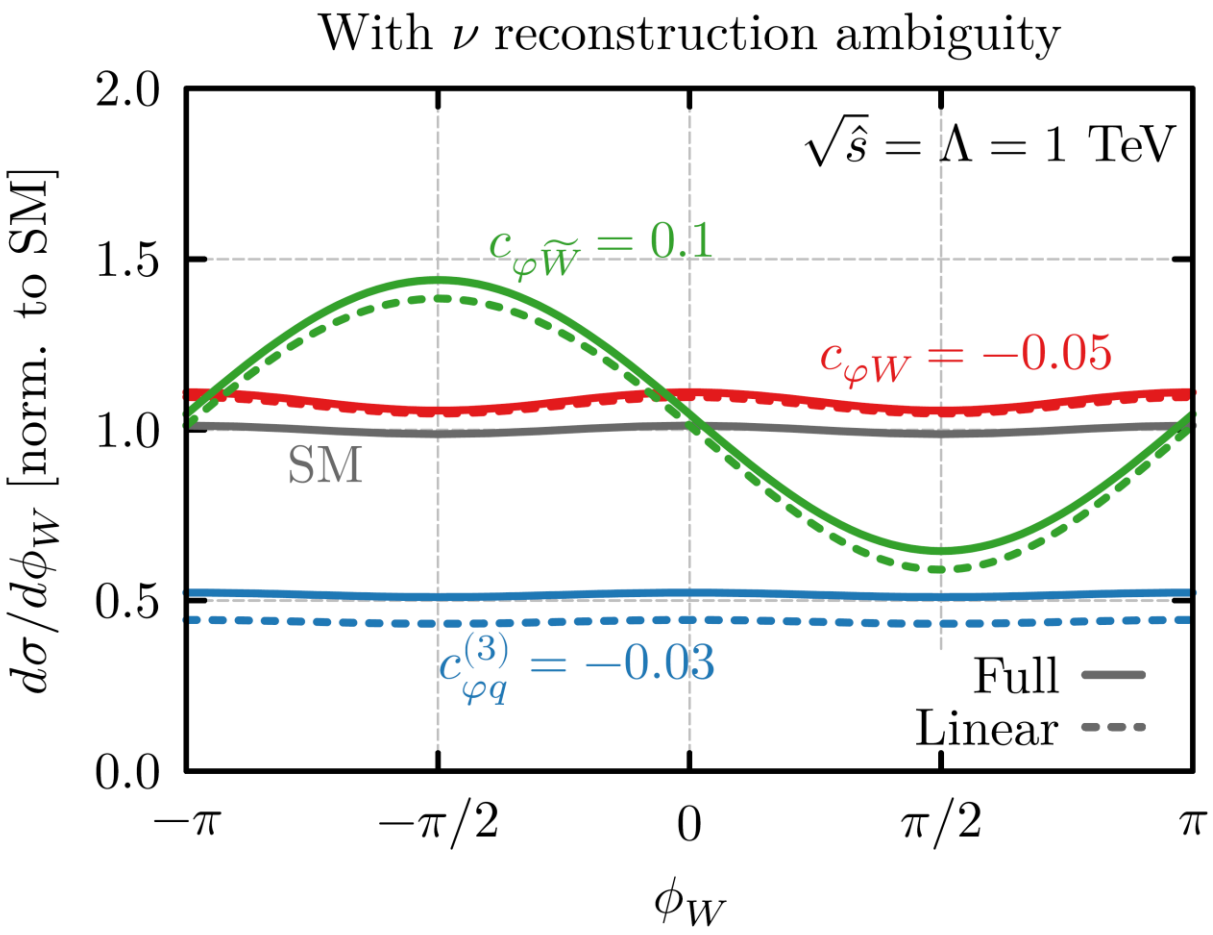

Differential in p_T^h and ϕ_W

$$\sigma^{int}_{\mathcal{O}^{(3)}_{\varphi q}} \sim \frac{\hat{s}}{\Lambda^2}$$

ν reconstruction

$(\phi_W \to \pi - \phi_W)$

$$\sigma^{int}_{\mathcal{O}_{\varphi W}} \sim \frac{\sqrt{\hat{s}} M_W}{\Lambda^2} \sin(\phi_W)$$

$$\sigma^{int}_{\mathcal{O}_{\varphi \widetilde{W}}} \sim \frac{\sqrt{\hat{s}} M_W}{\Lambda^2} \sin(\phi_W)$$

$$p_T^h \in \{200, 400, 600, 800, 1000, \infty\}\,\text{GeV} \qquad \phi_W \in [-\pi, 0],\ [0, \pi]$$

Wh.

95% C.L. on $c_{\varphi q}^{(3)}$

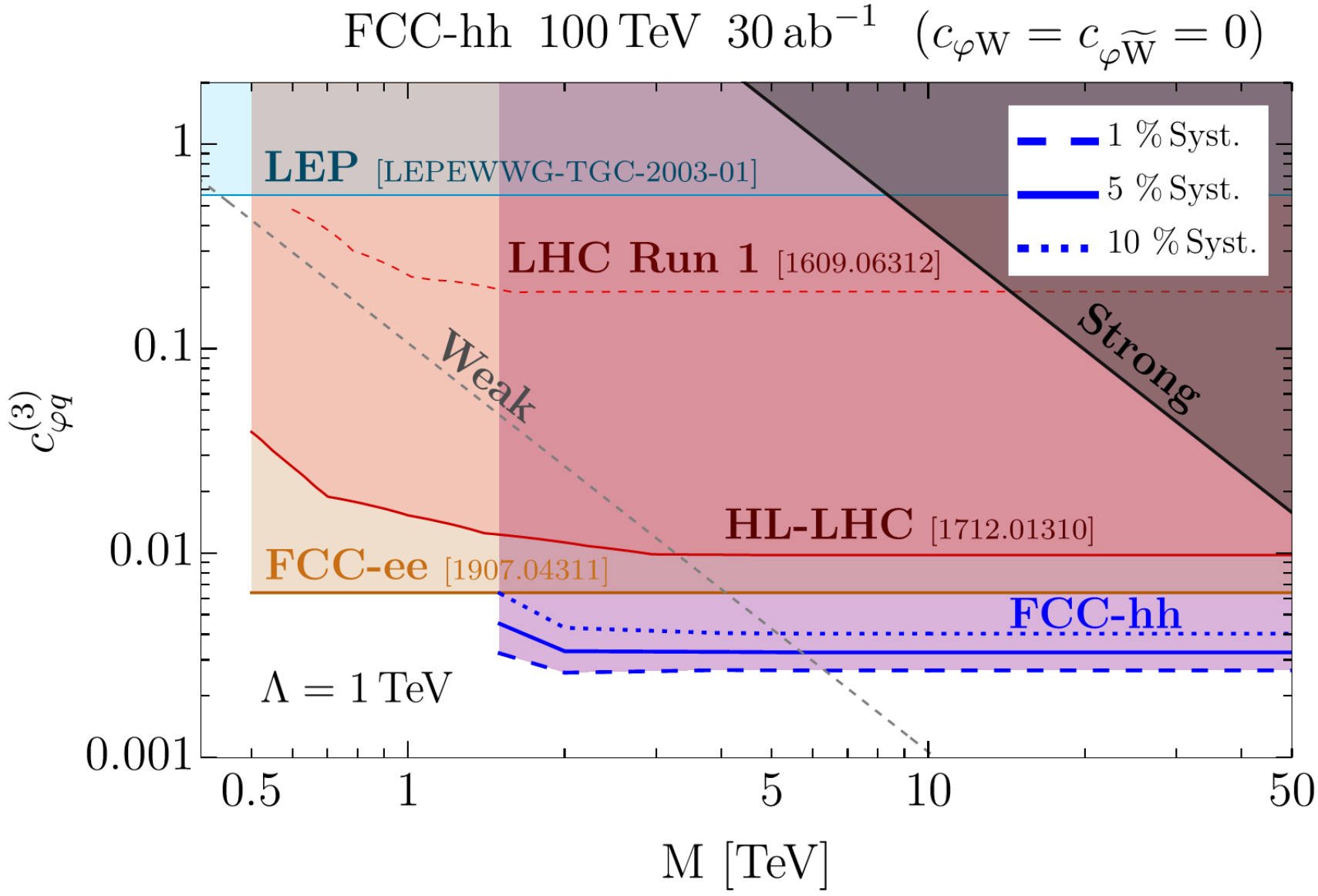

Wh. 95% C.L. on the bosonic operators

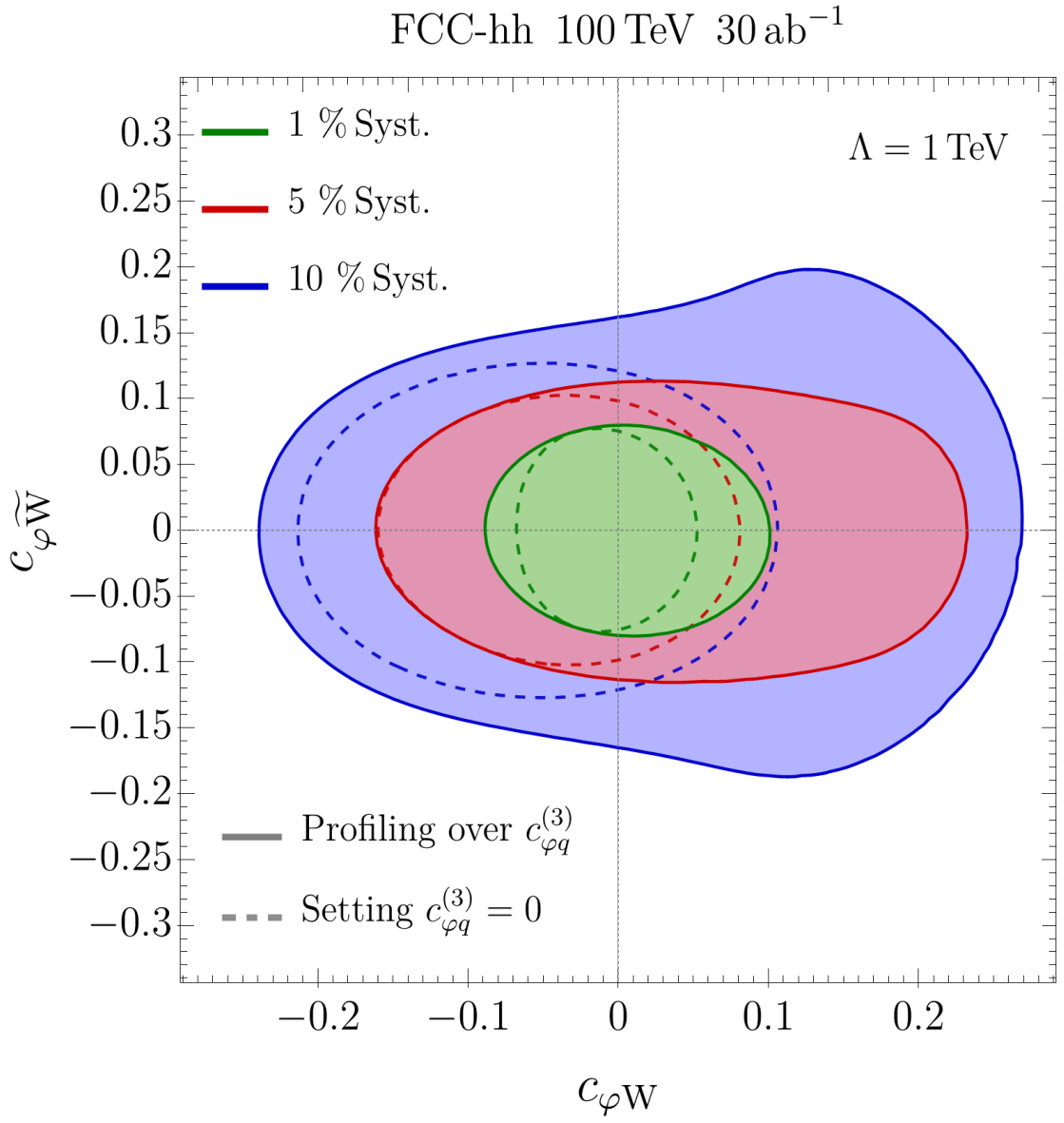

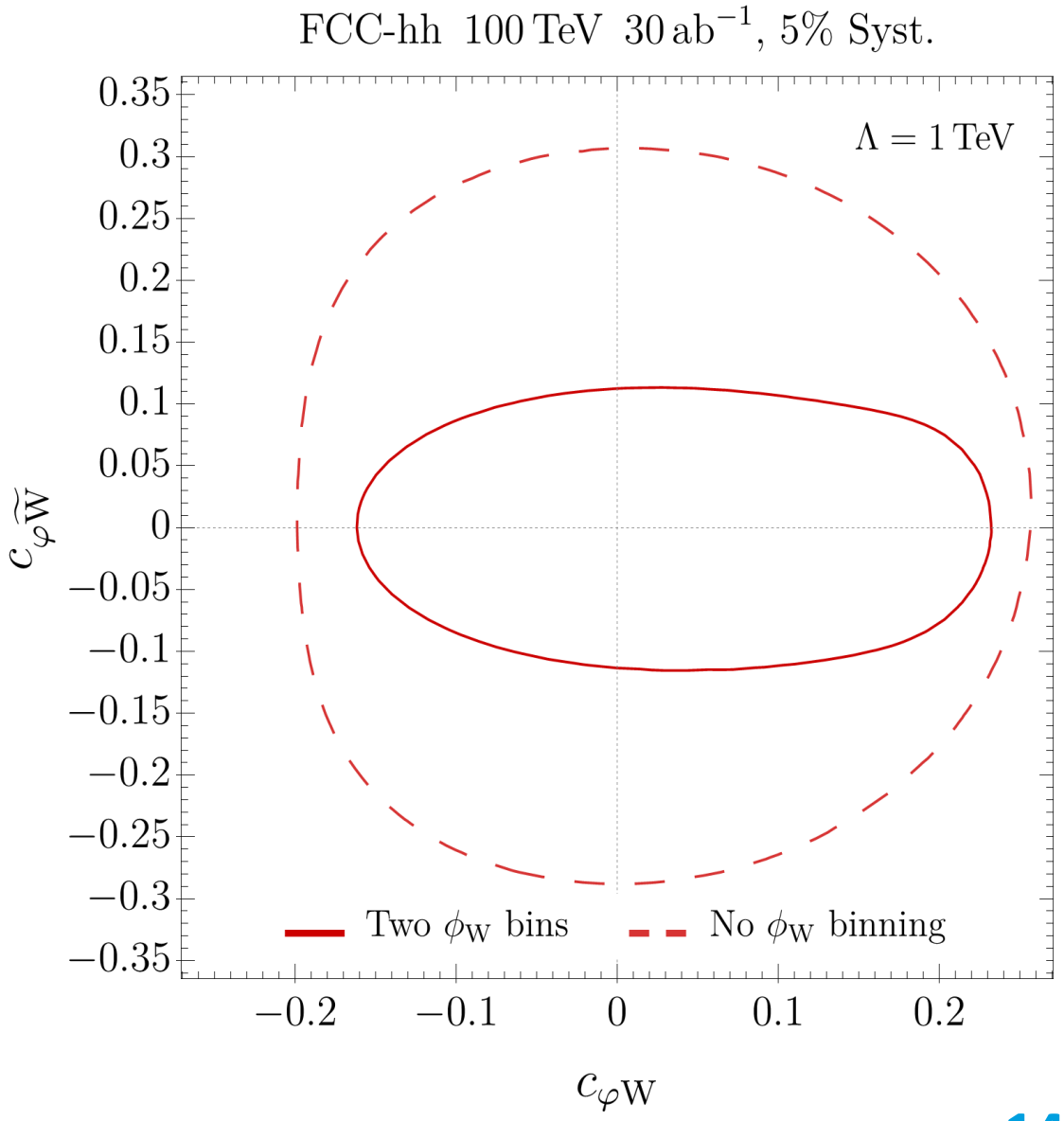

Diphoton Zh.

arXiv 2011.13941 (JHEP 04 (2021) 154)

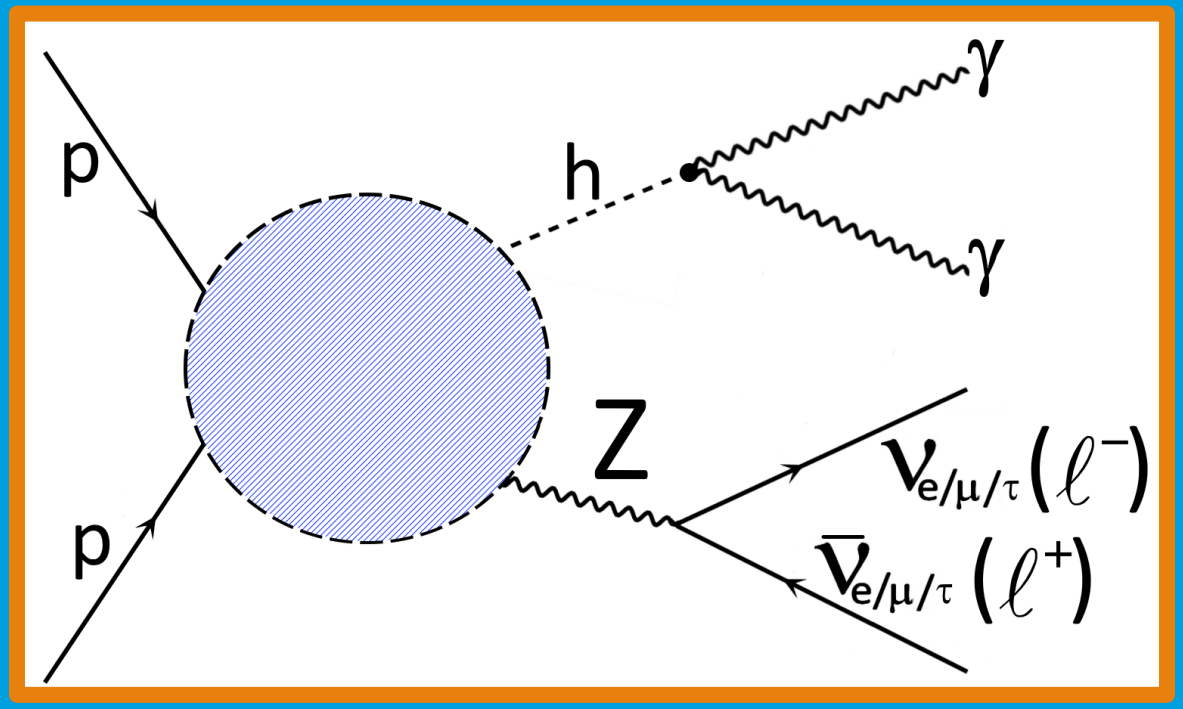

$$pp \to Zh \to l^+l^- \left(\nu\bar{\nu}\right)\gamma\gamma$$

Zh. What New Physics can we probe?

- Assumptions: SMEFT + Dim. 6 op. in Warsaw basis + Flav. Univ.

High-energy behaviour

$$\frac{c_{\varphi q}^{(3)}}{\Lambda^2}\left(\overline{Q}_L\sigma^a\gamma^\mu Q_L\right)\left(iH^\dagger\sigma^a\overleftrightarrow{D}_\mu H\right)$$

$$\frac{c_{\varphi q}^{(1)}}{\Lambda^2}\left(\overline{Q}_L\gamma^\mu Q_L\right)\left(iH^\dagger\overleftrightarrow{D}_\mu H\right)$$

$$\frac{c_{\varphi u}}{\Lambda^2}\left(\overline{u}_R\gamma^\mu u_R\right)\left(iH^\dagger\overleftrightarrow{D}_\mu H\right)$$

$$\frac{c_{\varphi d}}{\Lambda^2}\left(\overline{d}_R\gamma^\mu d_R\right)\left(iH^\dagger\overleftrightarrow{D}_\mu H\right)$$

$$\rightarrow \quad \frac{\mathcal{A}_{BSM}}{\mathcal{A}_{SM}} \sim \hat{s} = E_{CM}^2$$

Zh.

Interference patterns

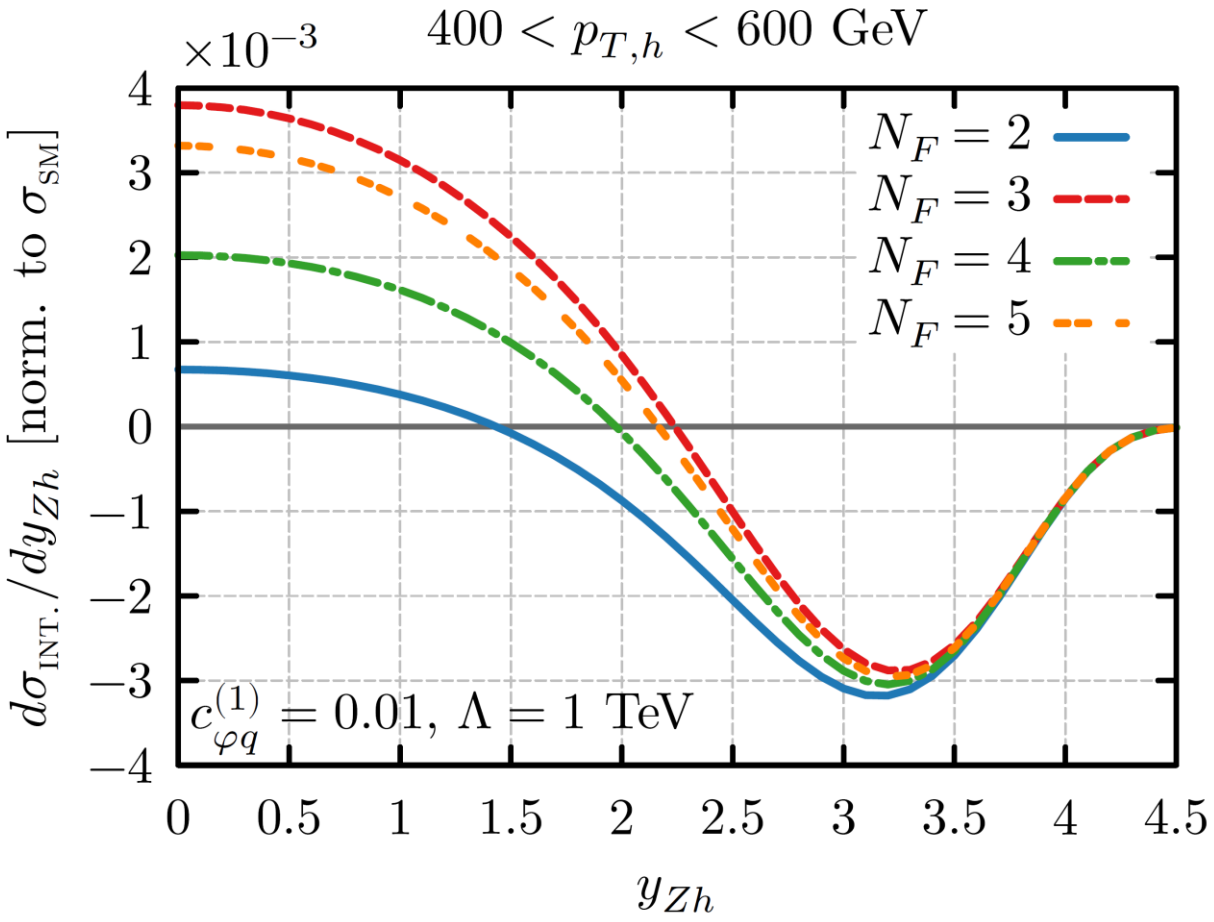

$$\sigma^{int}_{\mathcal{O}^{(1)}_{\varphi q}} \propto s^2_W Q - T_3$$

Cancellation of up and down contributions

$$\sigma^{int}_{\mathcal{O}_{\varphi u(d)}} \propto g_R^{Zu(d)}$$

Suppression by SM coupling

Differential in p_T and rapidity

$$\mathrm{Min}\{p_T^h, p_T^Z\} \in \{200, 400, 600, 800, 1000, \infty\}\ \mathrm{GeV}$$

$$|y_{Zh}| \in [0, 2),\ [2, 6]$$

(Slightly different rapidity binning for $Z \to \nu\bar{\nu}$)

Vh. Best possible bounds for $c_{\varphi q}^{(3)}$

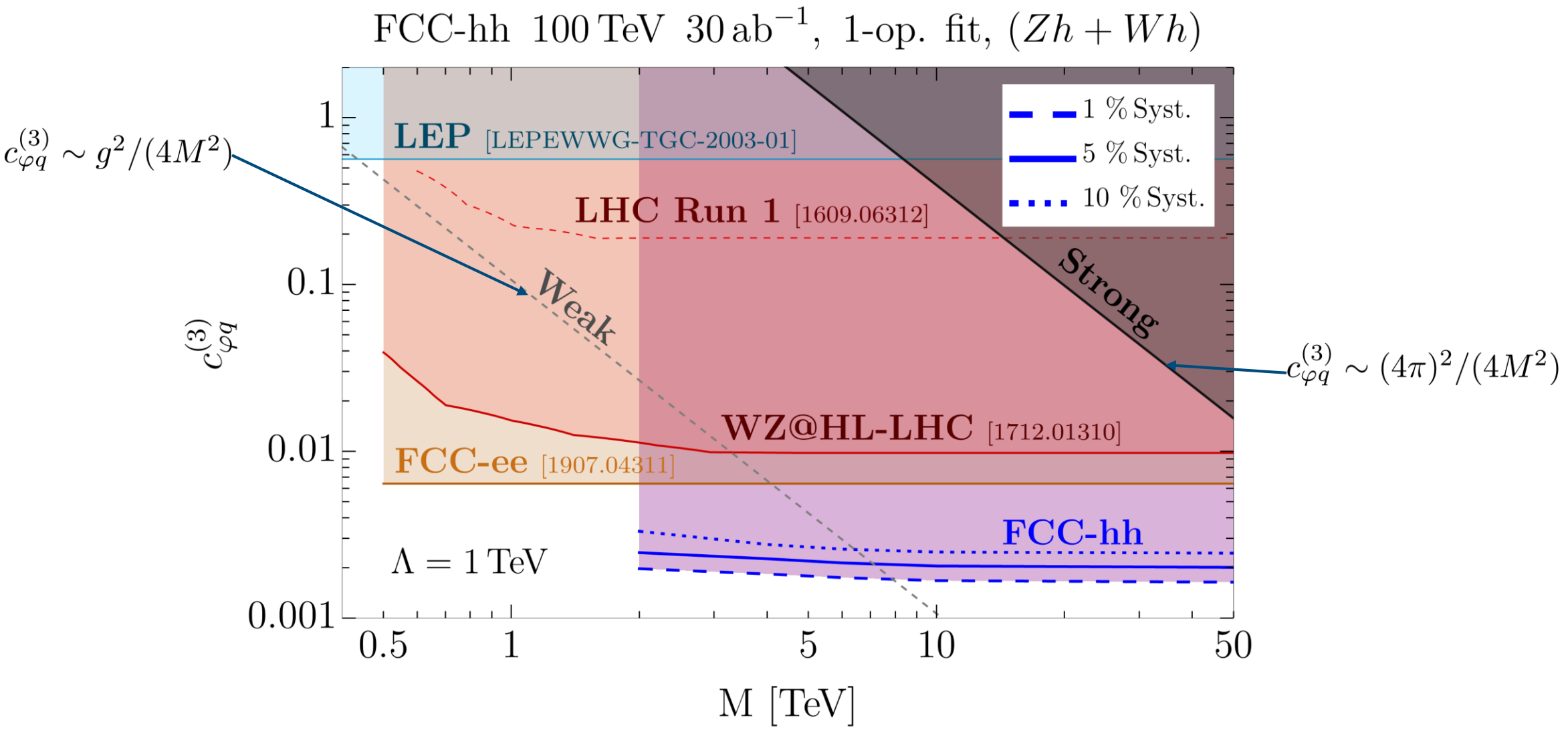

Vh.

The power of combining

- 95% CL bounds

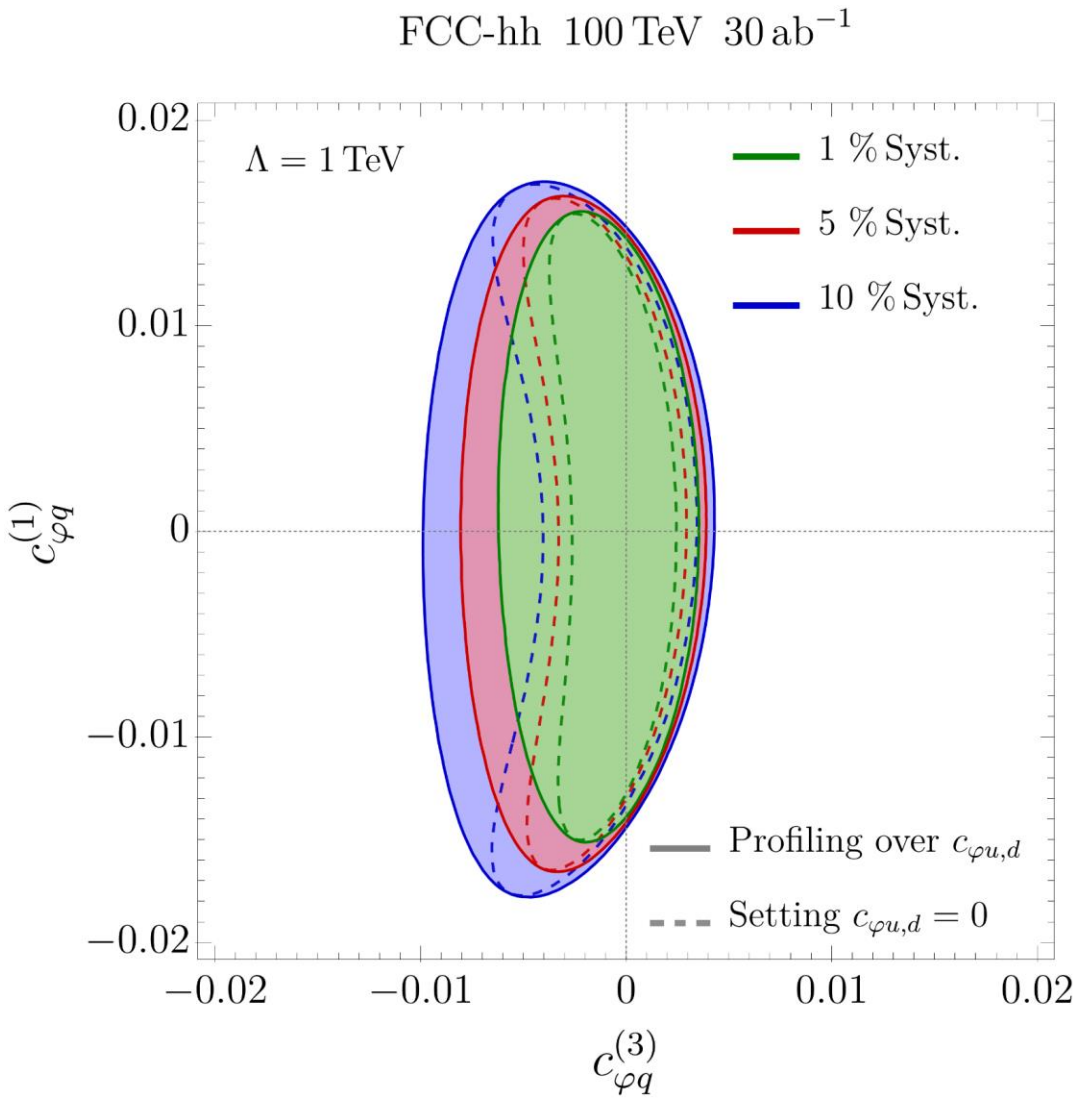

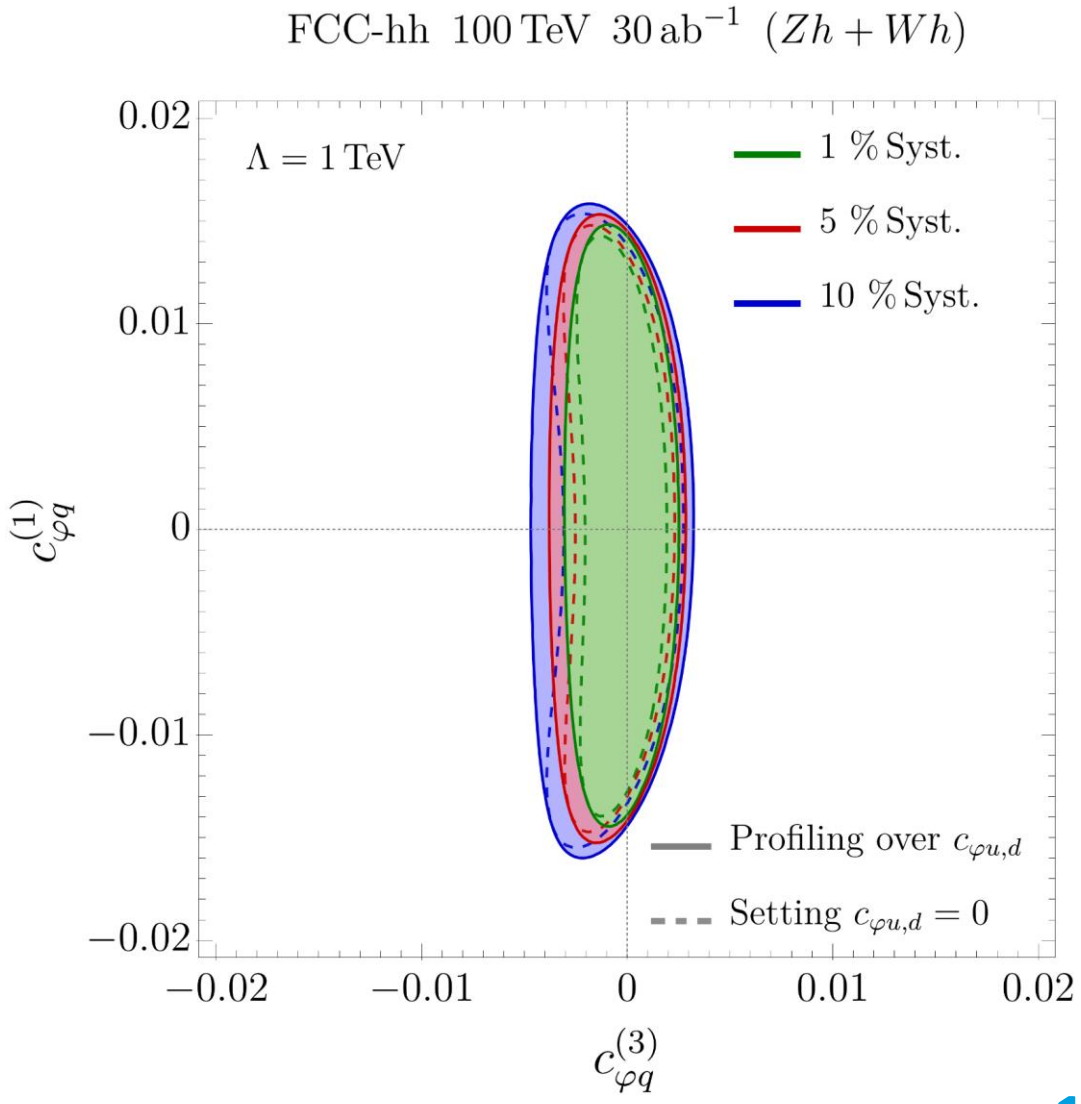

Vh. Sizeable impact on aTGC bounds

$$c_{\varphi q}^{(3)} = +\frac{\Lambda^2}{4m_W^2} g^2 \left(\delta g_L^{Zu} - \delta g_L^{Zd} - c_{\rm W}^2\, \delta g_{1z}\right)$$

$$c_{\varphi q}^{(1)} = -\frac{\Lambda^2}{4m_W^2} g^2 \left(\delta g_L^{Zu} + \delta g_L^{Zd} + \frac{1}{3}\left(t_{\rm W}^2 \delta\kappa_\gamma - s_{\rm W}^2 \delta g_{1z}\right)\right)$$

$$c_{\varphi u} = -\frac{\Lambda^2}{2m_W^2} g^2 \left(\delta g_R^{Zu} + \frac{2}{3}\left(t_{\rm W}^2 \delta\kappa_\gamma - s_{\rm W}^2 \delta g_{1z}\right)\right)$$

$$c_{\varphi d} = -\frac{\Lambda^2}{2m_W^2} g^2 \left(\delta g_R^{Zd} - \frac{1}{3}\left(t_{\rm W}^2 \delta\kappa_\gamma - s_{\rm W}^2 \delta g_{1z}\right)\right)$$

$$\mathcal{L}_{TGC} \supset ie\left(1+\delta\kappa_\gamma\right) A^{\mu\nu} W_\mu^+ W_\nu^- + ig\, c_W \left(1+\delta g_{1z}\right)\left(W_{\mu\nu}^+ W^{-,\mu} - W_{\mu\nu}^- W^{+,\mu}\right) Z^\nu$$

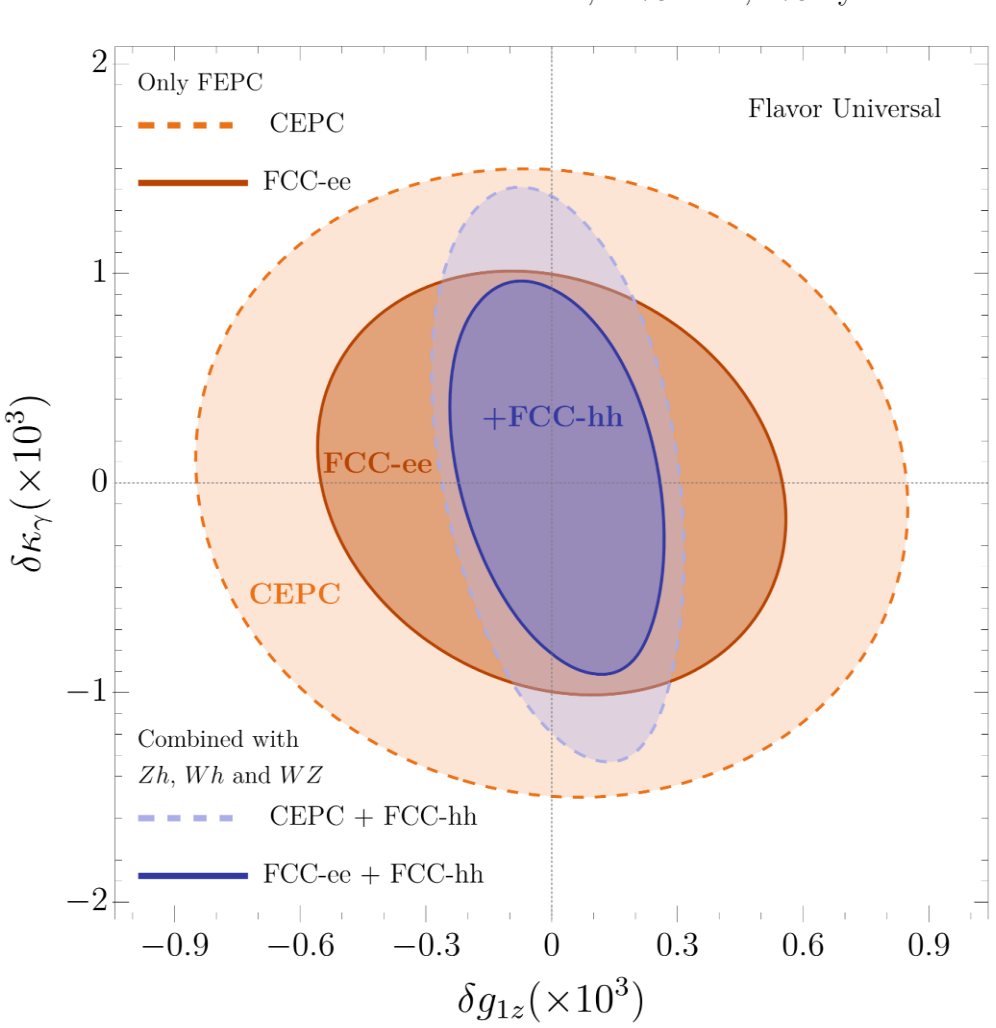

Clear complementarity with future lepton colliders

Vh. Comparing our bounds with other colliders

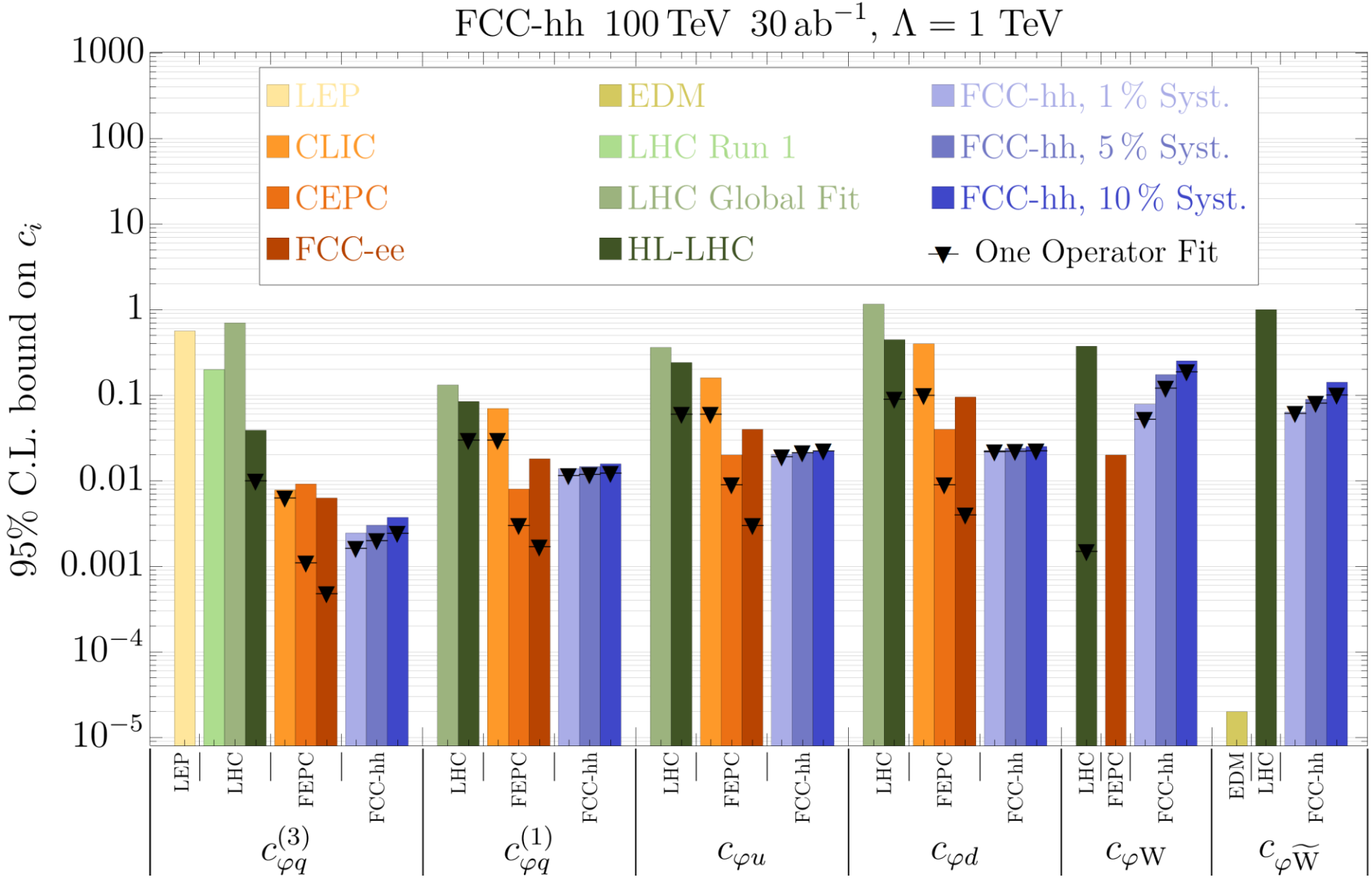

Let them be quarks, Higgs.

arXiv 2208.11134

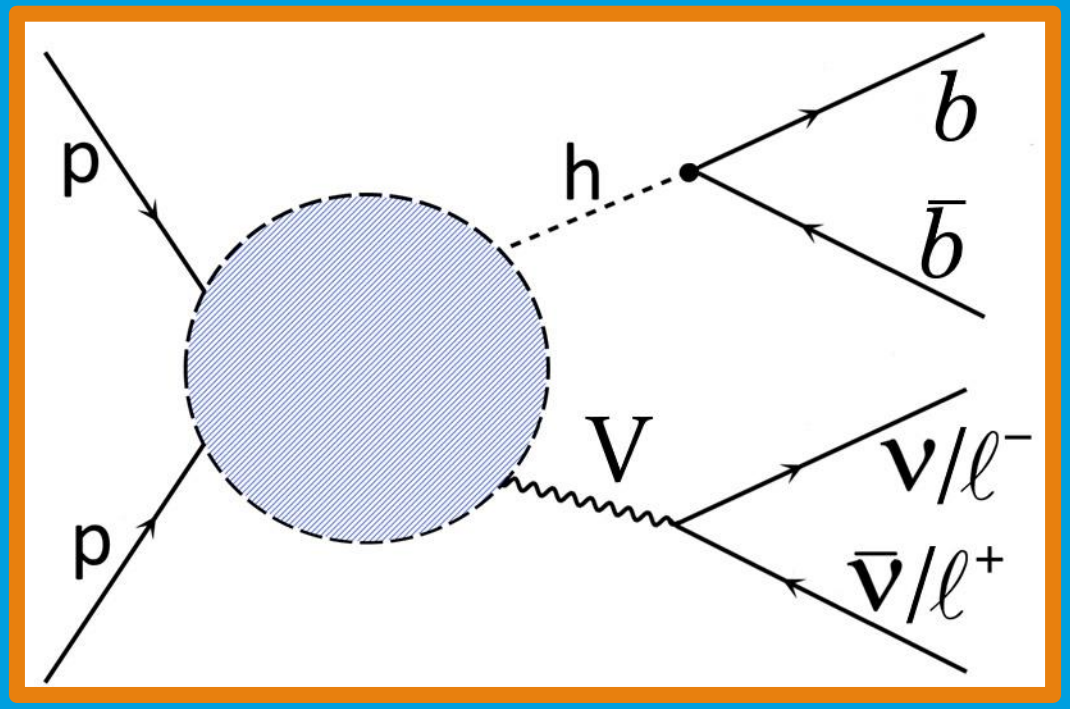

$$pp \to Vh \to \ell(\nu)\ell(\nu)b\bar{b}$$

Vh. Combining regimes

Boosted

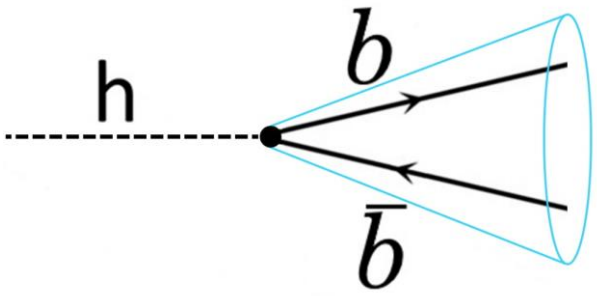

ATLAS, 2008.02508

DOI: 10.1016/j.physletb.2021.136204 28th April 2021

Measurement of the associated production of a Higgs boson decaying into b-quarks with a vector boson at high transverse momentum in pp collisions at $\sqrt{s} = 13$ TeV with the ATLAS detector

The ATLAS Collaboration

(Not the same as ATLAS-CONF-2021-051!!)

Scale-invariant tagging

Gouzevitch et al, 1303.6636
Bishara et al, 1611.03860

With use of Mass-drop tagging

Butterworth et al, 0802.2470

Resolved

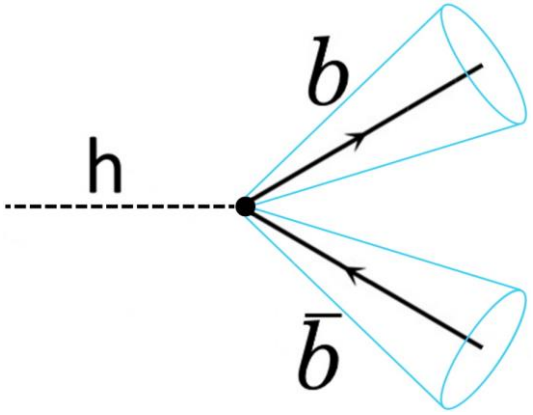

ATLAS, 2007.02873

DOI: 10.1140/epjc/s10052-020-08677-2 9th March 2021

Measurements of WH and ZH production in the $H \to b\bar{b}$ decay channel in pp collisions at 13 TeV with the ATLAS detector

The ATLAS Collaboration

Adding Resolved category: 10-17% improvement at LHC.

+Projections for FCC-hh based on CDR

Vh. Direct comparison LHC vs FCC-hh

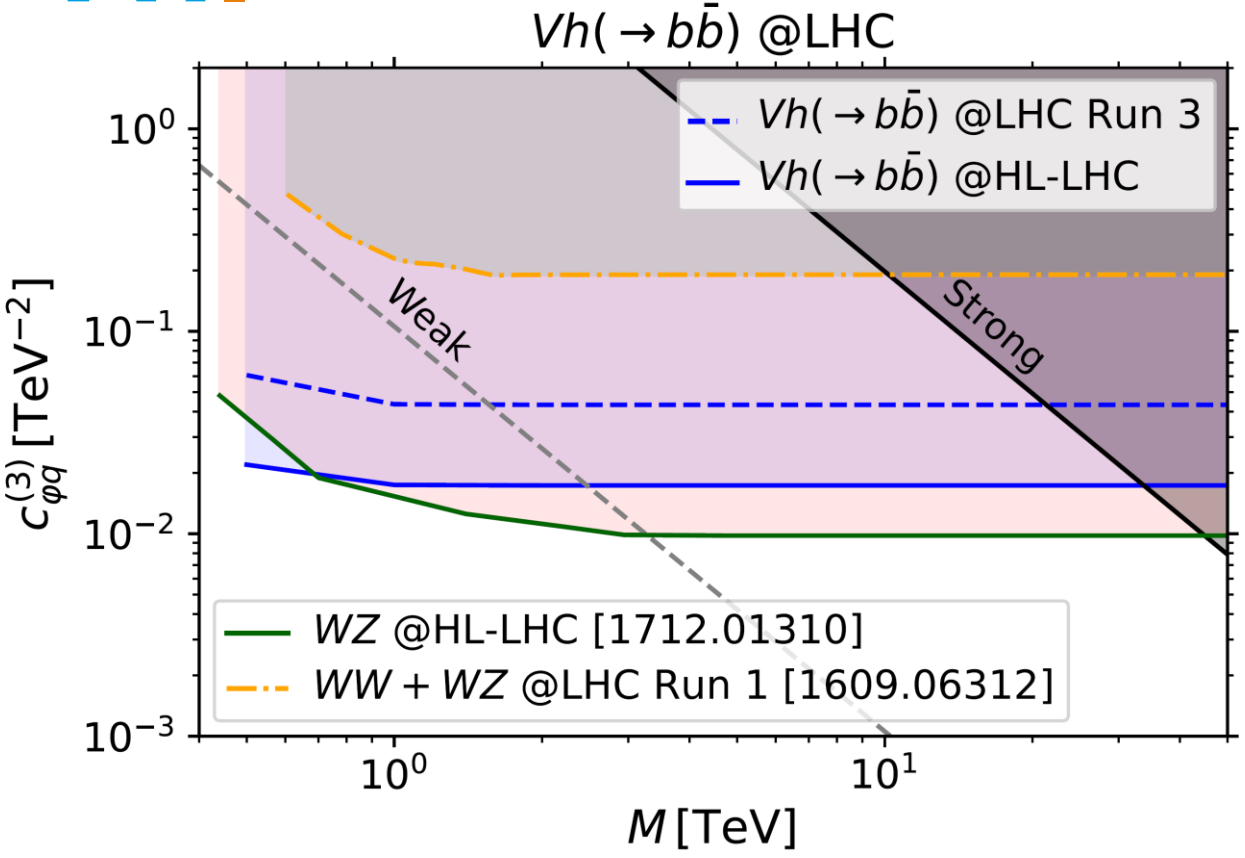

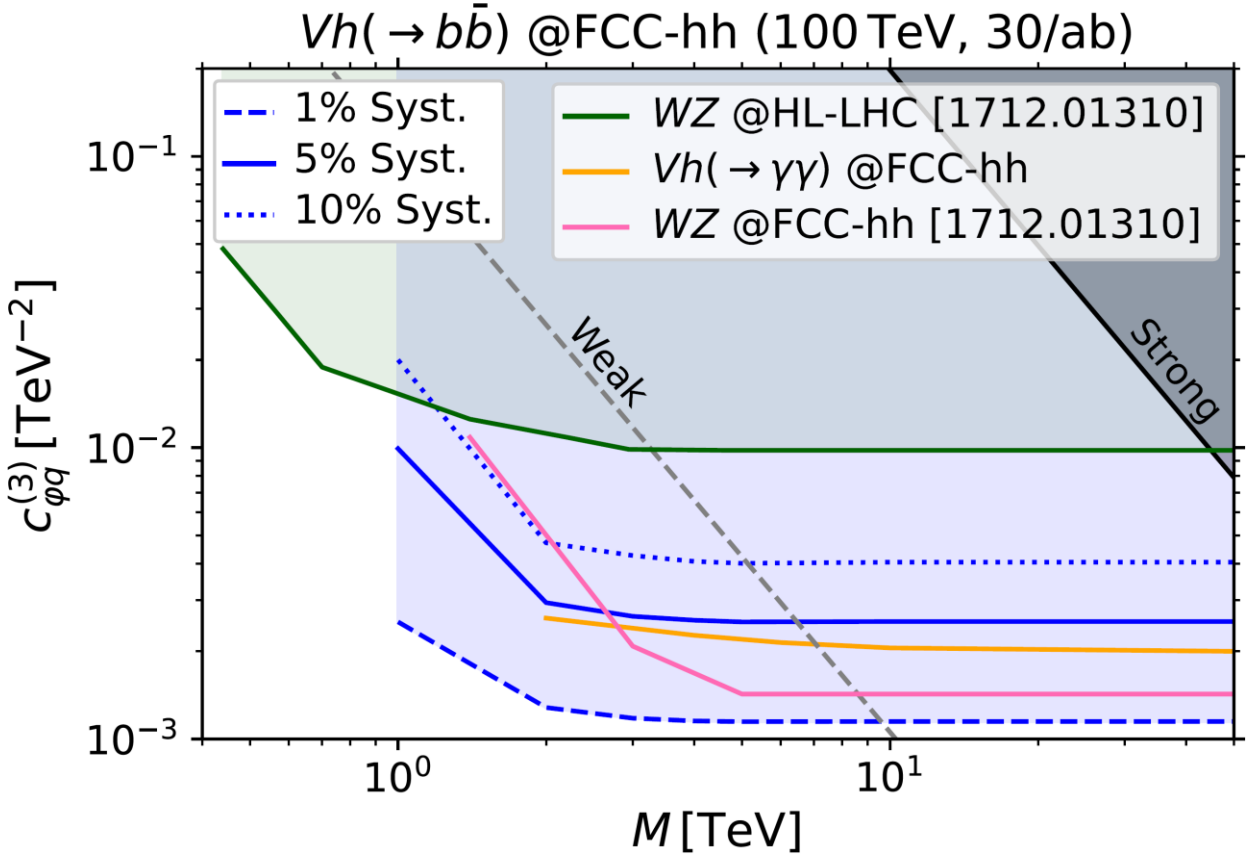

LHC Run 3 → (~2x) **HL-LHC** → (~5x) **FCC-hh**

LHC Run 3 is limited by statistics

$(h \to)\ \gamma\gamma \approx b\bar{b}$ @FCC-hh

Vh. Rapidity binning effects.

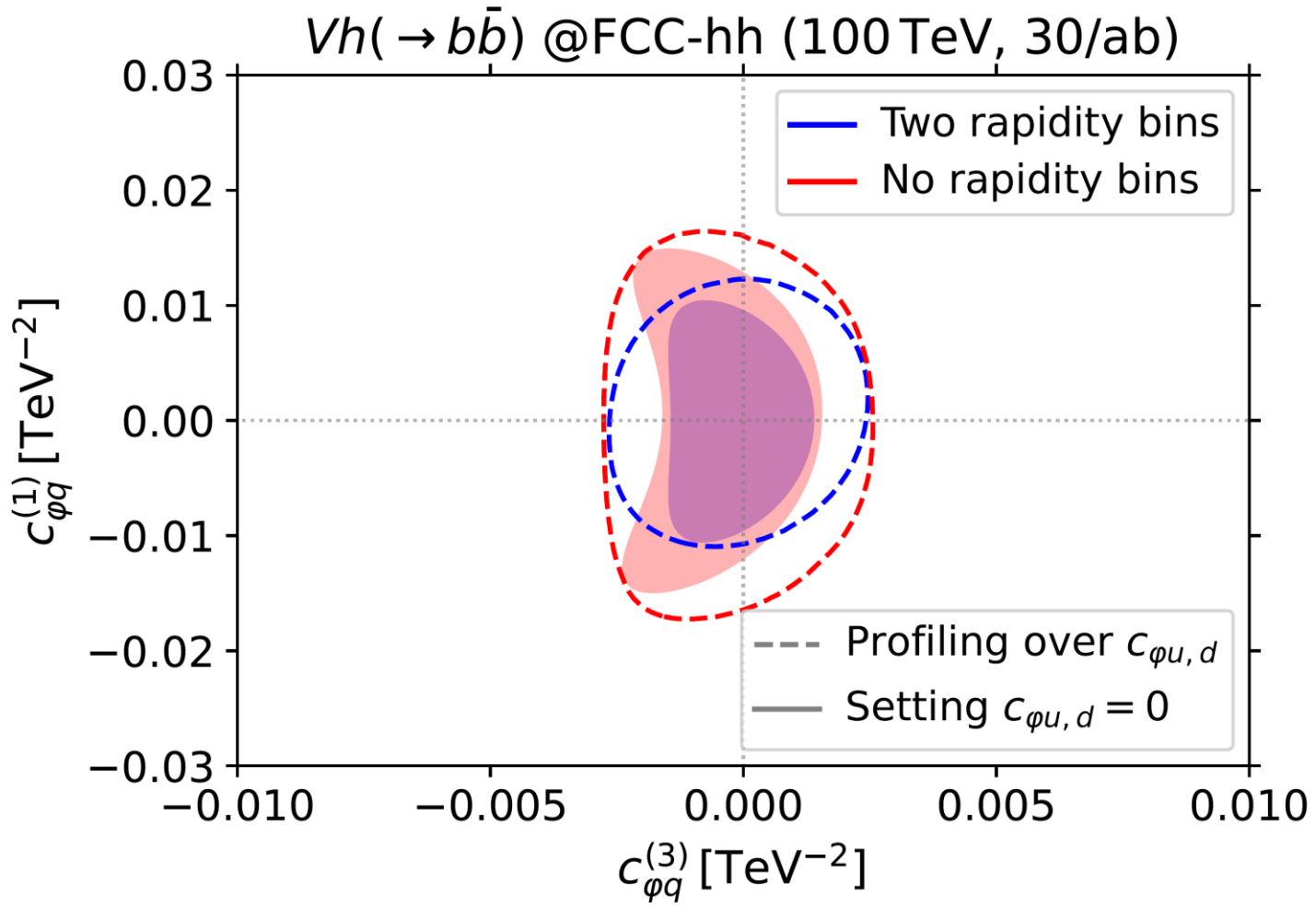

Significant impact on $\mathcal{O}_{\varphi q}^{(1)}$ due to the lift of the cancellation.

Conclusions

- $(W, Z)\, h$ is an interesting diboson channel that probes several operators.
- A simple p_T binning yields competitive sensitivity to $\mathcal{O}_{\varphi q}^{(3)}$.
- $h \to b\bar{b}$ allows to perform these studies at (HL-)LHC, but with limitations.
- $h \to \gamma\gamma$ will become available at FCC-hh, opening new possibilities.
- In Wh , a binning in ϕ_W gives an observable linear in $\mathcal{O}_{\varphi \widetilde{W}}$.
- In Zh, a binning in rapidity improves the sensitivity to $\mathcal{O}_{\varphi q}^{(1)}$.
- At FCC-hh, $h \to \gamma\gamma$ and $h \to b\bar{b}$ achieve similar results in different ways.
- Wh and Zh with are not exploration channels, but important to probe different directions.

Thank you for your attention

Contact

www.manchester.ac.uk

Alejo N. Rossia
HEP Theory Group – Dept. Of Physics and Astronomy
E-mail: alejo dot rossia at manchester dot ac dot uk
http://www.hep.man.ac.uk/

Appendix.

For even more details, read our papers or contact us.

Wh.

Signal

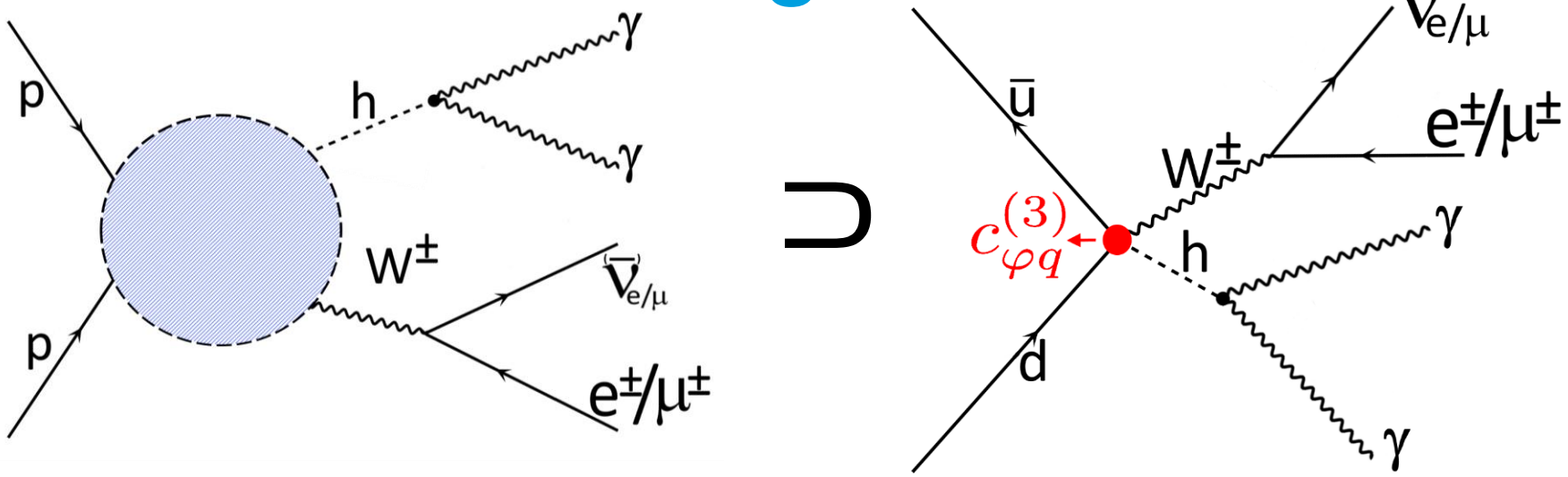

Background

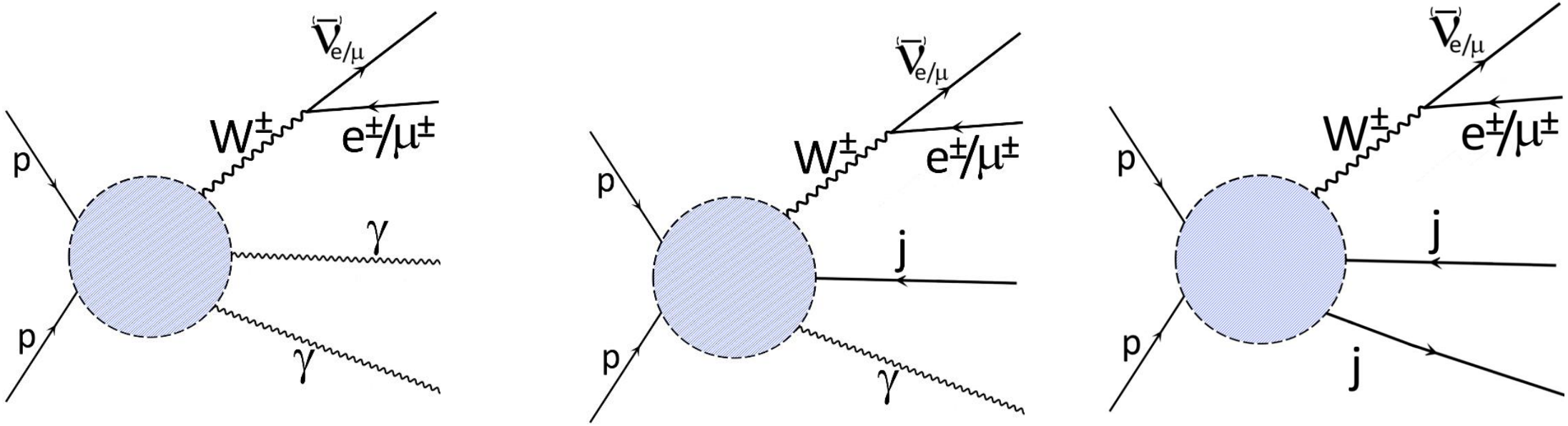

Wh. Simulation details

- Montecarlo generation: Madgraph5_aMC@NLO v.2.6.5; showering: Pythia 8.2; detector simulation: Delphes v.3.4.1 with FCC-hh card.
- Signal and $W\gamma\gamma$ simulated at FO, the rest simulated at LO. QED k-factor for the signal.
- Parton level generation cuts:

	Wh	$W\gamma\gamma$	$Wj\gamma$ and Wjj
$p^{\ell}_{T,\mathrm{min}}$ [GeV]		30 (all samples)	
$p^{\gamma,j}_{T,\mathrm{min}}$ [GeV]		50 (all samples)	
$\not{E}_{T,\mathrm{min}}$ [GeV]		100 (all samples)	
$\lvert\eta^{j,\ell}_{\mathrm{max}}\rvert$		6.1 (all samples)	
$\Delta R^{\gamma\gamma,\gamma j,\gamma\ell}_{\mathrm{min}}$	–	0.01	0.01
$\Delta R^{\gamma\gamma,\gamma j,jj}_{\mathrm{max}}$	–	2.5	2
$m^{\gamma\gamma,\gamma j,jj}$ [GeV]	–	[50,300]	[50,250]
$p^{h,\gamma\gamma}_{T,\mathrm{min}}$ [GeV]	{150,350,550,750}	{100,300,500,700}	–
$p^{\ell\nu}_{T,\mathrm{min}}$ [GeV]	–	–	{100,300,500,700}

Wh. Analysis details

- Selection cuts and cutflow in the third p_T^h bin:

	Selection cuts
$p_{T,\min}^{\ell}$ [GeV]	30
$p_{T,\min}^{\gamma}$ [GeV]	50
$\not{E}_{T,\,\min}$ [GeV]	100
$m_{\gamma\gamma}$ [GeV]	$[120, 130]$
$\Delta R_{\max}^{\gamma\gamma}$	$\{1.3, 0.9, 0.75, 0.6, 0.6\}$
$p_{T,\max}^{Wh}$ [GeV]	$\{300, 500, 700, 900, 900\}$

Selection cuts / efficiency	$\xi^{(3)}_{h\to\gamma\gamma}$	$\xi^{(3)}_{\gamma\gamma}$	$\xi^{(3)}_{j\gamma}$	$\xi^{(3)}_{jj}$
$\geq 1\ell^{\pm}$ with $p_T > 30$ GeV	0.86	0.46	0.94	0.94
$\geq 2\gamma$ each with $p_T > 50$ GeV	0.50	0.18	$5.7 \cdot 10^{-3}$	$8.7 \cdot 10^{-7}$
$\not{E}_T > 100\,\text{GeV}$	0.49	0.16	$5.1 \cdot 10^{-3}$	$8.5 \cdot 10^{-7}$
$120\,\text{GeV} < m_{\gamma\gamma} < 130\,\text{GeV}$	0.46	$6 \cdot 10^{-3}$	$2 \cdot 10^{-4}$	$8.2 \cdot 10^{-8}$
$\Delta R^{\gamma\gamma} < \Delta R_{max}$	0.45	$4 \cdot 10^{-3}$	$3.1 \cdot 10^{-5}$	$6.4 \cdot 10^{-8}$
$p_T^{Wh} < p_{T,max}^{Wh}$	0.41	$7 \cdot 10^{-4}$	$1.1 \cdot 10^{-5}$	$4.7 \cdot 10^{-8}$

Wh. How big is the background?

- Events per bin for the relevant processes

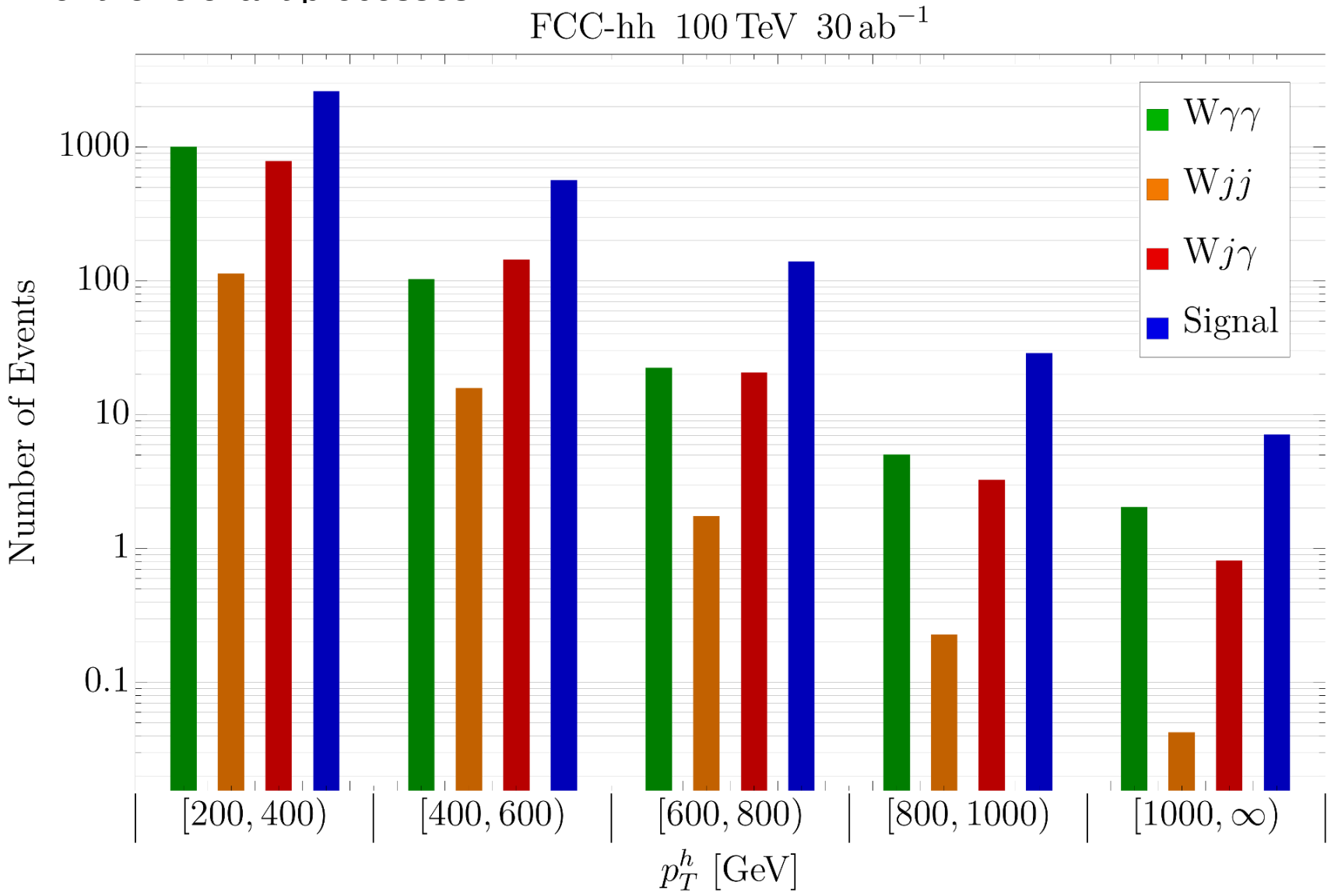

Wh.

More results

- 95% CL bounds

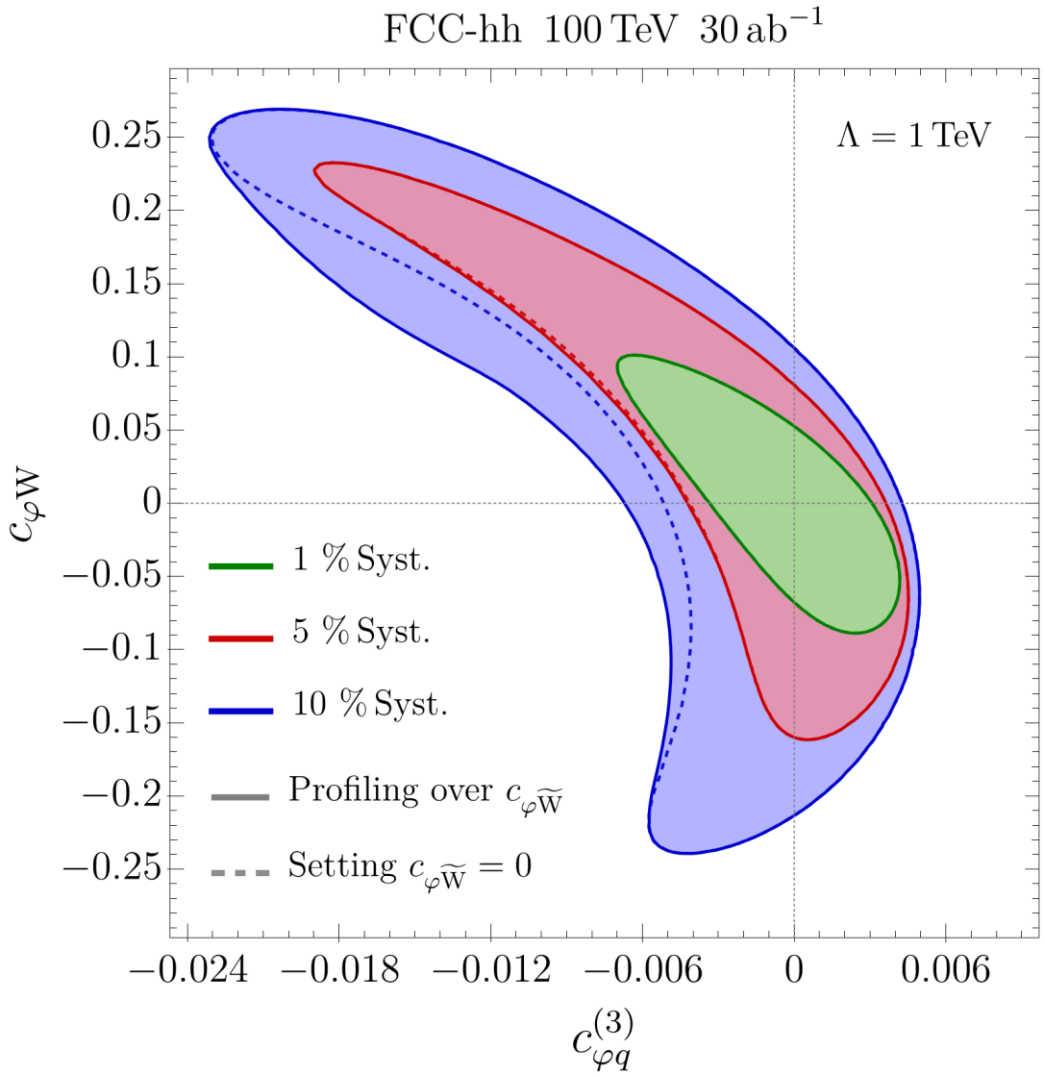

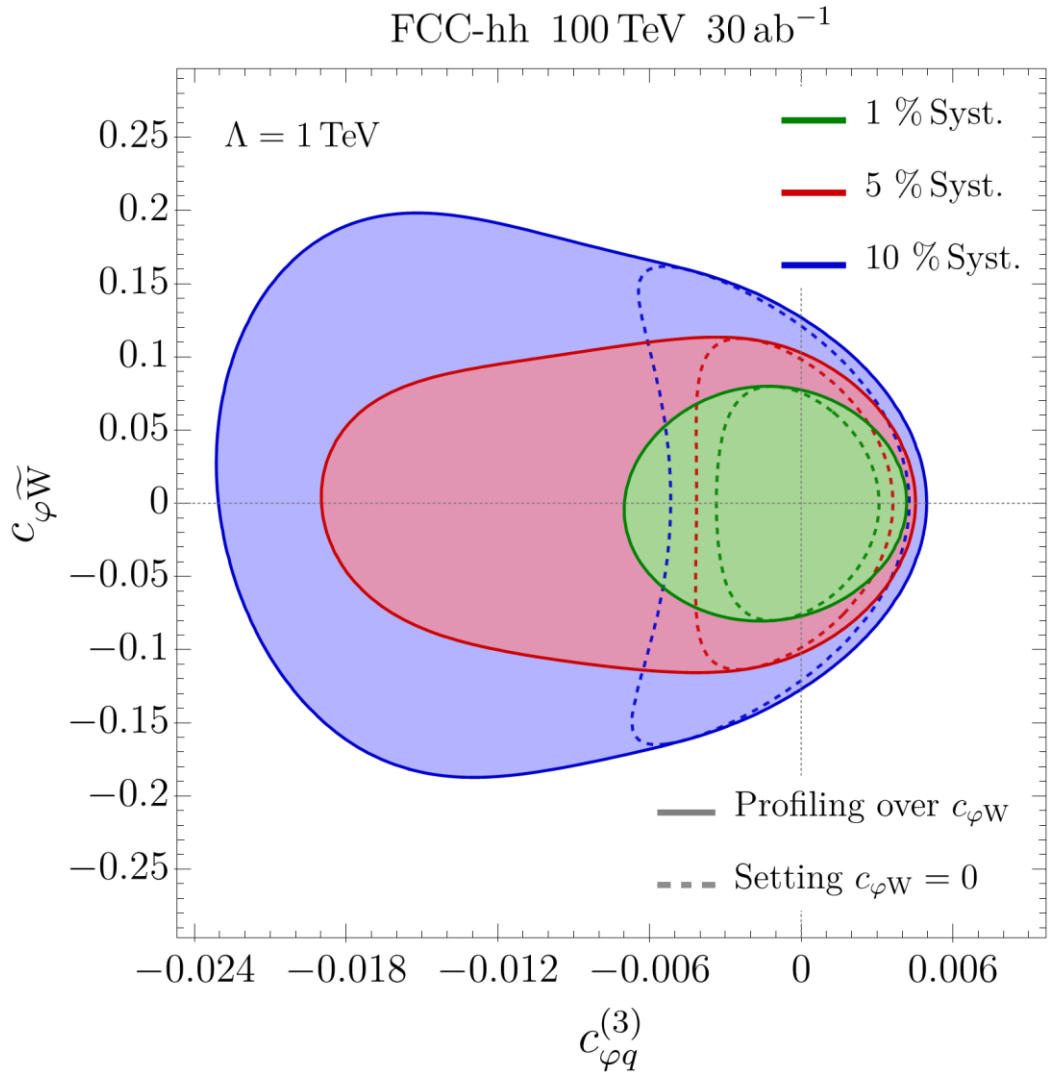

Wh.

More results

- 95% CL bounds summary

Coefficient	Profiled Fit		One Operator Fit	
$c_{\varphi q}^{(3)}$	$[-5.1, 3.4] \times 10^{-3}$	1% syst.	$[-2.7, 2.5] \times 10^{-3}$	1% syst.
	$[-11.6, 3.8] \times 10^{-3}$	5% syst.	$[-3.3, 2.9] \times 10^{-3}$	5% syst.
	$[-20.6, 4.1] \times 10^{-3}$	10% syst.	$[-4.0, 3.5] \times 10^{-3}$	10% syst.
$c_{\varphi \mathrm{W}}$	$[-7.1, 7.9] \times 10^{-2}$	1% syst.	$[-5.3, 4.3] \times 10^{-2}$	1% syst.
	$[-13.0, 17.5] \times 10^{-2}$	5% syst.	$[-12.1, 6.8] \times 10^{-2}$	5% syst.
	$[-20.0, 25.2] \times 10^{-2}$	10% syst.	$[-18.8, 9.0] \times 10^{-2}$	10% syst.
$c_{\varphi \widetilde{\mathrm{W}}}$	$[-6.4, 6.4] \times 10^{-2}$	1% syst.	$[-6.1, 6.1] \times 10^{-2}$	1% syst.
	$[-9.0, 8.8] \times 10^{-2}$	5% syst.	$[-8.1, 8.1] \times 10^{-2}$	5% syst.
	$[-13.5, 14.2] \times 10^{-2}$	10% syst.	$[-10.1, 10.1] \times 10^{-2}$	10% syst.

Simulation details

- Montecarlo generation: Madgraph5_aMC@NLO v.2.7.3; showering: Pythia 8.2; detector simulation: Delphes v.3.4.1 with FCC-hh card. SMEFT@NLO UFO (http://feynrules.irmp.ucl.ac.be/wiki/SMEFTatNLO)
- Signal simulated at LO and corrected to (QCD+QED) NLO with k-factors. Gluon initiated processes simulated at LO. The rest simulated at QCD NLO.
- Parton level generation cuts:

Cut	Channel	
	$Z \to \nu\bar{\nu}$	$Z \to l^+l^-$
$p_{T,\min}^{j}$ [GeV]	30	
$p_{T,\min}^{\gamma}$ [GeV]	50	
$p_{T,\min}^{l}$	0	30 (only for LO samples)
$\lvert\eta_{max}^{\gamma,j}\rvert$	6.1^{1}	
$\lvert\eta_{max}^{l}\rvert$	∞	6.1
$\Delta R^{\ell,\gamma l}$	0.01	
$\Delta R^{\gamma\gamma}$	0.25 (0.01 for LO samples)	
$p_T^{V,j}$	$\{0, 200, 400, 600, 800, 1200, \infty\}$	

Zh. Analysis details

- Selection cuts and binning:

$Z \to \nu\bar{\nu}$		$Z \to l^-l^+$
Bins of $\lvert y^h \rvert$	Bins of $min\{p_T^h, p_T^Z\}$	Bins of $\lvert y^{Zh} \rvert$
$[0, 2), [2, 6]$	$[200, 400)$	$[0, 2), [2, 6]$
	$[400, 600)$	
$[0, 1.5), [1.5, 6]$	$[600, 800)$	
$[0, 1), [1, 6]$	$[800, 1000)$	
	$[1000, \infty)$	

	Selection cuts
$p_{T,\min}^{\ell}$ [GeV]	30
$p_{T,\min}^{\gamma}$ [GeV]	50
$m_{\gamma\gamma}$ [GeV]	$[120, 130]$
$m_{l^+l^-}$ [GeV]	$[81, 101]$
$\Delta R_{\max}^{\gamma\gamma}$	$\{1.3, 0.9, 0.75, 0.6, 0.6\}$
$\Delta R_{\max}^{l^+l^-}$	$\{1.2, 0.8, 0.6, 0.5, 0.4\}$
$p_{T,\max}^{Zh}$ [GeV]	$\{200, 600, 1100, 1500, 1900\}$

- K-factors for signal in 1+QCD+QED format

p_{Tmin} bin [GeV]	$Zh \to \ell\ell\gamma\gamma$	$Zh \to \nu\nu\gamma\gamma$	$Wh \to \nu\ell\gamma\gamma$
$0 - 200$	$1 + 0.59 - 0.07 = 1.52$	$1 + 0.26 - 0.06 = 1.20$	$1 + 0.17 - 0.04 = 1.13$
$200 - 400$	$1 + 0.52 - 0.09 = 1.43$	$1 + 0.31 - 0.09 = 1.22$	$1 + 0.28 - 0.09 = 1.19$
$400 - 600$	$1 + 0.64 - 0.14 = 1.50$	$1 + 0.37 - 0.14 = 1.23$	$1 + 0.28 - 0.17 = 1.11$
$600 - 800$	$1 + 0.69 - 0.18 = 1.51$	$1 + 0.40 - 0.18 = 1.22$	$1 + 0.35 - 0.24 = 1.11$
$800 - 1000$	$1 + 0.70 - 0.24 = 1.46$	$1 + 0.40 - 0.24 = 1.16$	$1 + 0.39 - 0.32 = 1.07$
$1000 - \infty$	$1 + 0.69 - 0.32 = 1.37$	$1 + 0.40 - 0.32 = 1.08$	$1 + 0.36 - 0.40 = 0.96$

Zh.

Analysis details

- Cutflows

Cuts / Efficiency	$q\bar{q} \to Zh$	Wh	$W\gamma\gamma$	$Z\gamma\gamma$	$gg \to Zh$
$0\ \ell^{\pm}$ in acc. region	1	0.30	0.44	1	0.97
$\geq 2\,\gamma$ in acc. region	0.60	0.19	0.30	0.72	0.60
$m_{\gamma\gamma} \in [120, 130]$ GeV	0.58	0.17	7.7×10^{-3}	1.3×10^{-2}	0.59
$p_{T,\mathrm{min}} \geq 400$ GeV	0.42	0.061	6.9×10^{-4}	2.9×10^{-3}	0.37
$p_T^{Zh} \leq p_{T,max}^{Zh}$	0.40	0.057	1.1×10^{-4}	2.8×10^{-3}	0.33

Cuts / Efficiency	$q\bar{q} \to Zh \to \ell^+\ell^-\gamma\gamma$	$Z\gamma\gamma \to \ell^+\ell^-\gamma\gamma$	$gg \to Zh \to \ell^+\ell^-\gamma\gamma$
$2\ \ell^{\pm}$ in acc. region	0.85	0.74	0.75
$\geq 2\,\gamma$ in acc. region	0.51	0.54	0.46
$m_{\gamma\gamma} \in [120, 130]$ GeV	0.50	9.4×10^{-3}	0.45
$m_{l^+l^-} \in [81, 101]$ GeV	0.47	8.8×10^{-3}	0.42
$p_{T,\mathrm{min}} \geq 400$ GeV	0.35	2.2×10^{-3}	0.26
$p_T^{Zh} \leq p_{T,max}^{Zh}$	0.33	2.1×10^{-3}	0.23

Zh.

Signal and background

- Wh is part of the signal because it is affected by $\boldsymbol{\sigma^{(3)}_{\varphi q}}$.

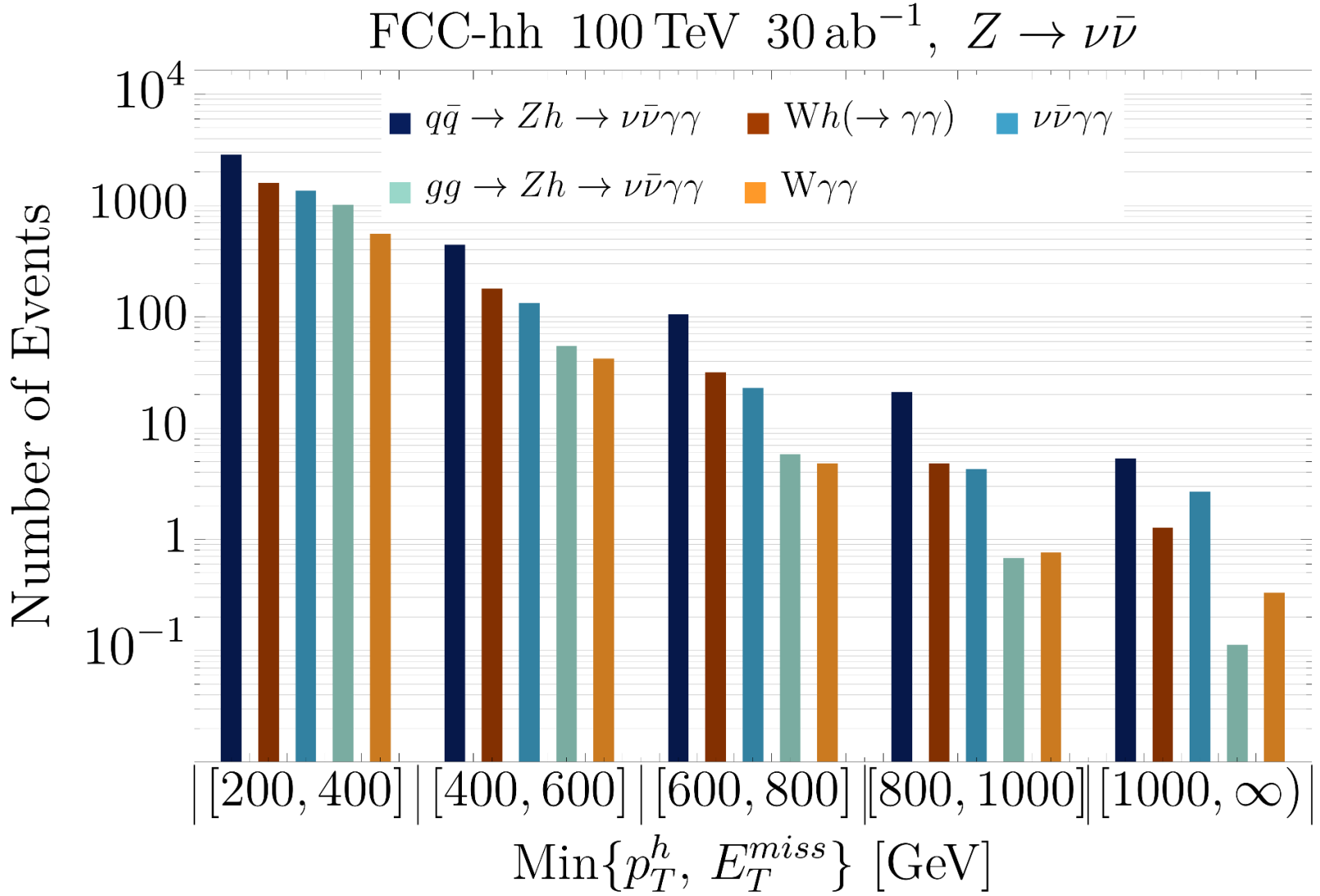

More results

- Events per bin for the relevant processes in the leptonic channel.

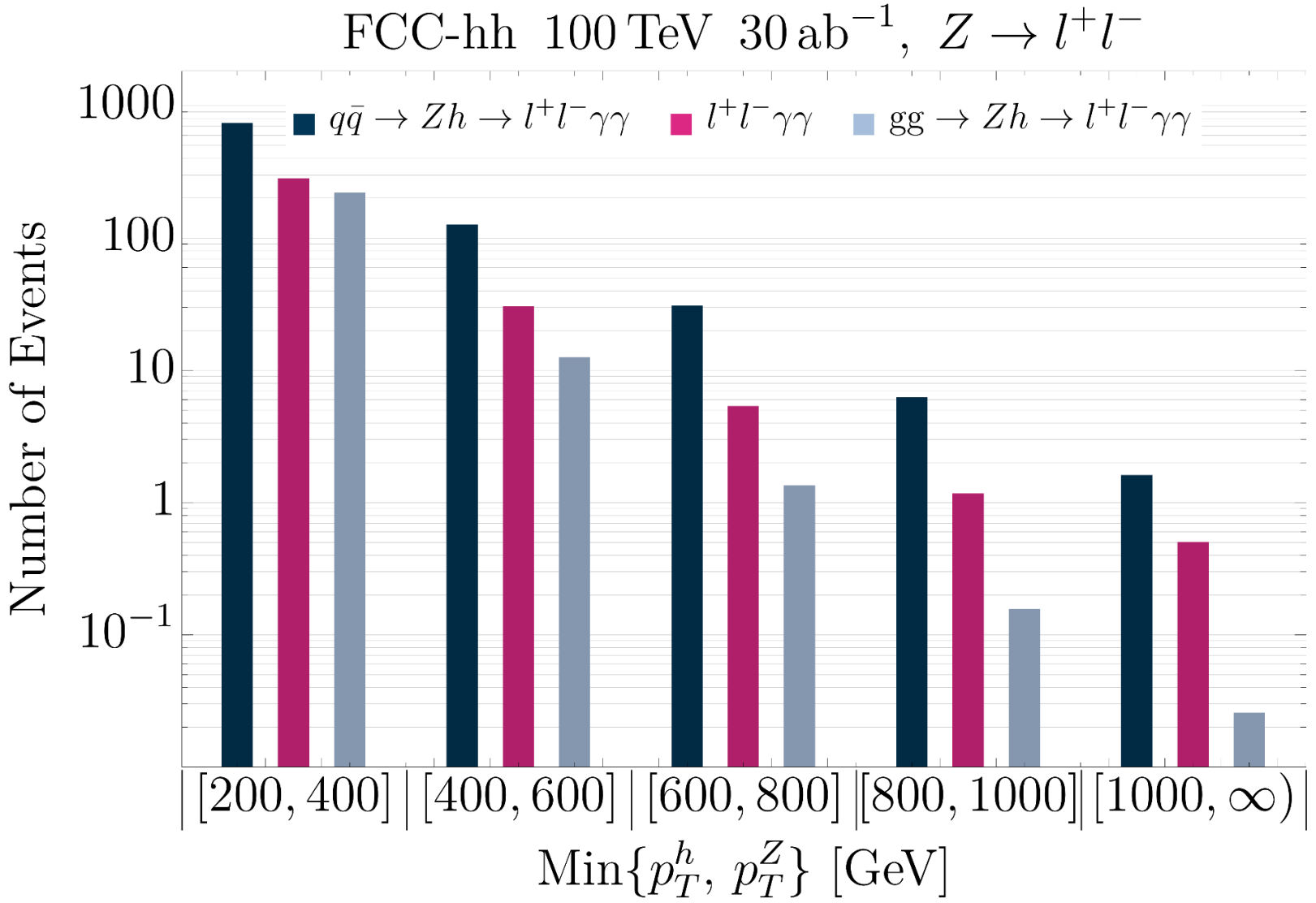

Zh.

More results

- 95% CL bounds

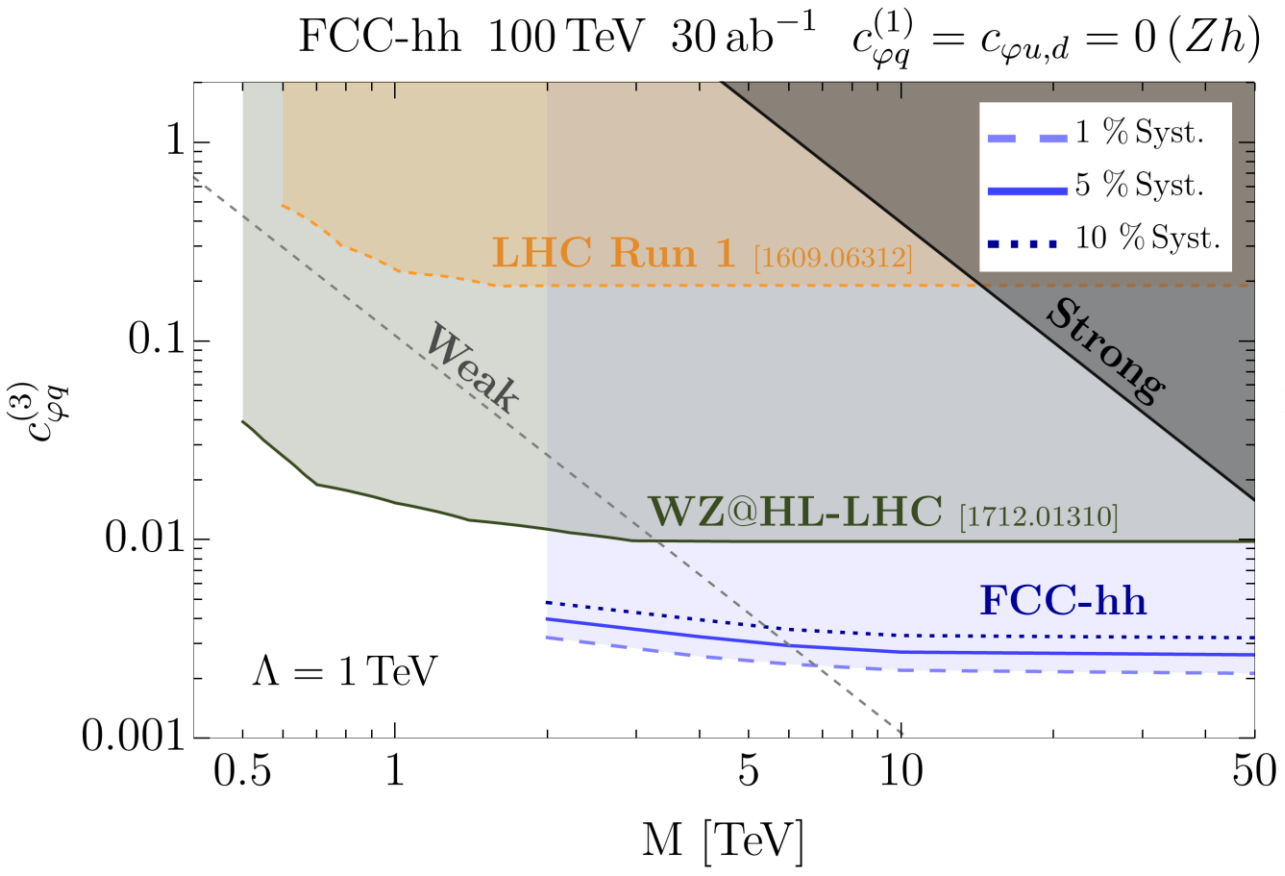

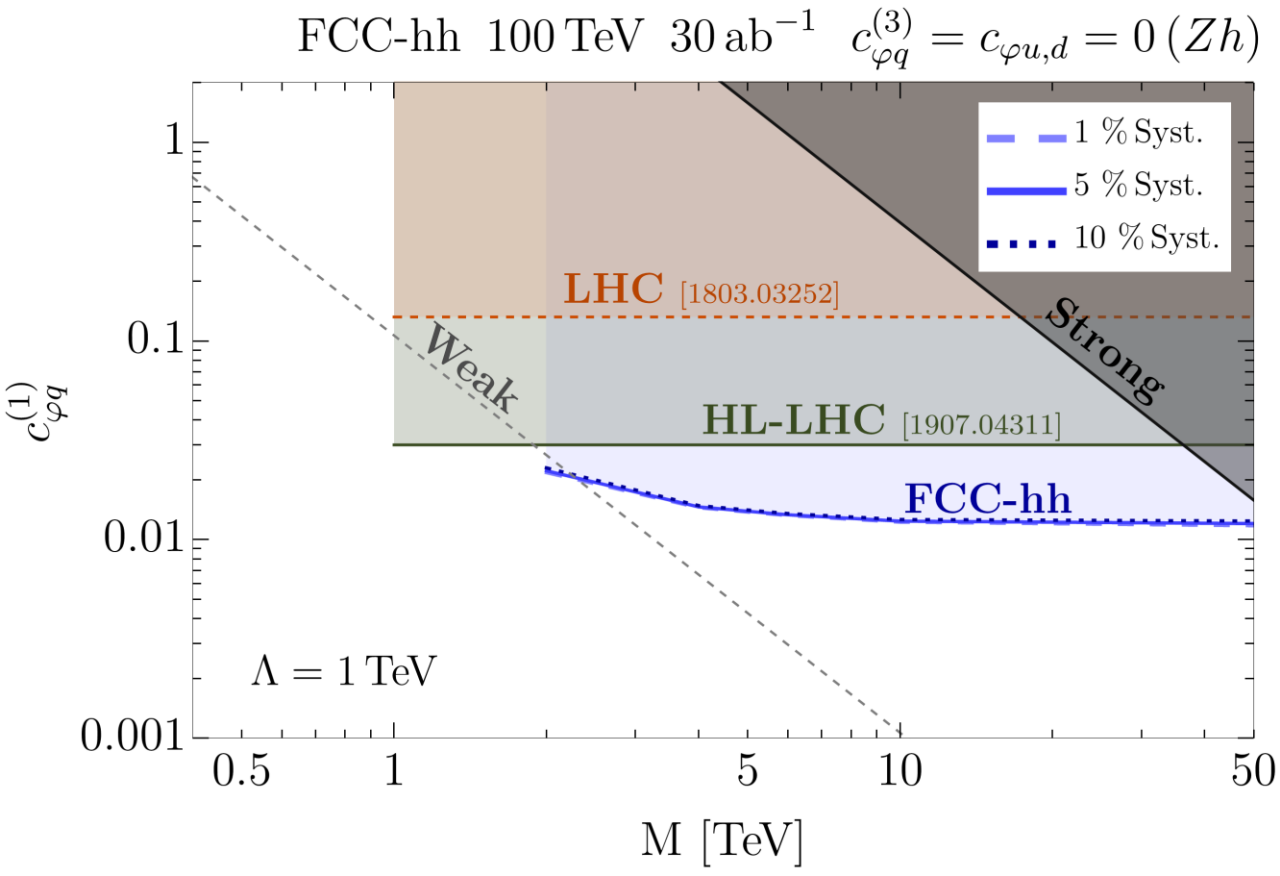

More results

- 95% CL bounds summary

Coefficient	Profiled Fit		One Operator Fit	
$c_{\varphi q}^{(3)}$	$[-5.2, 3.1] \times 10^{-3}$	1% syst.	$[-2.1, 2.0] \times 10^{-3}$	1% syst.
	$[-6.7, 3.3] \times 10^{-3}$	5% syst.	$[-2.6, 2.4] \times 10^{-3}$	5% syst.
	$[-8.2, 3.7] \times 10^{-3}$	10% syst.	$[-3.2, 2.8] \times 10^{-3}$	10% syst.
$c_{\varphi q}^{(3)}$ $(+Wh)$	$[-2.5, 2.1] \times 10^{-3}$	1% syst.	$[-1.6, 1.6] \times 10^{-3}$	1% syst.
	$[-3.0, 2.4] \times 10^{-3}$	5% syst.	$[-2.0, 1.9] \times 10^{-3}$	5% syst.
	$[-3.7, 2.7] \times 10^{-3}$	10% syst.	$[-2.4, 2.2] \times 10^{-3}$	10% syst.
$c_{\varphi q}^{(1)}$	$[-1.3, 1.4] \times 10^{-2}$	1% syst.	$[-1.1, 1.15] \times 10^{-2}$	1% syst.
	$[-1.5, 1.5] \times 10^{-2}$	5% syst.	$[-1.1, 1.2] \times 10^{-2}$	5% syst.
	$[-1.6, 1.5] \times 10^{-2}$	10% syst.	$[-1.2, 1.2] \times 10^{-2}$	10% syst.
$c_{\varphi u}$	$[-2.0, 1.6] \times 10^{-2}$	1% syst.	$[-1.9, 0.89] \times 10^{-2}$	1% syst.
	$[-2.1, 1.7] \times 10^{-2}$	5% syst.	$[-2.1, 0.96] \times 10^{-2}$	5% syst.
	$[-2.2, 1.8] \times 10^{-2}$	10% syst.	$[-2.2, 1.0] \times 10^{-2}$	10% syst.
$c_{\varphi d}$	$[-2.1, 2.3] \times 10^{-2}$	1% syst.	$[-1.4, 2.2] \times 10^{-2}$	1% syst.
	$[-2.2, 2.4] \times 10^{-2}$	5% syst.	$[-1.5, 2.2] \times 10^{-2}$	5% syst.
	$[-2.3, 2.5] \times 10^{-2}$	10% syst.	$[-1.5, 2.2] \times 10^{-2}$	10% syst.

Vh. UV models: Spin-1 triplets

$L_\mu \sim (1,3)_0$

$$\mathcal{L}_{BSM} = \frac{1}{4}F^a_{L,\mu\nu}F^{a,\mu\nu}_L + \frac{m_L^2}{2}L_\mu L^\mu + \gamma_H L^a_\mu \frac{i}{2}H^\dagger\sigma^a \overleftrightarrow{D}^\mu H + \sum_f \gamma_f L^a_\mu \bar{f}\gamma^\mu\sigma^a f$$

$$c^{(3)}_{\varphi q} = -\frac{\gamma_H\gamma_q}{2m_L^2}$$

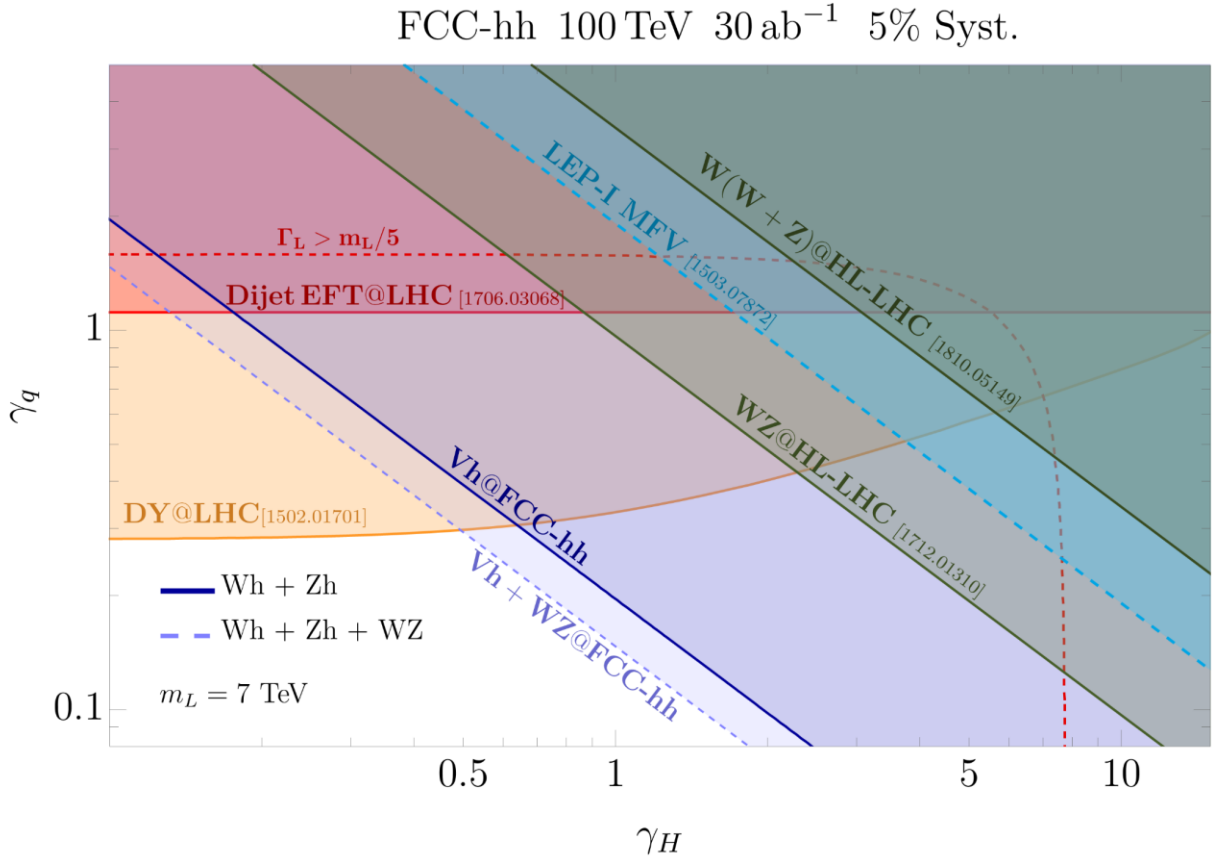

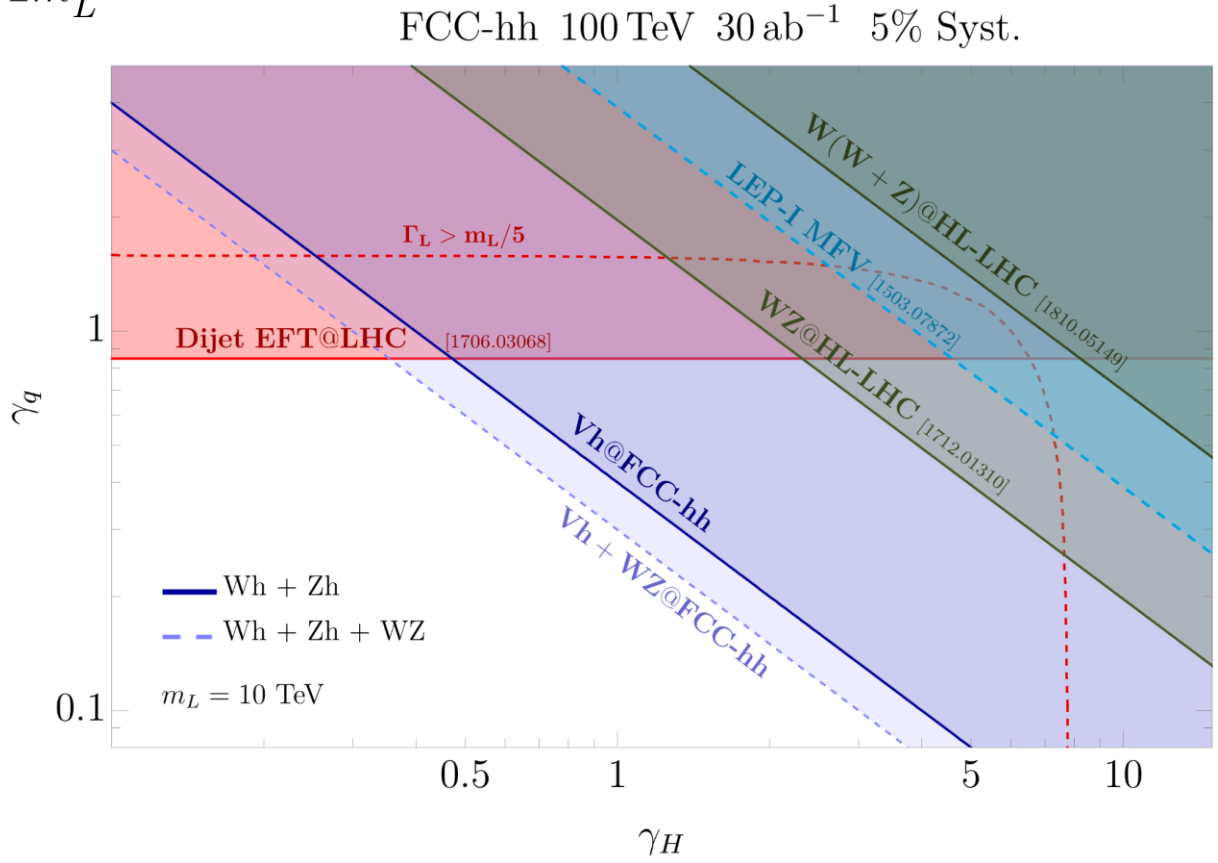

Preliminary results with scale-invariant b-tagging

- 95% CL bounds on aTGCs for Universal Theories.

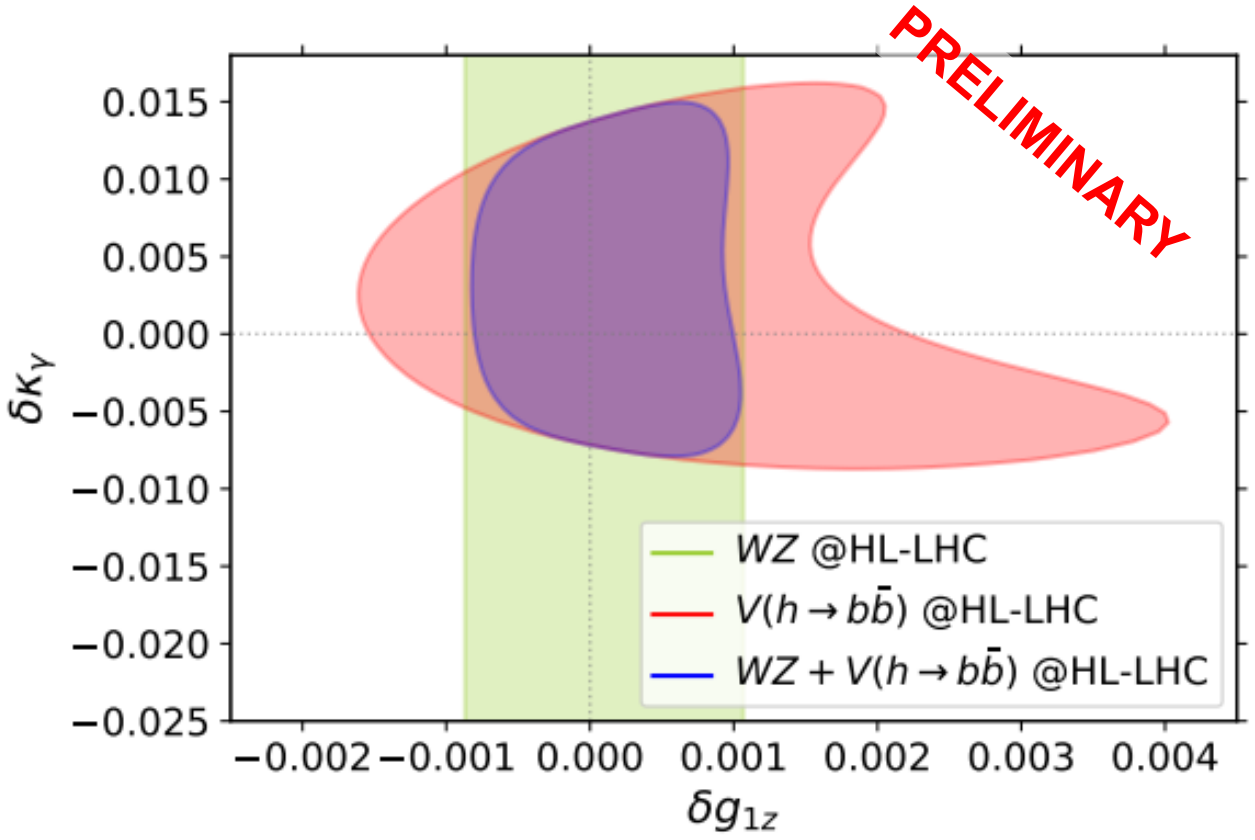

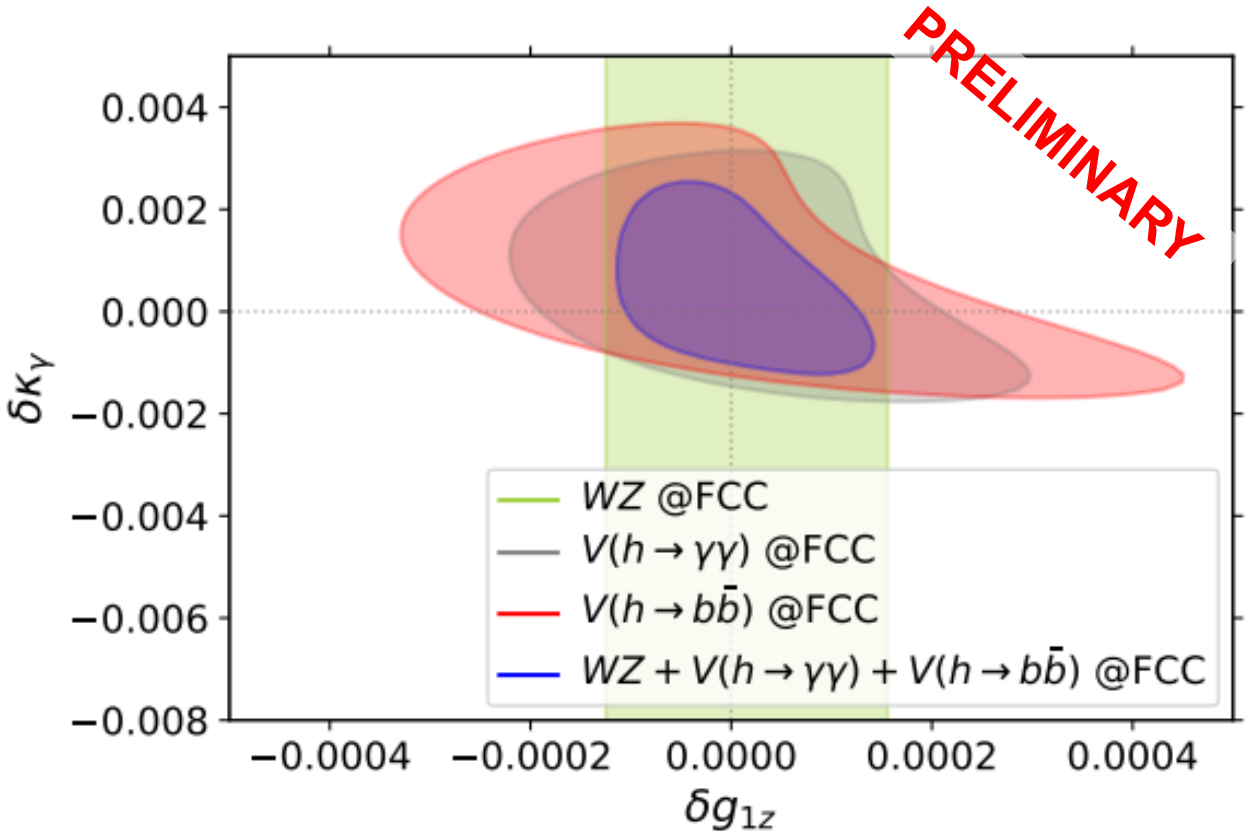

Vh. Future experiments timeline

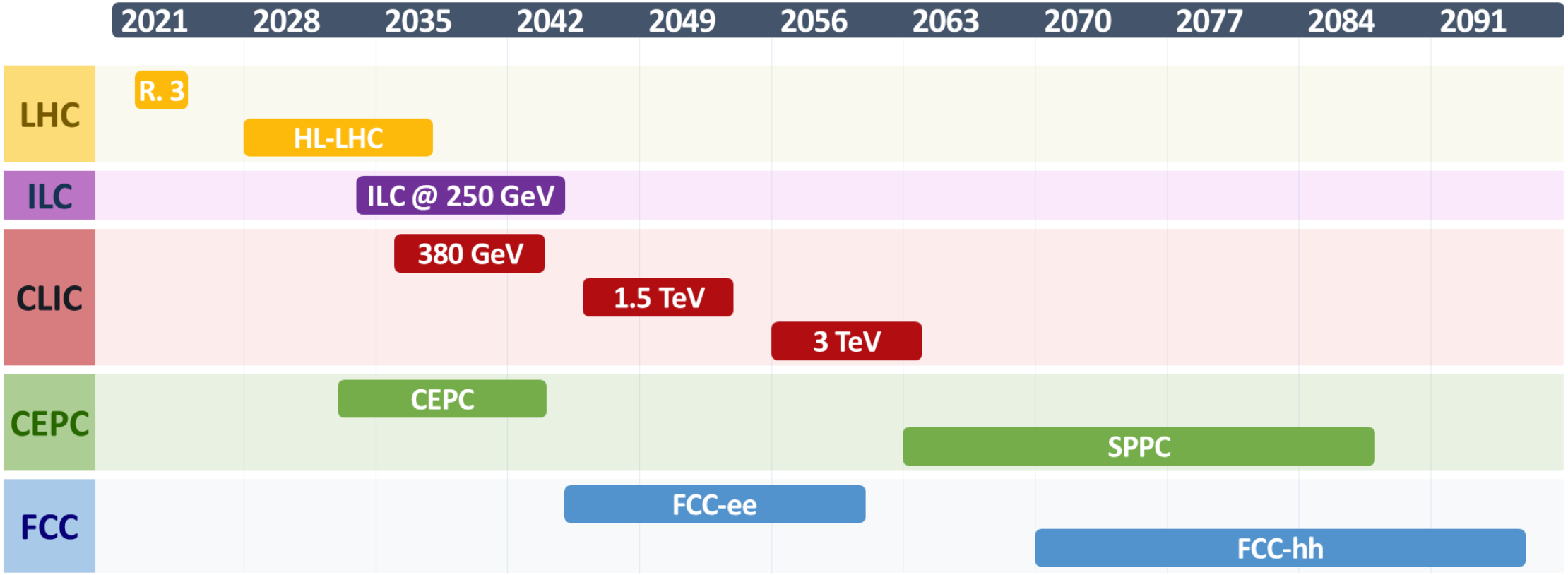

Vh.

Tagging algorithm

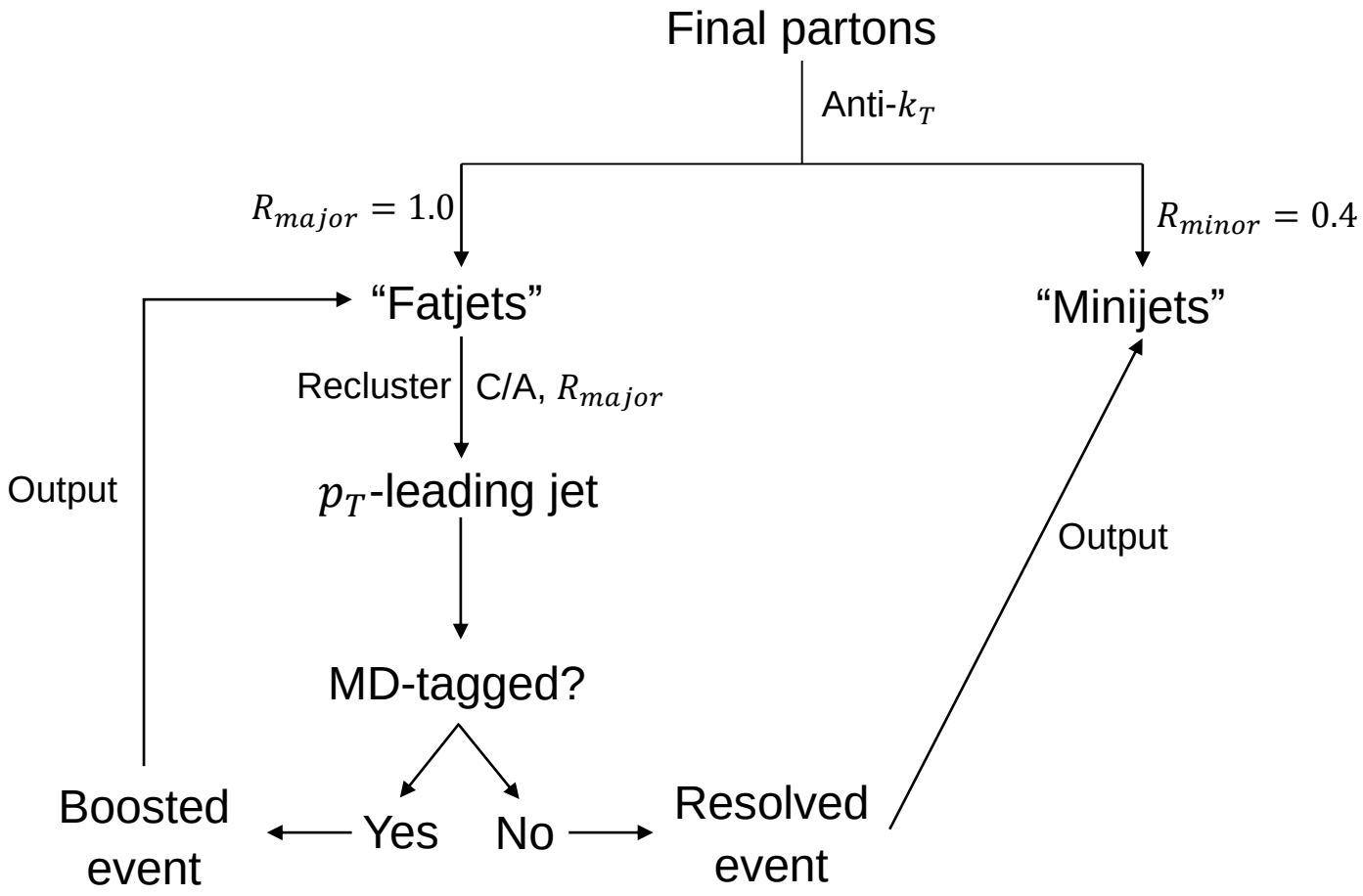

Vh. (b-)Tagging algorithm

$\exists\ (b, c, j)$ final parton within $\Delta R \leq R_{minor}$ of Minijet → b –tag for Minijet with prob. $eff_{(b,c,j)}^{LHC/FCC}$

For Boosted events

+1 b-tag for MDT jet per b-tagged Minijet within $\Delta R \leq 0.2$

Enough for Resolved events

$$\text{eff}_b^{\text{LHC}} = \begin{cases} 0 & \text{if } p_T \leq 20\,\text{GeV or } |\eta| > 2.5 \\ 0.8\tanh(0.003 p_T)\frac{30}{1+0.086 p_T} & \text{else} \end{cases}$$

$$\text{eff}_c^{\text{LHC}} = \begin{cases} 0 & \text{if } p_T \leq 20\,\text{GeV or } |\eta| > 2.5 \\ 0.2\tanh(0.02 p_T)\frac{1}{1+0.0034 p_T} & \text{else} \end{cases}$$

$$\text{eff}_j^{\text{LHC}} = \begin{cases} 0 & \text{if } p_T \leq 20\,\text{GeV or } |\eta| > 2.5 \\ 0.002\tanh(7.3 \cdot 10^{-6} \cdot p_T) & \text{else} \end{cases}$$

$$\text{eff}_b^{\text{FCC}} = \begin{cases} 0 & \text{if } p_T \leq 20\,\text{GeV or } |\eta| > 4.5 \\ 0.85 & \text{else} \end{cases}$$

$$\text{eff}_c^{\text{FCC}} = \begin{cases} 0 & \text{if } p_T \leq 20\,\text{GeV or } |\eta| > 4.5 \\ 0.05 & \text{else} \end{cases}$$

$$\text{eff}_j^{\text{FCC}} = \begin{cases} 0 & \text{if } p_T \leq 20\,\text{GeV or } |\eta| > 4.5 \\ 0.01 & \text{else} \end{cases}$$

	Collider	Electrons		Muons		Light Jets	b-jets
		Loose	Tight	Loose	Tight		
p_T [GeV]	LHC	> 7	> 27	> 7	> 25	> 30 (> 20)	> 20
	FCC-hh	> 30		> 30		> 30	
$\lvert\eta\rvert$	LHC	< 2.5		< 2.7		< 4.5 (< 2.5)	< 2.5
	FCC-hh	< 6.0		< 6.0		< 6.0	< 4.5

Table 8: Acceptance regions for charged leptons, light non-b-tagged jets and b-tagged jets used in our analysis for LHC, HL-LHC and FCC-hh. The acceptance regions of LHC and HL-LHC are equal. In the case of light jets at LHC, the minimum p_T outside (between) the parenthesis applies to the jets that fulfill the $|\eta|$ condition outside (between) the parenthesis, see text for details. All the values were chosen following refs. [13, 14, 38]

Selection cuts	Boosted category		Resolved category	
	(HL-)LHC	FCC-hh	(HL-)LHC	FCC-hh
$p^{b}_{T,\text{min}}$ [GeV]	-		20	
$p^{b,\text{leading}}_{T,\text{min}}$ [GeV]	-		45	-
η^{b}_{max}	-		2.5	4.5
$\eta^{h_{\text{cand}}}_{\text{max}}$	2.0	4.5	-	
$\Delta R^{\text{max}}_{bb}$	-		2.0	
$E^{\text{miss}}_{T,\text{min}}$ [GeV]	$\begin{cases} 50 \text{ if } \ell = e \\ 90 \text{ if } \ell = \mu \end{cases}$	-	$\begin{cases} 30 \text{ if } \ell = e \\ 90 \text{ if } \ell = \mu \end{cases}$	-
$\lvert\Delta y(W, h_{\text{cand}})\rvert_{\text{max}}$	1.4	1.2	-	
$m_{h_{\text{cand}}}$ [GeV]	[90, 120]			

Table 10: Summary of the selection cuts in the 1-lepton category for LHC and FCC-hh analyses.

Vh.

$h \to b\bar{b}$

Selection cuts	Boosted category		Resolved category	
	(HL-)LHC	FCC-hh	(HL-)LHC	FCC-hh
$p^{b}_{T,\mathrm{min}}$ [GeV]	-		20	
$p^{b,\mathrm{leading}}_{T,\mathrm{min}}$ [GeV]	-		45	-
η^{b}_{max}	-		2.5	4.5
$\eta^{h_{\mathrm{cand}}}_{\mathrm{max}}$	2.0	4.5	-	
$\Delta R^{\mathrm{max}}_{bb}$	-		1.5	
$H_{T,\mathrm{min}}$ [GeV]	-		130	-
$\Delta\phi(E^{\mathrm{miss}}_{T}, h_{\mathrm{cand}})$	$[120°, 240°]$		$[120°, 240°]$	
$\Delta\phi(b_1, b_2)$	-		$[0, 140]°$	$[0, 110]°$
$\Delta\phi(E^{\mathrm{miss}}_{T}, b\mathrm{-jets})$	-		$[20°, 340°]$	
$E^{\mathrm{miss}}_{T,\mathrm{min}}$ [GeV]	270	-	150	-
$m_{h_{\mathrm{cand}}}$ [GeV]	$[90, 120]$			

Table 9: Summary of the selection cuts in the 0-lepton category for both LHC and FCC-hh analyses.

Vh.

$h \to b\bar{b}$

Selection cuts	Boosted category		Resolved category	
	(HL-)LHC	FCC-hh	(HL-)LHC	FCC-hh
$p_{T,\text{min}}^{b}$ [GeV]	-		20	
$p_{T,\text{min}}^{b,\text{leading}}$ [GeV]	-		45	-
η_{max}^{b}	-		2.5	4.5
$\eta_{\text{max}}^{h_{\text{cand}}}$	2.0	4.5	-	
$\Delta R_{bb}^{\text{max}}$	-		1.5	2.0
Leptons	$\exists\,\ell$ with $p_T > 27\,\text{GeV}$ and $\lvert\eta\rvert < 2.5$	-	$p_{T,\text{min}}^{\ell,\text{lead}}$=27 GeV	-
$\Delta y(Z, h_{\text{cand}})_{\text{max}}$	1.0		-	
$m_{\ell\ell}$ [GeV]	[66, 116]		[81, 101]	
max. p_T^{ℓ} imbalance	0.8	0.5	-	
$p_{T,\text{min}}^{Z,E_T^{\text{miss}}}$ [GeV]	90 if $\ell = \mu$	200	-	
$m_{h_{\text{cand}}}$ [GeV]	[90, 120]			
$p_{T,\text{min}}^{Z}$ [GeV]	200	-	-	-

Table 11: Summary of the selection cuts in the 2-lepton category for the LHC and FCC-hh analyses.

Vh.

$h \to b\bar{b}$

Cuts / Eff.	Zh		Wh		$Wb\bar{b}$		$Zb\bar{b}$		$t\bar{t}$	
	LHC	FCC	LHC	FCC	LHC	FCC	LHC	FCC	LHC	FCC
0 $\ell^{\pm}$	1	1	0.32	0.41	0.34	0.40	0.78	1	0.98	1
0 UT jets	0.37	0.22	0.036	0.019	0.02	0.009	0.12	0.061	0.011	0.022
1 MDT DBT jet	0.29	0.19	0.026	0.012	0.014	0.005	0.048	0.018	0.0018	0.0012
$\eta_{\max}^{h_{\text{cand}}}$	0.26	0.19	0.022	0.012	0.012	0.005	0.044	0.018	0.0016	0.0012
$\Delta\phi(E_T^{\text{miss}}, h_{\text{cand}})$	0.26	0.19	0.022	0.012	0.012	0.005	0.044	0.018	0.0016	0.0012
E_T^{miss}	0.12	-	0.007	-	0.003	-	0.013	-	0.0005	-
$m_{h_{\text{cand}}}$	0.12	0.19	0.007	0.012	0.0008	0.001	0.003	0.003	$4 \cdot 10^{-5}$	0.0001

Table 12: Cutflow for the boosted events in the 0-lepton category at LHC and FCC-hh. The acceptance regions for charged leptons and jets at the different colliders are defined in the text. A dash means that the particular cut was not applied. UT, MDT and BDT stand for untagged, mass-drop-tagged and doubly-b-tagged respectively.

Cuts / Eff.	Zh		Wh		$Wb\bar{b}$		$Zb\bar{b}$		$t\bar{t}$	
	LHC	FCC	LHC	FCC	LHC	FCC	LHC	FCC	LHC	FCC
0 $\ell^{\pm}$	1	1	0.32	0.40	0.34	0.4	0.78	1	0.98	1
0 UT jets	0.37	0.22	0.036	0.019	0.020	0.092	0.12	0.061	0.011	0.022
2 res. b-jets	0.028	0.0037	0.0027	0.003	0.0016	0.0061	0.015	0.025	$6 \cdot 10^{-5}$	$1 \cdot 10^{-5}$
ΔR_{bb}	0.027	0.003	0.0024	0.0003	0.0006	0.0002	0.0035	0.0034	$1 \cdot 10^{-5}$	$4 \cdot 10^{-8}$
H_T	0.027	-	0.0024	-	0.0006	-	0.0035	-	$1 \cdot 10^{-5}$	-
$p_{T,\min}^{b,\text{leading}}$	0.027	-	0.0024	-	0.0006	-	0.0035	-	$1 \cdot 10^{-5}$	-
$\Delta\phi(E_T^{\text{miss}}, h_{\text{cand}})$	0.027	0.0030	0.0024	0.0003	0.0006	0.0002	0.0035	0.0034	$1 \cdot 10^{-5}$	$4 \cdot 10^{-8}$
$\Delta\phi(b_1, b_2)$	0.027	0.0026	0.0024	0.0003	0.0006	0.0002	0.0035	0.0029	$1 \cdot 10^{-5}$	$4 \cdot 10^{-8}$
$\Delta\phi(E_T^{\text{miss}}, b\text{−jets})$	0.027	0.0026	0.0024	0.0003	0.0006	0.0002	0.0035	0.0003	$1 \cdot 10^{-5}$	$4 \cdot 10^{-8}$
E_T^{miss}	0.027	-	0.0024	-	0.0006	-	0.0035	-	$1 \cdot 10^{-5}$	-
$m_{h_{\text{cand}}}$	0.027	0.0026	0.0024	0.0003	$3 \cdot 10^{-5}$	$2 \cdot 10^{-5}$	10^{-4}	0.0001	$< 10^{-5}$	$< 4 \cdot 10^{-8}$

Table 13: Cutflow for the resolved events in the 0-lepton category at the LHC and FCC-hh. A dash means that the particular cut was not applied and UT stands for untagged.

Vh.

$h \to b\bar{b}$

Coefficient	Profiled Fit		One-Operator Fit	
$c_{\varphi q}^{(3)}$ [TeV^{-2}]	$[-9.2, 4.4] \times 10^{-2}$	1% syst.	$[-5.9, 4.0] \times 10^{-2}$	1% syst.
	$[-11.1, 4.6] \times 10^{-2}$	5% syst.	$[-6.8, 4.3] \times 10^{-2}$	5% syst.
	$[-14.5, 4.9] \times 10^{-2}$	10% syst.	$[-8.3, 4.6] \times 10^{-2}$	10% syst.
$c_{\varphi q}^{(1)}$ [TeV^{-2}]	$[-1.4, 1.4] \times 10^{-1}$	1% syst.	$[-1.2, 1.1] \times 10^{-1}$	1% syst.
	$[-1.4, 1.4] \times 10^{-1}$	5% syst.	$[-1.2, 1.1] \times 10^{-1}$	5% syst.
	$[-1.5, 1.5] \times 10^{-1}$	10% syst.	$[-1.3, 1.1] \times 10^{-1}$	10% syst.
$c_{\varphi u}$ [TeV^{-2}]	$[-2.1, 1.4] \times 10^{-1}$	1% syst.	$[-1.9, 1.1] \times 10^{-1}$	1% syst.
	$[-2.1, 1.4] \times 10^{-1}$	5% syst.	$[-1.9, 1.1] \times 10^{-1}$	5% syst.
	$[-2.2, 1.5] \times 10^{-1}$	10% syst.	$[-2.0, 1.2] \times 10^{-1}$	10% syst.
$c_{\varphi d}$ [TeV^{-2}]	$[-2.0, 2.6] \times 10^{-1}$	1% syst.	$[-1.6, 2.0] \times 10^{-1}$	1% syst.
	$[-2.1, 2.4] \times 10^{-1}$	5% syst.	$[-1.6, 2.0] \times 10^{-1}$	5% syst.
	$[-2.2, 2.5] \times 10^{-1}$	10% syst.	$[-1.7, 2.1] \times 10^{-1}$	10% syst.

Table 17: Bounds at 95% C.L. on the coefficients of the $\mathcal{O}_{\varphi q}^{(3)}$, $\mathcal{O}_{\varphi q}^{(1)}$, $\mathcal{O}_{\varphi u}$ and $\mathcal{O}_{\varphi d}$ operators for 13 TeV LHC with integrated luminosity of 139 fb^{-1}. **Left column:** Global fit, profiled over the other coefficients. **Right column:** One-operator fit (i.e. setting the other coefficients to zero).

Vh.

$h \to b\bar{b}$

Coefficient	Profiled Fit		One-Operator Fit	
$c_{\varphi q}^{(3)}$ [TeV^{-2}]	$[-5.9, 3.2] \times 10^{-2}$	1% syst.	$[-3.7, 2.9] \times 10^{-2}$	1% syst.
	$[-7.9, 3.5] \times 10^{-2}$	5% syst.	$[-4.3, 3.2] \times 10^{-2}$	5% syst.
	$[-10.6, 4.0] \times 10^{-2}$	10% syst.	$[-5.4, 3.6] \times 10^{-2}$	10% syst.
$c_{\varphi q}^{(1)}$ [TeV^{-2}]	$[-1.2, 1.1] \times 10^{-1}$	1% syst.	$[-10.4, 8.5] \times 10^{-2}$	1% syst.
	$[-1.2, 1.2] \times 10^{-1}$	5% syst.	$[-10.6, 8.7] \times 10^{-2}$	5% syst.
	$[-1.3, 1.3] \times 10^{-1}$	10% syst.	$[-11.1, 9.3] \times 10^{-2}$	10% syst.
$c_{\varphi u}$ [TeV^{-2}]	$[-1.8, 1.2] \times 10^{-1}$	1% syst.	$[-16.6, 8.7] \times 10^{-2}$	1% syst.
	$[-1.9, 1.2] \times 10^{-1}$	5% syst.	$[-16.8, 9.0] \times 10^{-2}$	5% syst.
	$[-2.0, 1.4] \times 10^{-1}$	10% syst.	$[-17.5, 9.7] \times 10^{-2}$	10% syst.
$c_{\varphi d}$ [TeV^{-2}]	$[-1.7, 2.0] \times 10^{-1}$	1% syst.	$[-1.3, 1.7] \times 10^{-1}$	1% syst.
	$[-1.8, 2.1] \times 10^{-1}$	5% syst.	$[-1.3, 1.7] \times 10^{-1}$	5% syst.
	$[-1.9, 2.2] \times 10^{-1}$	10% syst.	$[-1.4, 1.8] \times 10^{-1}$	10% syst.

Table 19: Bounds at 95% C.L. on the coefficients of the $\mathcal{O}_{\varphi q}^{(3)}$, $\mathcal{O}_{\varphi q}^{(1)}$, $\mathcal{O}_{\varphi u}$ and $\mathcal{O}_{\varphi d}$ operators for 13 TeV LHC with integrated luminosity of 300 fb^{-1}.

Vh.

$h \to b\bar{b}$

Coefficient	Profiled Fit		One-Operator Fit	
$c_{\varphi q}^{(3)}$ [TeV^{-2}]	$[-2.1, 1.4] \times 10^{-2}$	1% syst.	$[-1.1, 1.0] \times 10^{-2}$	1% syst.
	$[-3.9, 1.9] \times 10^{-2}$	5% syst.	$[-1.7, 1.5] \times 10^{-2}$	5% syst.
	$[-6.7, 2.7] \times 10^{-2}$	10% syst.	$[-2.9, 2.3] \times 10^{-2}$	10% syst.
$c_{\varphi q}^{(1)}$ [TeV^{-2}]	$[-7.6, 6.5] \times 10^{-2}$	1% syst.	$[-6.3, 4.5] \times 10^{-2}$	1% syst.
	$[-9.1, 8.3] \times 10^{-2}$	5% syst.	$[-7.2, 5.4] \times 10^{-2}$	5% syst.
	$[-10.4, 10.4] \times 10^{-2}$	10% syst.	$[-8.7, 6.9] \times 10^{-2}$	10% syst.
$c_{\varphi u}$ [TeV^{-2}]	$[-11.5, 5.9] \times 10^{-2}$	1% syst.	$[-11.1, 3.9] \times 10^{-2}$	1% syst.
	$[-13.5, 8.2] \times 10^{-2}$	5% syst.	$[-12.4, 4.9] \times 10^{-2}$	5% syst.
	$[-16.1, 10.7] \times 10^{-2}$	10% syst.	$[-14.4, 6.8] \times 10^{-2}$	10% syst.
$c_{\varphi d}$ [TeV^{-2}]	$[-1.0, 1.2] \times 10^{-1}$	1% syst.	$[-6.6, 10.6] \times 10^{-2}$	1% syst.
	$[-1.3, 1.5] \times 10^{-1}$	5% syst.	$[-8.0, 12.0] \times 10^{-2}$	5% syst.
	$[-1.6, 1.8] \times 10^{-1}$	10% syst.	$[-10.4, 14.4] \times 10^{-2}$	10% syst.

Table 21: Bounds at 95% C.L. on the coefficients of the $\mathcal{O}_{\varphi q}^{(3)}$, $\mathcal{O}_{\varphi q}^{(1)}$, $\mathcal{O}_{\varphi u}$ and $\mathcal{O}_{\varphi d}$ operators for 14 TeV HL-LHC with integrated luminosity of $3\,\text{ab}^{-1}$.

Vh.

$h \to b\bar{b}$

Coefficient	Profiled Fit		One-Operator Fit	
$c_{\varphi q}^{(3)}$ [TeV^{-2}]	$[-2.0, 2.1] \times 10^{-3}$	1% syst.	$[-1.1, 1.1] \times 10^{-3}$	1% syst.
	$[-4.9, 3.7] \times 10^{-3}$	5% syst.	$[-2.5, 2.4] \times 10^{-3}$	5% syst.
	$[-7.6, 5.1] \times 10^{-3}$	10% syst.	$[-4.0, 3.6] \times 10^{-3}$	10% syst.
$c_{\varphi q}^{(1)}$ [TeV^{-2}]	$[-9.1, 10.7] \times 10^{-3}$	1% syst.	$[-8.1, 8.2] \times 10^{-3}$	1% syst.
	$[-13.6, 14.5] \times 10^{-3}$	5% syst.	$[-11.4, 11.3] \times 10^{-3}$	5% syst.
	$[-16.3, 16.4] \times 10^{-3}$	10% syst.	$[-13.2, 13.1] \times 10^{-3}$	10% syst.
$c_{\varphi u}$ [TeV^{-2}]	$[-15.9, 9.0] \times 10^{-3}$	1% syst.	$[-6.2, 4.9] \times 10^{-3}$	1% syst.
	$[-27.0, 13.5] \times 10^{-3}$	5% syst.	$[-24.9, 8.2] \times 10^{-3}$	5% syst.
	$[-30.4, 16.4] \times 10^{-3}$	10% syst.	$[-30.2, 10.4] \times 10^{-3}$	10% syst.
$c_{\varphi d}$ [TeV^{-2}]	$[-17.9, 23.6] \times 10^{-3}$	1% syst.	$[-9.8, 23.0] \times 10^{-3}$	1% syst.
	$[-22.0, 26.5] \times 10^{-3}$	5% syst.	$[-14.0, 24.5] \times 10^{-3}$	5% syst.
	$[-25.1, 29.5] \times 10^{-3}$	10% syst.	$[-16.9, 26.4] \times 10^{-3}$	10% syst.

Table 3: Bounds at 95% C.L. on the coefficients of the $\mathcal{O}_{\varphi q}^{(3)}$, $\mathcal{O}_{\varphi q}^{(1)}$, $\mathcal{O}_{\varphi u}$ and $\mathcal{O}_{\varphi d}$ operators for FCC-hh with integrated luminosity of 30 ab^{-1}. **Left column:** Bounds from the global fit, profiled over the other coefficients. **Right column:** Bounds from a one-operator fit (i.e. setting the other coefficients to zero).

Vh.

$h \to b\bar{b}$

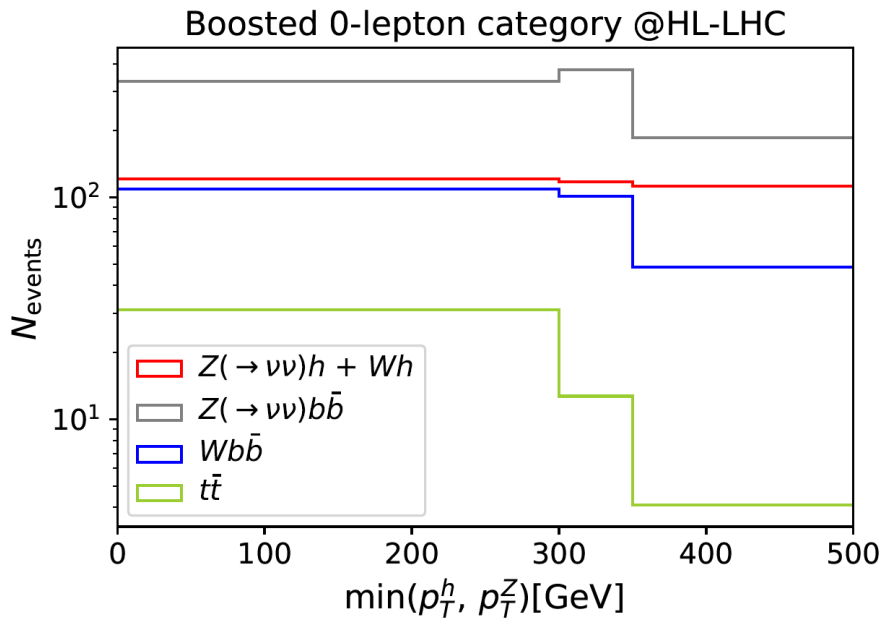
Boosted 0-lepton category @HL-LHC
N_{events}
10^2
10^1
$Z(\to \nu\nu)h + Wh$
$Z(\to \nu\nu)b\bar{b}$
$Wb\bar{b}$
$t\bar{t}$
0
100
200
300
400
500
$\min(p_T^h, p_T^Z)$[GeV]

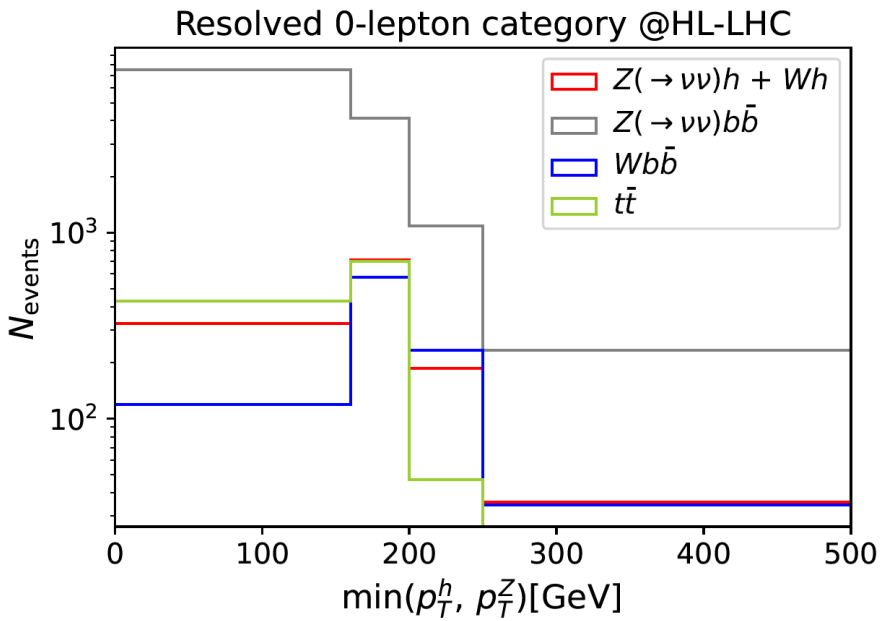
Resolved 0-lepton category @HL-LHC
N_{events}
10^3
10^2
$Z(\to \nu\nu)h + Wh$
$Z(\to \nu\nu)b\bar{b}$
$Wb\bar{b}$
$t\bar{t}$
0
100
200
300
400
500
$\min(p_T^h, p_T^Z)$[GeV]

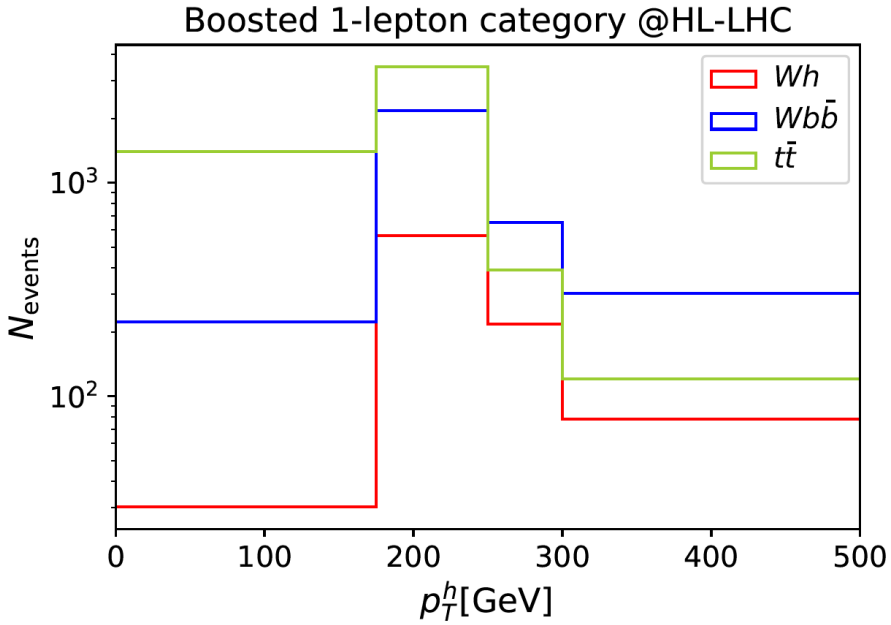
Boosted 1-lepton category @HL-LHC
N_{events}
10^3
10^2
Wh
$Wb\bar{b}$
$t\bar{t}$
0
100
200
300
400
500
p_T^h[GeV]

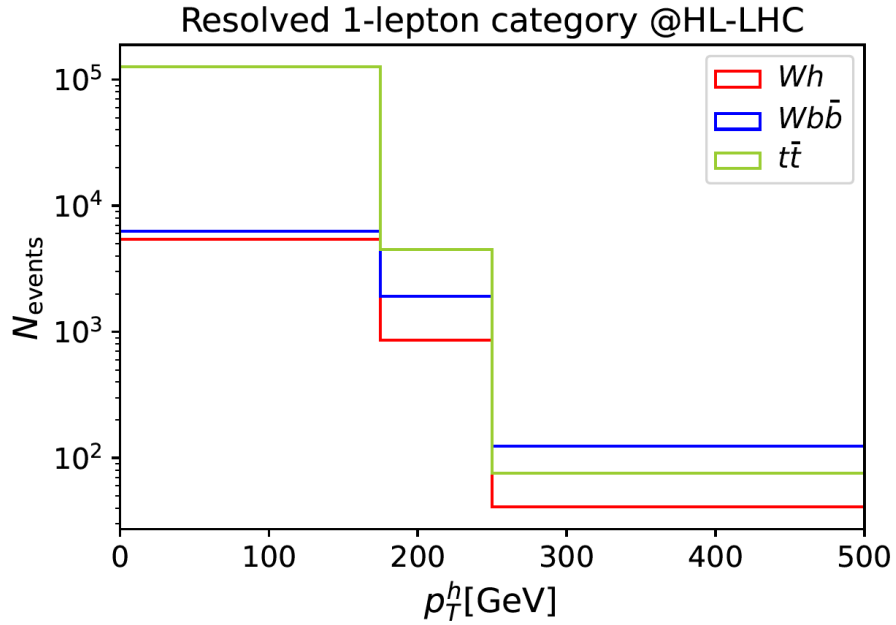
Resolved 1-lepton category @HL-LHC
N_{events}
10^5
10^4
10^3
10^2
Wh
$Wb\bar{b}$
$t\bar{t}$
0
100
200
300
400
500
p_T^h[GeV]

Vh.

$h \to b\bar{b}$

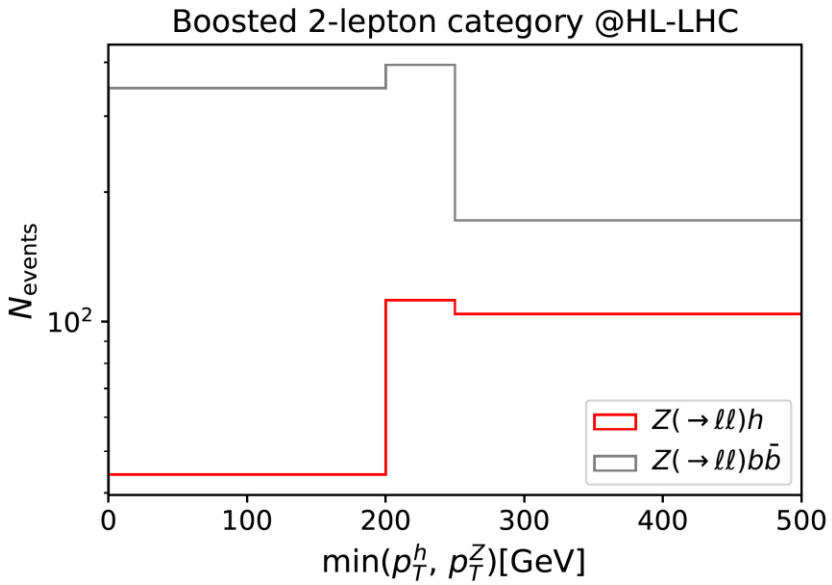
Boosted 2-lepton category @HL-LHC
N_{events}
10^2
$Z(\to \ell\ell)h$
$Z(\to \ell\ell)b\bar{b}$
0
100
200
300
400
500
$\min(p_T^h, p_T^Z)$[GeV]

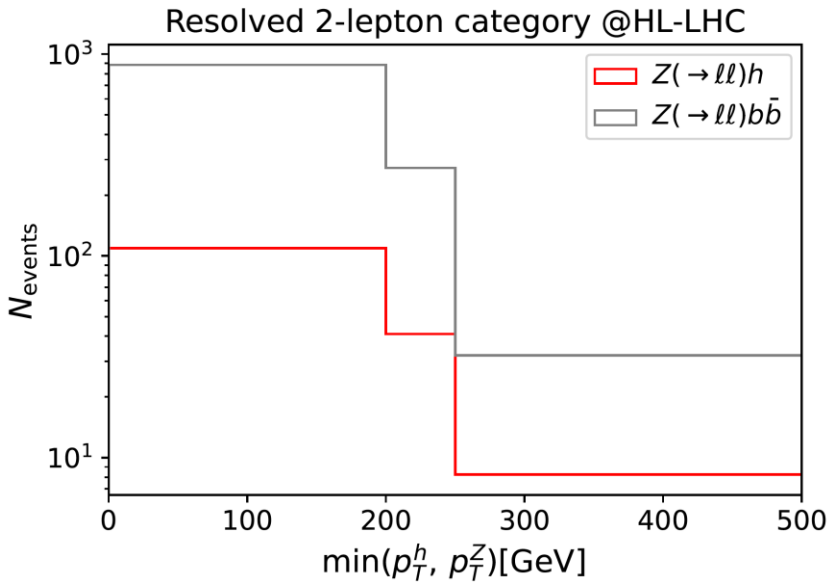
Resolved 2-lepton category @HL-LHC
N_{events}
10^3
10^2
10^1
$Z(\to \ell\ell)h$
$Z(\to \ell\ell)b\bar{b}$
0
100
200
300
400
500
$\min(p_T^h, p_T^Z)$[GeV]

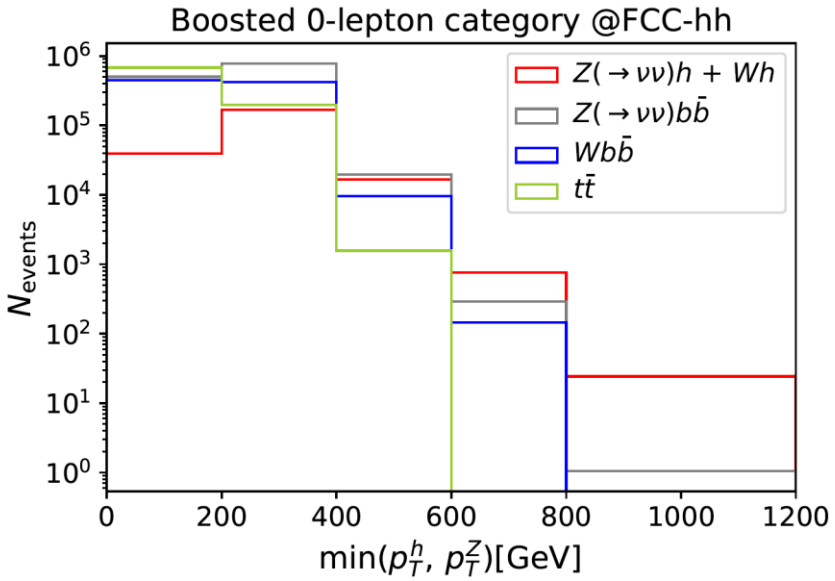
Boosted 0-lepton category @FCC-hh
N_{events}
10^6
10^5
10^4
10^3
10^2
10^1
10^0
$Z(\to \nu\nu)h + Wh$
$Z(\to \nu\nu)b\bar{b}$
$Wb\bar{b}$
$t\bar{t}$
0
200
400
600
800
1000
1200
$\min(p_T^h, p_T^Z)$[GeV]

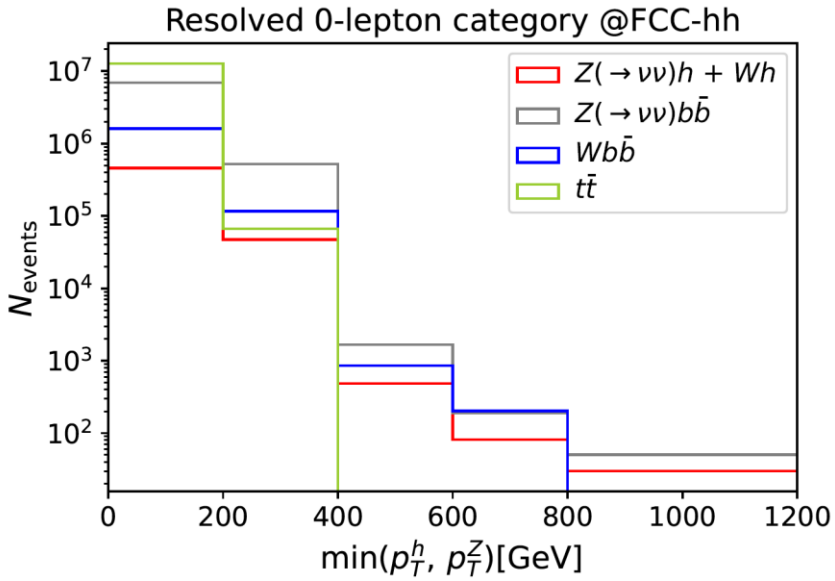
Resolved 0-lepton category @FCC-hh
N_{events}
10^7
10^6
10^5
10^4
10^3
10^2
$Z(\to \nu\nu)h + Wh$
$Z(\to \nu\nu)b\bar{b}$
$Wb\bar{b}$
$t\bar{t}$
0
200
400
600
800
1000
1200
$\min(p_T^h, p_T^Z)$[GeV]

Vh.

$h \to b\bar{b}$

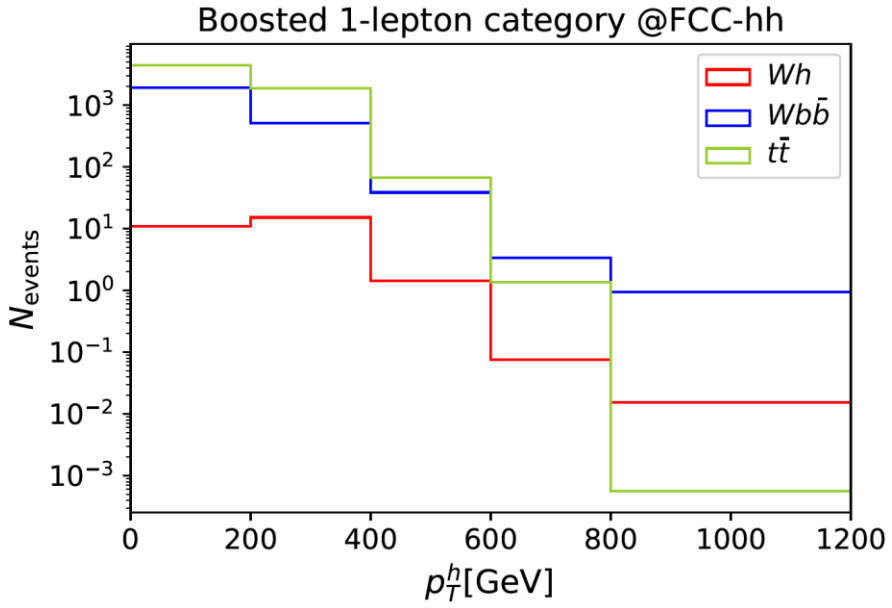
Boosted 1-lepton category @FCC-hh
Wh
$Wb\bar{b}$
$t\bar{t}$
N_{events}
p_T^h[GeV]

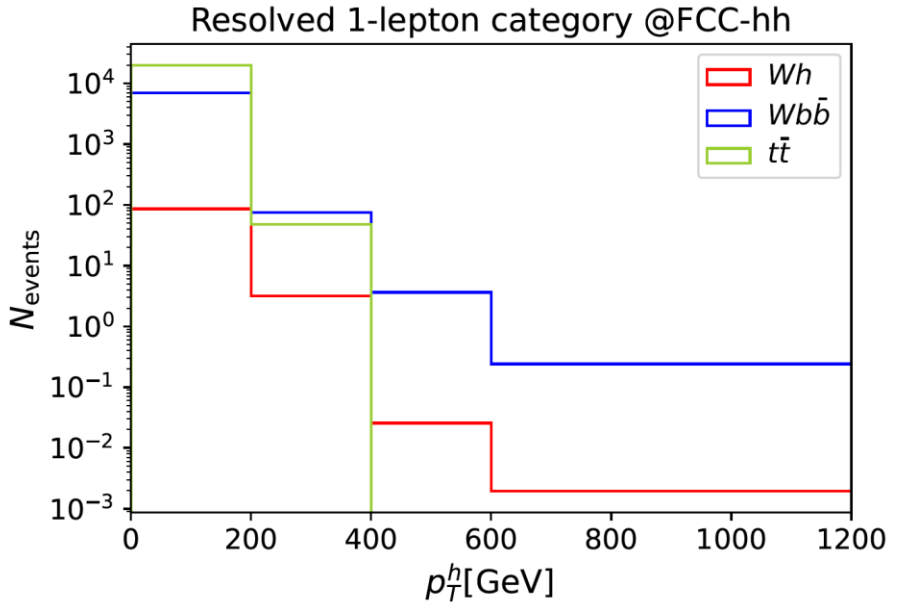
Resolved 1-lepton category @FCC-hh
Wh
$Wb\bar{b}$
$t\bar{t}$
N_{events}
p_T^h[GeV]

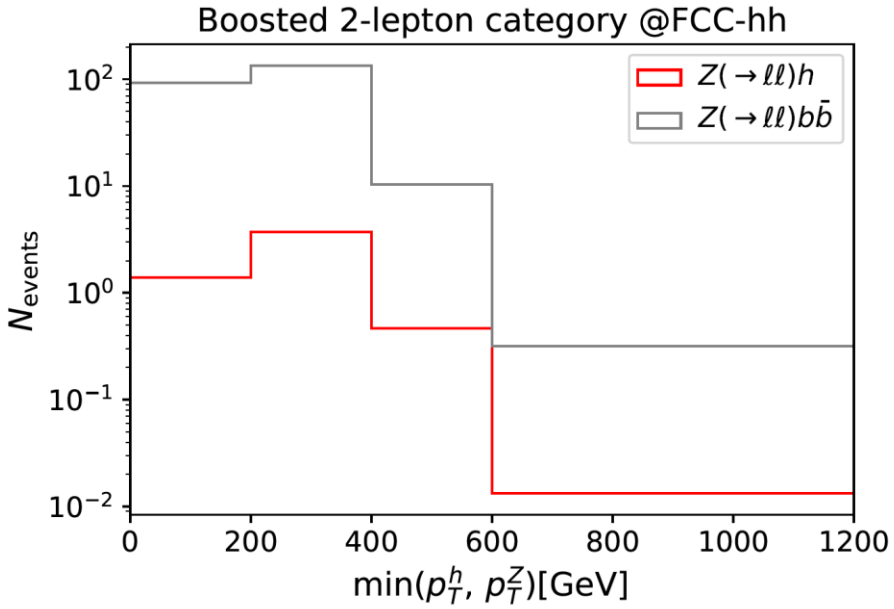
Boosted 2-lepton category @FCC-hh
$Z(\to \ell\ell)h$
$Z(\to \ell\ell)b\bar{b}$
N_{events}
min(p_T^h, p_T^Z)[GeV]

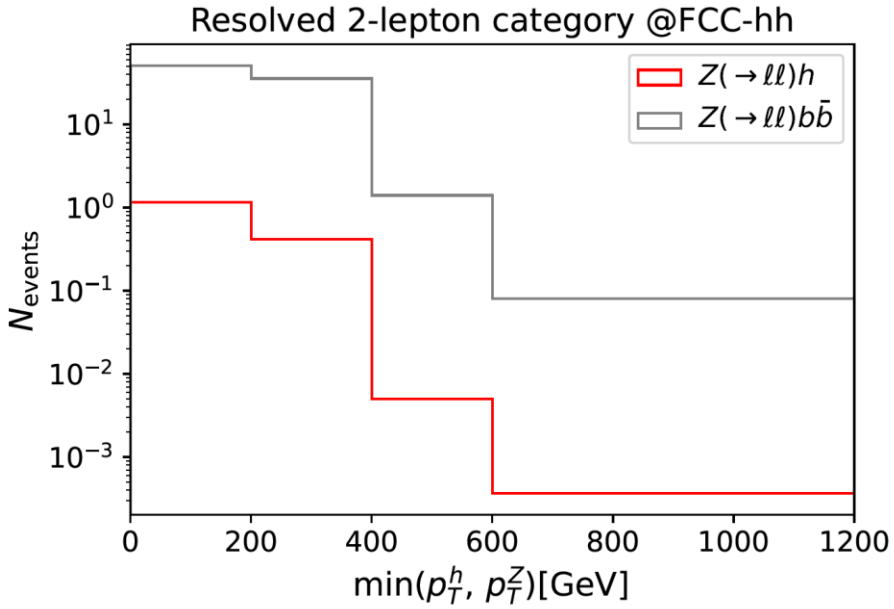
Resolved 2-lepton category @FCC-hh
$Z(\to \ell\ell)h$
$Z(\to \ell\ell)b\bar{b}$
N_{events}
min(p_T^h, p_T^Z)[GeV]

Vh.

$h \to b\bar{b}$

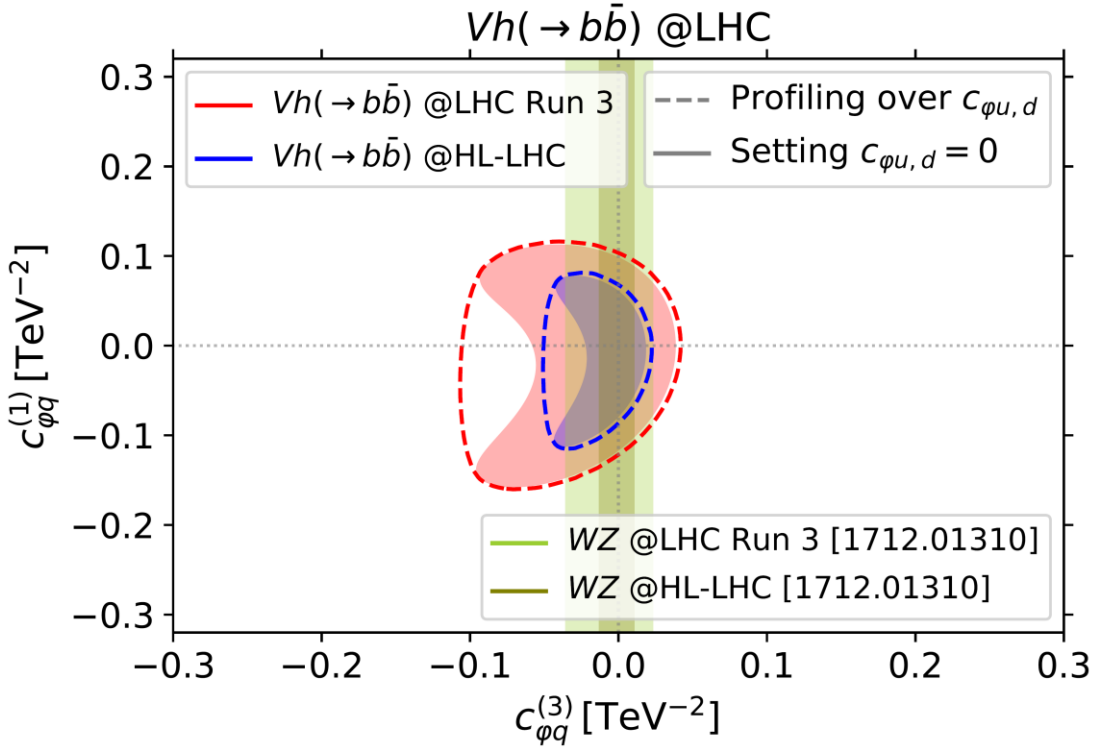
$Vh(\to b\bar{b})$ @LHC
$Vh(\to b\bar{b})$ @LHC Run 3
$Vh(\to b\bar{b})$ @HL-LHC
Profiling over $c_{\varphi u,\,d}$
Setting $c_{\varphi u,\,d} = 0$
WZ @LHC Run 3 [1712.01310]
WZ @HL-LHC [1712.01310]
$c_{\varphi q}^{(1)}$ [TeV^{-2}]
$c_{\varphi q}^{(3)}$ [TeV^{-2}]

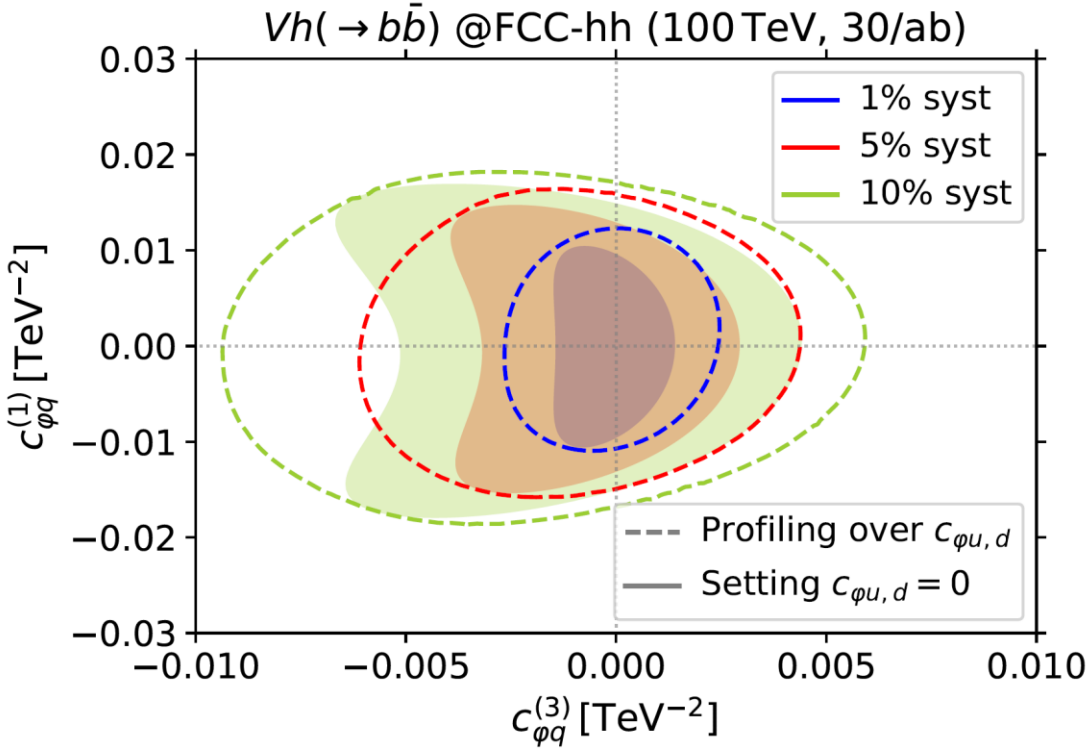
$Vh(\to b\bar{b})$ @FCC-hh (100 TeV, 30/ab)
1% syst
5% syst
10% syst
Profiling over $c_{\varphi u,\,d}$
Setting $c_{\varphi u,\,d} = 0$
$c_{\varphi q}^{(1)}$ [TeV^{-2}]
$c_{\varphi q}^{(3)}$ [TeV^{-2}]

Vh.

$h \to b\bar{b}$

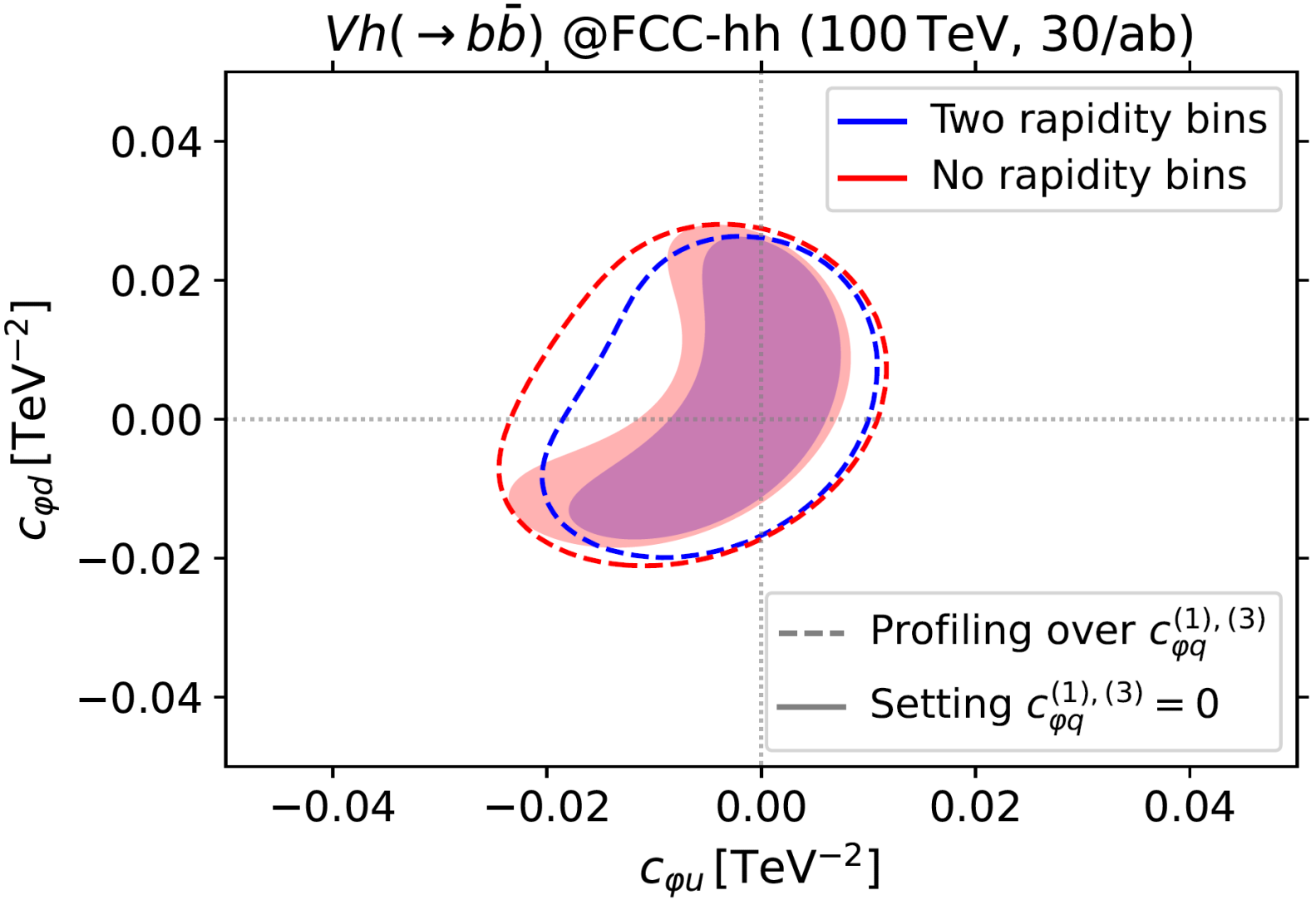
$Vh(\to b\bar{b})$ @FCC-hh (100 TeV, 30/ab)
Two rapidity bins
No rapidity bins
Profiling over $c_{\varphi q}^{(1),(3)}$
Setting $c_{\varphi q}^{(1),(3)} = 0$
$c_{\varphi d}$ [TeV^{-2}]
$c_{\varphi u}$ [TeV^{-2}]
0.04
0.02
0.00
−0.02
−0.04
−0.04
−0.02
0.00
0.02
0.04

Vh.

$h \to b\bar{b}$

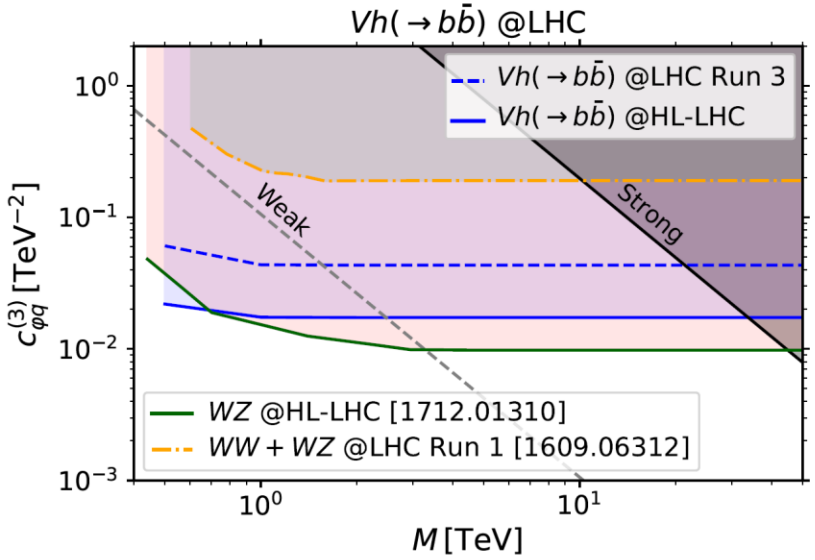
$Vh(\to b\bar{b})$ @LHC
$Vh(\to b\bar{b})$ @LHC Run 3
$Vh(\to b\bar{b})$ @HL-LHC
Weak
Strong
WZ @HL-LHC [1712.01310]
$WW + WZ$ @LHC Run 1 [1609.06312]
$c^{(3)}_{\varphi q}$ [TeV^{-2}]
M [TeV]

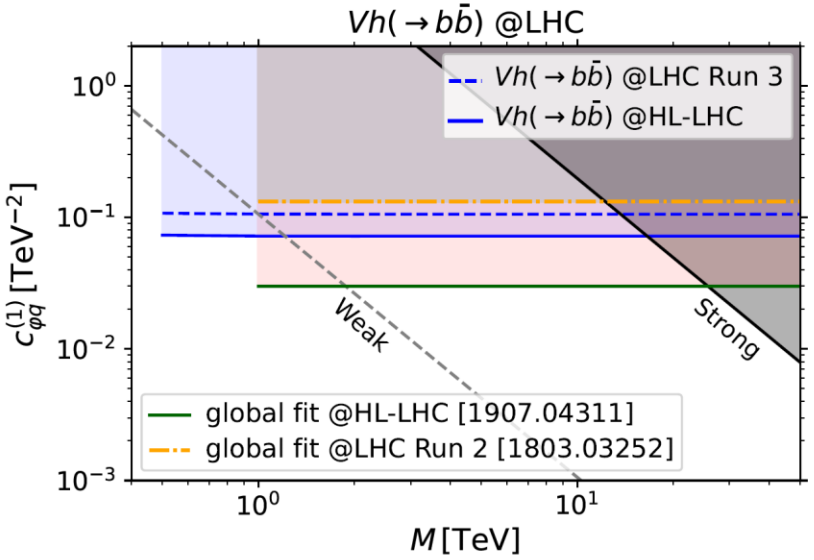
$Vh(\to b\bar{b})$ @LHC
$Vh(\to b\bar{b})$ @LHC Run 3
$Vh(\to b\bar{b})$ @HL-LHC
Weak
Strong
global fit @HL-LHC [1907.04311]
global fit @LHC Run 2 [1803.03252]
$c^{(1)}_{\varphi q}$ [TeV^{-2}]
M [TeV]

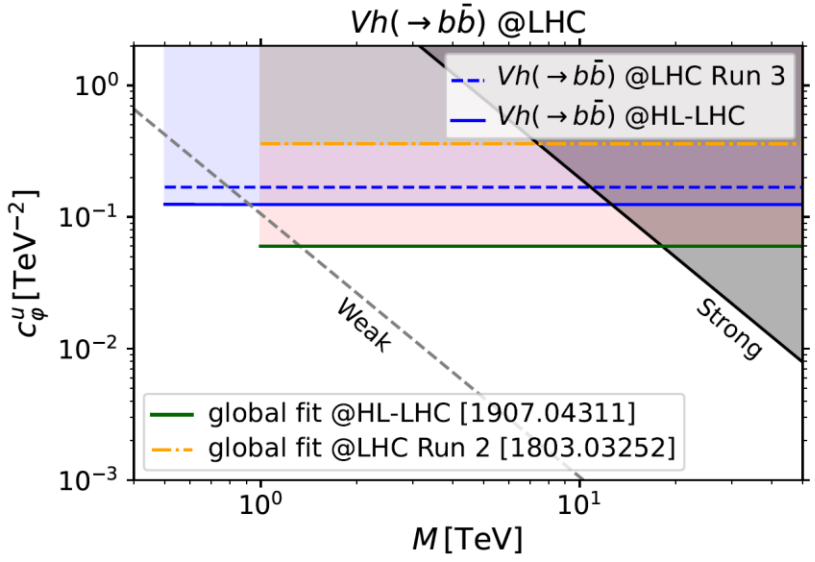
$Vh(\to b\bar{b})$ @LHC
$Vh(\to b\bar{b})$ @LHC Run 3
$Vh(\to b\bar{b})$ @HL-LHC
Weak
Strong
global fit @HL-LHC [1907.04311]
global fit @LHC Run 2 [1803.03252]
c^{u}_{φ} [TeV^{-2}]
M [TeV]

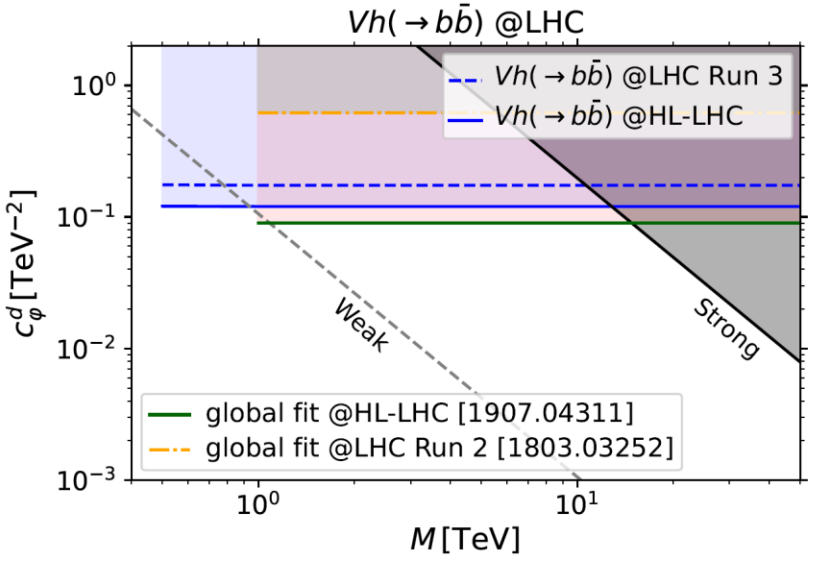
$Vh(\to b\bar{b})$ @LHC
$Vh(\to b\bar{b})$ @LHC Run 3
$Vh(\to b\bar{b})$ @HL-LHC
Weak
Strong
global fit @HL-LHC [1907.04311]
global fit @LHC Run 2 [1803.03252]
c^{d}_{φ} [TeV^{-2}]
M [TeV]

Vh.

$h \to b\bar{b}$

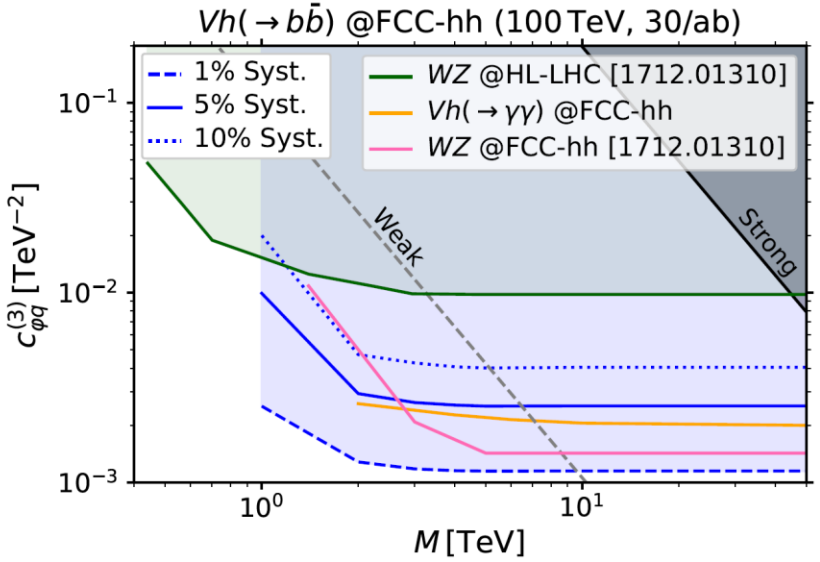
$Vh(\to b\bar{b})$ @FCC-hh (100 TeV, 30/ab)
1% Syst.
5% Syst.
10% Syst.
WZ @HL-LHC [1712.01310]
$Vh(\to\gamma\gamma)$ @FCC-hh
WZ @FCC-hh [1712.01310]
Weak
Strong
$c^{(3)}_{\varphi q}$ [TeV^{-2}]
M [TeV]

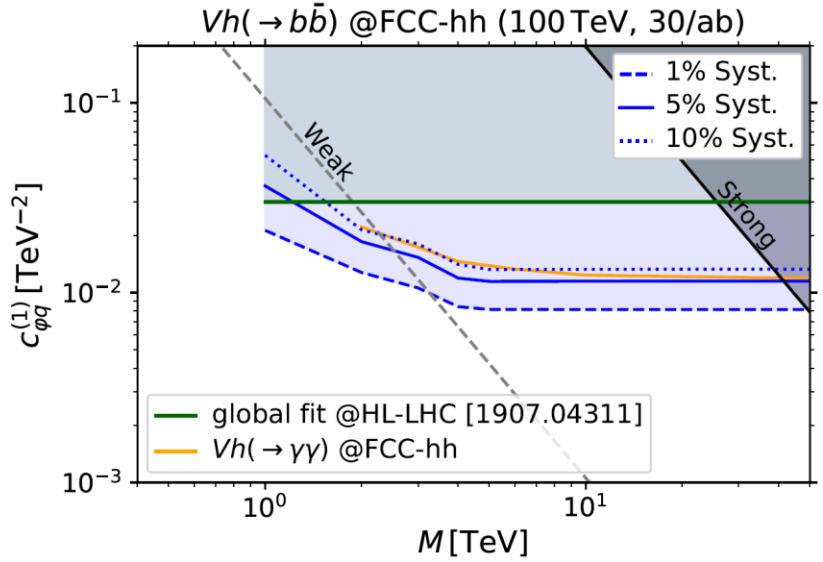
$Vh(\to b\bar{b})$ @FCC-hh (100 TeV, 30/ab)
1% Syst.
5% Syst.
10% Syst.
Weak
Strong
global fit @HL-LHC [1907.04311]
$Vh(\to\gamma\gamma)$ @FCC-hh
$c^{(1)}_{\varphi q}$ [TeV^{-2}]
M [TeV]

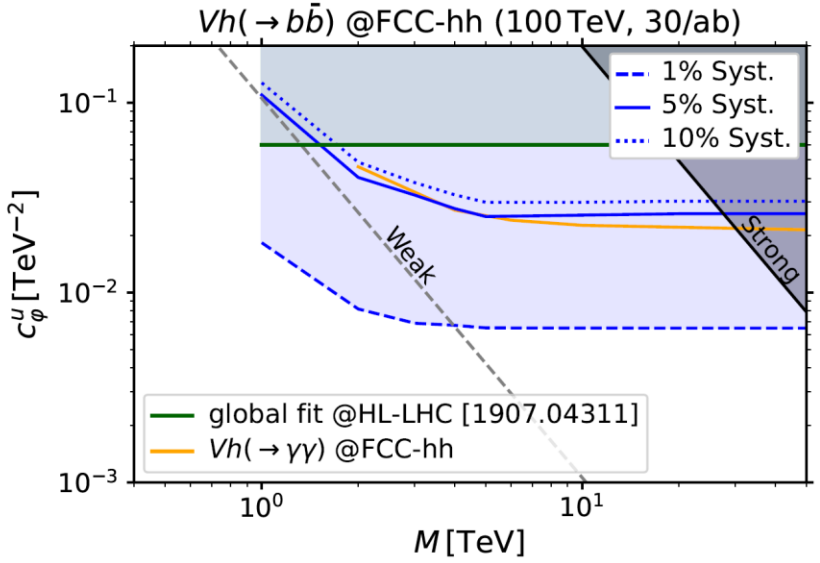
$Vh(\to b\bar{b})$ @FCC-hh (100 TeV, 30/ab)
1% Syst.
5% Syst.
10% Syst.
Weak
Strong
global fit @HL-LHC [1907.04311]
$Vh(\to\gamma\gamma)$ @FCC-hh
c^{u}_{φ} [TeV^{-2}]
M [TeV]

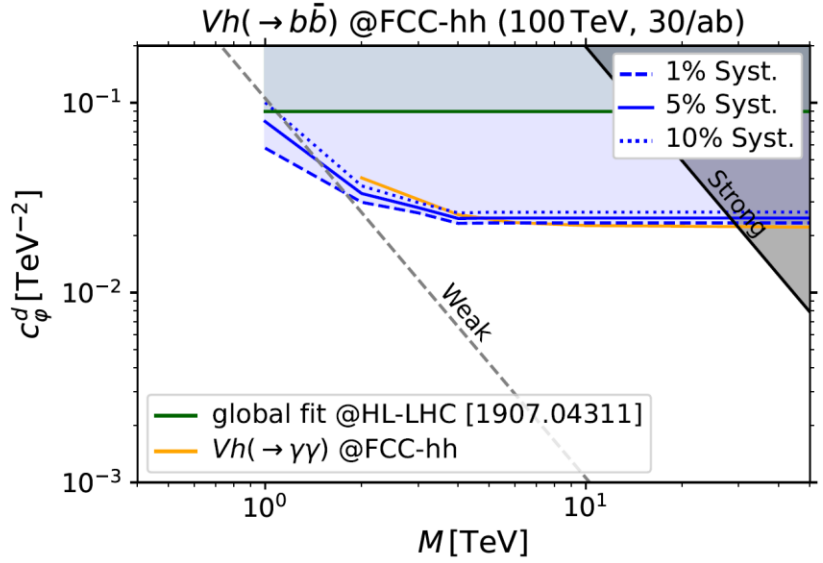
$Vh(\to b\bar{b})$ @FCC-hh (100 TeV, 30/ab)
1% Syst.
5% Syst.
10% Syst.
Weak
Strong
global fit @HL-LHC [1907.04311]
$Vh(\to\gamma\gamma)$ @FCC-hh
c^{d}_{φ} [TeV^{-2}]
M [TeV]

Vh.

$h \to b\bar{b}$

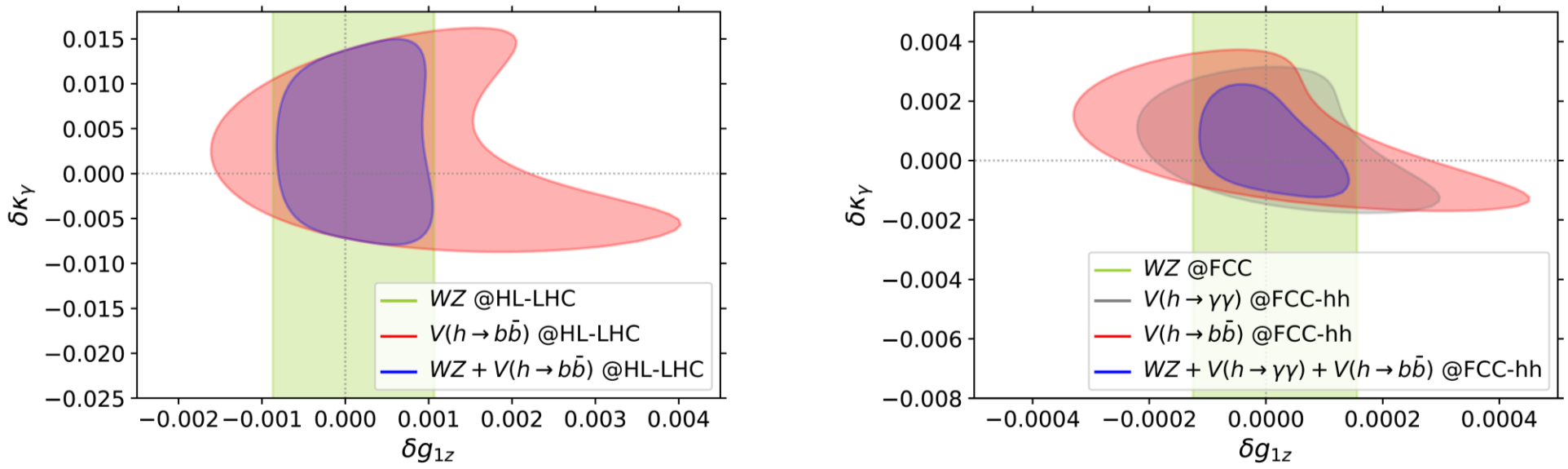

Figure 13: 95% C.L. bounds on the anomalous Triple Gauge Couplings δg_{1z} and $\delta\kappa_\gamma$ for Universal Theories. We show the bounds obtained from our analysis of $Vh(\to b\bar{b})$ at the HL-LHC and the FCC-hh, and compare them to the bounds obtained from different studies. Additionally, we present the results of combining the bounds from all the analyses we are comparing for each of the two colliders, respectively. **Left panel:** Bounds at the HL-LHC. We compare our results from $Vh(\to b\bar{b})$ with the bounds from the leptonic WZ channel [3]. **Right panel:** Bounds at the FCC-hh. We compare our results from $Vh(\to b\bar{b})$ with the bounds from the leptonic WZ channel [3] and from $Vh(\to \gamma\gamma)$ [5].

Vh.

Dimension-6 operators in Vh

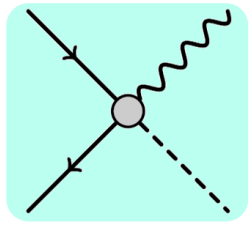
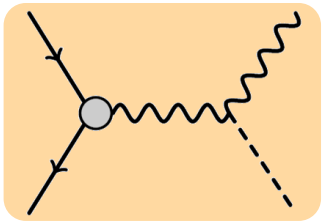
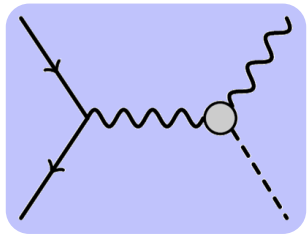
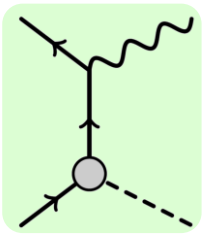

$$\mathcal{O}_{\varphi D} = \left(H^\dagger D^\mu H\right)^* \left(H^\dagger D_\mu H\right)$$

$$\mathcal{O}_{\varphi \mathrm{W}} = H^\dagger H\, W^{a,\mu\nu} W^a_{\mu\nu}$$

$$\mathcal{O}_{\varphi \widetilde{\mathrm{W}}} = H^\dagger H\, W^{a,\mu\nu} \widetilde{W}^a_{\mu\nu}$$

$$\mathcal{O}_{\varphi \mathrm{B}} = H^\dagger H\, B^{\mu\nu} B_{\mu\nu}$$

$$\mathcal{O}_{\varphi \widetilde{\mathrm{B}}} = H^\dagger H\, B^{\mu\nu} \widetilde{B}_{\mu\nu}$$

$$\mathcal{O}_{\varphi \mathrm{WB}} = H^\dagger \sigma^a H\, B^{\mu\nu} W^a_{\mu\nu}$$

$$\mathcal{O}_{\varphi \widetilde{\mathrm{WB}}} = H^\dagger \sigma^a H\, B^{\mu\nu} \widetilde{W}^a_{\mu\nu}$$

$$\mathcal{O}_{u\mathrm{W}} = (\bar{q}_L \sigma^{\mu\nu} u_R)\, \tau^I \tilde{H} W^I_{\mu\nu}$$

$$\mathcal{O}_{d\mathrm{W}} = (\bar{q}_L \sigma^{\mu\nu} d_R)\, \tau^I H W^I_{\mu\nu}$$

$$\mathcal{O}_{u\mathrm{B}} = (\bar{q}_L \sigma^{\mu\nu} u_R)\, \tilde{H} B_{\mu\nu}$$

$$\mathcal{O}_{d\mathrm{B}} = (\bar{q}_L \sigma^{\mu\nu} d_R)\, H B_{\mu\nu}$$

$$\mathcal{O}_{\varphi ud} = (\bar{u}_R \gamma^\mu d_R) \left(i H^\dagger \overleftrightarrow{D}_\mu H\right)$$

$$\mathcal{O}^{(3)}_{\varphi q} = \left(\bar{Q}_L \sigma^a \gamma^\mu Q_L\right) \left(i H^\dagger \sigma^a \overleftrightarrow{D}_\mu H\right)$$

$$\mathcal{O}^{(1)}_{\varphi q} = \left(\bar{Q}_L \gamma^\mu Q_L\right) \left(i H^\dagger \overleftrightarrow{D}_\mu H\right)$$

$$\mathcal{O}_{\varphi u} = \left(\bar{u}_R \gamma^\mu u_R\right) \left(i H^\dagger \overleftrightarrow{D}_\mu H\right)$$

$$\mathcal{O}_{\varphi d} = \left(\bar{d}_R \gamma^\mu d_R\right) \left(i H^\dagger \overleftrightarrow{D}_\mu H\right)$$

$$\mathcal{O}_{u\varphi} = H^\dagger H \left(\bar{q}_L \tilde{H} u_R\right)$$

$$\mathcal{O}_{d\varphi} = H^\dagger H \left(\bar{q}_L H d_R\right)$$

MFV suppressed — **Sub-leading energy growth** — **No interference with SM for massless quarks**